

Article

Diachroneity Rules the Mid-Latitudes: A Test Case Using Late Neogene Planktic Foraminifera across the Western Pacific

Adriane R. Lam ^{1,*}, Martin P. Crundwell ², R. Mark Leckie ³, James Albanese ³ and Jacob P. Uzel ¹

¹ Department of Geological Sciences and Environmental Studies, Binghamton University, Binghamton, NY 13902, USA; jacobuzel88@gmail.com

² GNS Science, Lower Hutt 5010, New Zealand; m.crundwell@gns.cri.nz

³ Department of Geosciences, University of Massachusetts Amherst, Amherst, MA 01003, USA; mleckie@geo.umass.edu (R.M.L.); jamesalbanese6@gmail.com (J.A.)

* Correspondence: alam@binghamton.edu

Abstract: Planktic foraminifera are commonly used for first-order age control in deep-sea sediments from low-latitude regions based on a robust tropical–subtropical zonation scheme. Although multiple Neogene planktic foraminiferal biostratigraphic zonations for mid-latitude regions exist, quantification of diachroneity for the species used as datums to test paleobiogeographic patterns of origination and dispersal is lacking. Here, we update the age models for seven southwest-Pacific deep-sea sites using calcareous nannofossil and bolboform biostratigraphy and magnetostratigraphy, and use 11 sites between 37.9° N and 40.6° S in the western Pacific to correlate existing planktic foraminiferal biozonations and quantify the diachroneity of species used as datums. For the first time, northwest and southwest Pacific biozones are correlated and compared to the global tropical planktic foraminiferal biozonation. We find a high degree of diachroneity in the western Pacific, within and between the northwest and southwest regions, and between the western Pacific and the tropical zonation. Importantly, some datums that are found to be diachronous between regions have reduced diachroneity within regions. Much work remains to refine regional planktic foraminiferal biozonations and more fully understand diachroneity between the tropics and mid-latitudes. This study indicates that diachroneity is the rule for Late Neogene planktic foraminifera, rather than the exception, in mid-latitude regions.

Keywords: Tasman Sea; Kuroshio Current; Kuroshio Current Extension; Tasman Front; paleobiogeography; biostratigraphy; southwest Pacific; northwest Pacific; western equatorial Pacific; diachroneity



Citation: Lam, A.R.; Crundwell, M.P.; Leckie, R.M.; Albanese, J.; Uzel, J.P. Diachroneity Rules the Mid-Latitudes: A Test Case Using Late Neogene Planktic Foraminifera across the Western Pacific. *Geosciences* **2022**, *12*, 190. <https://doi.org/10.3390/geosciences12050190>

Academic Editors: Maria Rose Petrizzo, Lucilla Capotondi, Angela Cloke-Hayes and Jesus Martinez-Frias

Received: 26 February 2022

Accepted: 17 April 2022

Published: 26 April 2022

Publisher's Note: MDPI stays neutral with regard to jurisdictional claims in published maps and institutional affiliations.



Copyright: © 2022 by the authors. Licensee MDPI, Basel, Switzerland. This article is an open access article distributed under the terms and conditions of the Creative Commons Attribution (CC BY) license (<https://creativecommons.org/licenses/by/4.0/>).

1. Introduction

Planktic foraminifera are marine protists that are widespread in the global ocean today, and have been since at least the Middle Jurassic ([1–3]. Due to their abundance in deep-sea sediments, foraminifera have several uses, including but not limited to public outreach activities (e.g., [4]), taxonomic training (e.g., [5]), inferring open-ocean speciation processes (e.g., [6–11]) and, importantly, providing first-order age control. There is a robust, widely used, tropical-to-subtropical planktic foraminiferal biozonation for the Cenozoic [12,13], but other biostratigraphic studies conducted in mid-latitude regions of the world's oceans—specifically for the Pacific [14–20]—indicate that the tropical zonation is not appropriate for mid-latitude sites. Key reasons for this include the paucity of tropical water species in temperate water masses of the mid-latitudes, and the diachroneity of Cenozoic planktic foraminiferal species, which have been documented for regions across the world's oceans (e.g., [21–23]) and especially for the southwest Pacific (e.g., [24–30]). Recently published planktic foraminiferal occurrence data for the mid-latitudes of the northwest Pacific [31] further highlight the high degree of diachroneity across relatively short latitudinal distances (~5°) through the Late Neogene and Quaternary.

Studies from the southwest and northwest Pacific indicate that the key to establishing robust and meaningful biostratigraphic zonations is understanding the paleobiogeographic patterns that control species' first and last occurrences through space and time. Paleobiogeographic patterns of organisms have shed light on abiotic processes that contribute to dispersal patterns, speciation modes, and the causes of diachronous first and last appearances throughout the Phanerozoic (e.g., [32–41]). Thus, it is worth investigating patterns of diachroneity in planktic foraminifera at the local and regional levels, as such patterns can elucidate the drivers of evolutionary processes and, importantly, lay the groundwork for creating robust regional biostratigraphic zonations. In other words, planktic foraminiferal biostratigraphy is based on the paleobiogeographic patterns of species used as primary and secondary markers, and deeper understanding and quantification of the timing of evolution, dispersal, extirpation, and extinction events are powerful tools to interpret regional-to-global drivers of such patterns.

Dowsett [26] quantified the degree of synchrony of Pliocene planktic foraminifera and calcareous nannofossil datums at five Deep Sea Drilling Project Leg 90 sites in the southwest Pacific using the graphic correlation method. His study revealed that Pliocene datums were diachronous on the scale of 0.05–0.80 Myr. To follow up on the Dowsett [26] study, and to further assess and understand the timing of planktic foraminiferal evolutionary and dispersal patterns, we used biostratigraphic zonations and occurrence data developed for the southwest Pacific [14,18] this study, northwest Pacific [31,42], and western equatorial Pacific [15,43]. These data were used to (1) correlate Late Neogene (15–0 Ma) biozones from the mid-latitudes of the northwest Pacific to the mid-latitudes of the southwest Pacific (37.9° N to 40.6° S; Figure 1), to show how diachroneity affects biostratigraphic zonations and first-order age interpretations of sedimentary sections; and (2) quantify diachroneity across the western Pacific Ocean through the Late Neogene. We only investigated datums that are used as primary and secondary marker species to delineate biozones in the tropical zonation [13], biozones in the southwest Pacific [14,17,18], and the northwest Pacific [31]. For the first time, we correlated temperate northwest Pacific sites with the western equatorial Pacific and subtropical–temperate southwest Pacific sites, along with the global tropical zonations for planktic foraminifera [12,13] and calcareous nannofossils [44,45]. Data from the 11 sites used in this study further reveal the high degree of diachroneity within the mid-latitude regions—areas characterized by strong seasonality and steep latitudinal gradients in temperature, nutrients, and salinity today and through the Late Neogene (e.g., [46–49]).

Previous researchers have questioned the reliability of planktic foraminiferal datums, and have suggested that this group is better suited for evolutionary studies rather than biostratigraphic tools [50]. We disagree with this sentiment, and consider that the paleobiogeographic patterns of planktic foraminifera are powerful, underutilized signals for interpreting past ocean dynamics, inferring evolutionary responses to abiotic processes and, importantly, building robust regional biostratigraphic zonations. Rather than isochronous datums being the standard, we show that diachroneity of planktic foraminiferal datums is more common (with isochronous datums being rare) across and between mid-latitude regions, with diachroneity also apparent within and between low-latitude sites.

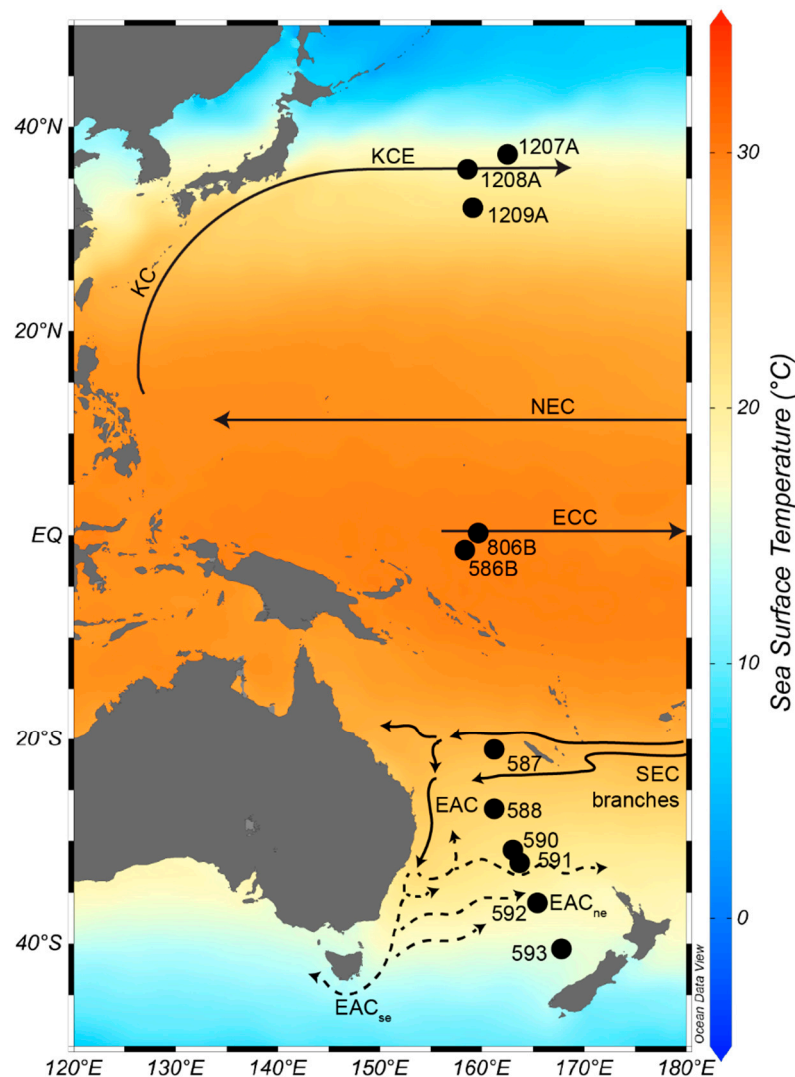


Figure 1. Modern-day sea surface temperature map of the western Pacific, with the 11 sites used in this study denoted by black circles. Major currents and eddy systems are denoted by solid and dashed lines, respectively. KCE, Kuroshio Current Extension; KC, Kuroshio Current; NEC, North Equatorial Current; ECC, Equatorial Counter Current; SEC branches, South Equatorial Current branches; EAC, East Australian Current; EAC_{ne}, north extension of East Australian Current; EAC_{se}, southern extension of East Australian Current. Map created using Ocean Data View [51] with sea surface temperature data from the World Ocean Atlas [52].

2. Materials and Methods

2.1. ODP and DSDP Sites Utilized

The sites used in this study lie in tropical, subtropical, and temperate or transitional water masses. The temperate and subtropical zones were defined by different criteria for both land and sea. For example, a mean annual temperature of 18 °C was applied for the boundary between warm subtropical waters and cold-water regions [53–55]. Today, seasonal monthly sea surface temperatures over the Shatsky Rise in the northwest Pacific vary between ~16 °C in February and ~26 °C in August [56]. Because this study spans much of the Neogene and Quaternary, oceanic zonal boundaries are likely to have shifted over time. Therefore, we applied broadly defined zonal criteria. The National Geographic Society defines the tropics as between the latitudes of the Tropic of Cancer in the Northern Hemisphere (~23.5° N) and the Tropic of Capricorn in the Southern Hemisphere (~23.5° S; [57]). The temperate zone is broadly defined as the regions between the

Tropic of Cancer and the Arctic Circle (~66.5° N), and between the Tropic of Capricorn and the Antarctic Circle (~66.5° S). According to the American Meteorological Society, the subtropics refers the warm part of the temperate region, from the tropics to approximately 35° N and 35° S latitude [58], which lies close to the mean annual 18 °C isotherm across the Shatsky Rise [56].

We investigated biogeographic patterns and diachroneity using sites drilled during Ocean Drilling Program (ODP) Leg 198 (Holes 1207A, 1208A, 1209A) in the northwest Pacific [59], ODP Leg 130 Hole 806B drilled in the western equatorial Pacific [60], and Deep Sea Drilling Project (DSDP) Leg 90 (Sites 586, 587, 588, 590, 591, 592, and 593) drilled in the southwest Pacific (Table 1; [61]). These sites have relatively continuous Late Neogene sequences that overlie major unconformities. For example, DSDP Site 593 in the southwest Pacific includes a hiatus between approximately 13.46 and 15.90 Ma [62]. The sites used in this study contain good preserved calcareous planktic microfossils and nannoplankton that are suitable for high-resolution biostratigraphic studies [18,31,42,43].

Table 1. Site latitude and longitude, water depths, core intervals utilized in this study, depths in the cores, and associated age of sediments.

Site	Latitude	Longitude	Water Depth (m)	Core Section, Interval (cm)	Depth in Cores (mbsf)	Age (Ma)
1207A	37.90° N	162.76° E	3100.8	1H-1, 29–31 to 18H-4, 78–80	0.29–162.08	0.018–12.304
1208A	36.29° N	158.22° E	3345.7	1H-1, 77–79 to 35X-2, 77–79	0.78–317.58	0.014–15.117
1209A	32.65° N	158.50° E	2387.2	1H-1, 27–29 to 11H-1, 77–79	0.27–94.48	0.019–7.161
806B	0.34° N	159.53° E	2519.9	1H-2, 12–14 to 66X-CC	1.62–627.51	0.230–22.800
586B	0.71° S	158.71° E	2207.0	1H-1, 51–53 to 21H-5, 50–52	1.92–197.31	0.097–7.391
587	21.20° S	161.59° E	1101.0	1H-1, 5–6 to 10H-6, 17–18	0.05–87.57	0.002–8.250
588	26.29° S	161.38° E	1533.0	1H-CC to 25H-CC	5.43–235.90	0.395–9.401
590	31.17° S	163.49° E	1299.0	1H-CC to 27H-CC	6.86–280.80	0.487–7.251
591	31.59° S	164.68° E	2131.0	1H-CC to 31H-CC	3.19–282.83	0.147–7.626
592	36.57° S	165.58° E	1088.0	1H-CC to 29X-CC	4.27–272.44	0.303–11.925
593	40.63° S	167.79° E	1068.0	1H-2, 87–89 to 45X-CC	2.38–427.39	0.112–18.049

Sites from Leg 198 were drilled on the Shatsky Rise—a large igneous province [63]. Through the Late Neogene, these sites moved relatively little, and largely remained above the carbonate compensation depth (CCD; [59]). Site 1207 was drilled on the northern high of the Shatsky Rise (the Shirshov Massif), Site 1208 was drilled on the central high (Orif Massif), and Site 1209 was drilled on the southern high (Tamu Massif; [64]). The sites transect the modern-day position of the Kuroshio Current Extension (KCE), with Site 1207 positioned on the northern edge of the current, and Site 1208 located below the axis of the current and its ecotone. Both sites currently lie within transitional (temperate) water masses created by the mixing of subtropical water masses brought poleward by the Kuroshio Current and subpolar water masses brought equatorward by the Oyashio Current (Figure 1). Site 1209 is located south of the KCE, in seasonal subtropical water masses. Carbonate preservation is generally good, but dissolution intervals are apparent in the deeper sections (Early–Middle Pliocene and Miocene) of Holes 1207A and 1208A, likely because these sites lie at deeper water depths compared to Hole 1209A (Table 1; [42]).

Ocean Drilling Program Leg 130 Site 806 was drilled on the northeastern margin of the Ontong Java Plateau, within the Indo-Pacific Warm Pool. The Ontong Java Plateau remained in equatorial waters for much of the Neogene, and sediments accumulated above the CCD [60]. Site 806 recovered a relatively complete Neogene sequence and terminated in the Oligocene, with good preservation of planktic foraminifera and calcareous nannofossils throughout [43,60,65].

Southwest Pacific sites from DSDP Leg 90 were drilled along a latitudinal transect of relatively shallow oceanic sites from the western equatorial Pacific to the temperate Tasman Sea region west of New Zealand (Figure 1). Cores drilled from the Lord Howe

Rise generally have high carbonate mass accumulation rates through the Neogene [49]. Water depths at the sites range from 1068–2207 m (Table 1), and calcareous microfossils and nannoplankton are very well preserved at all sites [66]. Hole 586B was drilled on the Ontong Java Plateau in the Indo-Pacific Warm Pool region, close to ODP Hole 806B (Figure 1). Sites 587 to 593 form a latitudinal transect from the subtropics to temperate mid-latitudes. The transect crosses the Tasman Front (TF)—the eastern extension of the East Australian Current [67] that forms the northern margin of the Subtropical Frontal Zone west of New Zealand. Sites 590 and 591 sit in subtropical water, while Sites 592 and 593 sit in temperate (transitional) water within the Subtropical Frontal Zone.

2.2. Foraminiferal Occurrence Data, Taxonomy, and Age Models

In order to investigate Late Neogene western Pacific Ocean's planktic foraminiferal paleobiogeographic patterns and directly correlate biostratigraphic zonations from the temperate mid-latitudes of the Northern to Southern hemispheres, we used the previously published Late Neogene planktic foraminiferal occurrence data and biostratigraphic zonations of Lam and Leckie [31] for ODP Leg 198 Holes 1207A, 1208A, and 1209A, Chaisson and Leckie [43] for ODP Leg 130 Hole 806B, and Jenkins and Srinivasan [18] for DSDP Leg 90 sites.

No updates to taxonomy or age models were made to the foraminiferal occurrence data and biostratigraphic schemes of Lam and Leckie [31] for ODP Holes 1207A, 1208A, and 1209A, as the planktic foraminiferal taxonomy was recently updated for these sites [42], and species' first and last occurrence dates were recently calibrated to the Geologic Time Scale 2020 (GTS 2020; [68]) by Lam and Leckie [31]. Relatedly, ODP Hole 806B planktic foraminiferal occurrence data and the age model for the hole were recently updated by Lam and Leckie [42]. The age model for Hole 806B was constructed using the calcareous nannoplankton biostratigraphy of Takayama [65], with ages updated to the datum dates in Sutherland et al. [69]. Thus, we used the updated taxonomy and recalibrated species' first and last occurrence dates for Hole 806B, as reported by Lam and Leckie [42].

We updated the planktic foraminiferal taxonomy for DSDP Leg 90 planktic foraminiferal occurrence data from Jenkins and Srinivasan [18] to that of Lam and Leckie [42], with additional taxonomic updates from Kennett and Srinivasan [17] and Wade et al. [70] for species not included in the taxonomic review of Lam and Leckie [42]. The Leg 90 foraminiferal occurrence data contained some species that were not distinguished from their closely related ancestors or descendants. We treated these on a case-by-case basis. For example, '*Globorotalia tosaensis*/*Globorotalia truncatulinoides*' was synonymized with *Truncorotalia truncatulinoides*; '*Globorotalia juanai*/*Globorotalia praemargaritae*' was changed to *Truncorotalia juanai*, and similarly, any species labeled '*Gr. praemargaritae*' was synonymized with *Tr. juanai*. From the Leg 90 occurrence data, we also removed '*Globorotalia plesirotunda*/*Globorotalia tumida*', as we viewed this column in the data as representing a species that was transitional between the two species. We also removed '*Neogloboquadrina humerosa*/*Neogloboquadrina dutertrei* plexus', '*Globorotalia crassaformis*/*Gr. tosaensis*', and the '*Globoconella puncticulata*/*Globoconella inflata* plexus'. Where only genus names were indicated (e.g., '*Globorotalia* sp. and sp. 2'), we removed those columns from the data. At Hole 586B, *Dentoglobigerina venezuelana* occurs quite high in the section. We suspect that this is due to the authors lumping *Globoquadrina conglomerata* with *Dt. venezuelana*; thus, the last occurrence of this species at the hole is likely inaccurate.

Even with the updated taxonomy, we should note that occurrence data from Leg 90 sites [18] do not include planktic foraminiferal morphospecies commonly identified in the southwest Pacific by micropaleontologists (e.g., *Globoconella puncticuloides*, *Globoconella mons*, and *Truncorotalia crassacarina*, which were not recognized in this study), meaning that species presented in the Leg 90 data likely lumped such morphospecies ranges with related taxa. In addition, expanded taxonomic work remains to be conducted for Neogene species with uncertain genus associations (e.g., *Hirsutella cibaensis* may be a globoconellid rather than a hirsutellid, and other figured specimens of *Hr. cibaensis* may belong to a different

species altogether; [71]). Such taxonomic uncertainties will be addressed by the Neogene Planktic Foraminiferal Working Group.

In this study, we also included 28 additional samples from DSDP Leg 90 Site 593 from the Microfossil Reference Centre collections at GNS Science to refine datums at the site (Supplementary Table S8). Our main focus with the incorporation of new Site 593 samples was to refine the first and last occurrences of species used to construct zones at this particular site (e.g., the last occurrence of *Paragloborotalia mayeri*, the first occurrence of *Globoconella puncticulata*). In addition, we also included species' occurrence data for Site 593 from Scott et al. [72].

Age models were created for DSDP Leg 90 sites based on magnetic reversal boundaries [73], calcareous nannofossil datums [74], and bolboform datums at Sites 592 [75] and 593 [76]. Ages of magnetic reversal boundaries and bolboform datums were updated to the GTS 2020 (Figure 2; [68]), and nannofossil datums were updated to the ages of those presented by Sutherland et al. [69]. In most cases, age models were created from a mix of magnetic reversal boundaries, nannofossil datums, and bolboform datums (Supplementary Table S1), because magnetostratigraphy was not well-resolved throughout the entire hole. Figures 3–8 rank the sites used in this study to indicate the robustness of the age models. A ranking of 1 indicates that the age model for the site is based entirely on magnetostratigraphy, a ranking of 2 indicates that the age model is a mix of magnetostratigraphic reversal boundaries and biostratigraphy, and a ranking of 3 indicates that the age model is solely based on biostratigraphy.

The depth of magnetic reversal boundaries was defined to occur between the samples that constrained the boundary (i.e., midpoint depth). For calcareous nannofossil and bolboform datums, species' first occurrences (bases) were calculated as the midpoint between the sample in which the species was present and the sample stratigraphically below in which the species was absent. Fossils' last occurrences (tops) were calculated as the midpoint between the sample that contained the species and the sample stratigraphically above in which the species was absent.

Using the updated taxonomy and age models for Leg 90 sites, we refined the biozones developed for the southwest Pacific by Kennett [43], as modified by Jenkins and Srinivasan ([18]; Supplementary Tables S2–S8). The updated biostratigraphy in the southwest Pacific should still be viewed as preliminary, as much work remains to further refine the biozones in this region and update the planktic foraminiferal taxonomy.

With the updated foraminiferal occurrence data and biostratigraphic zonations for the Leg 90 sites, along with occurrence data and zonations for the Leg 198 holes and equatorial Pacific Hole 806B, we investigated patterns of diachroneity among species, and how such diachroneity affects age interpretations of zonal boundaries. We focused only on planktic foraminiferal species used as primary (species that denote zone boundaries) and secondary (species' datums that occur within zones) datums in the global tropical zonation [12,13] and mid-latitude subtropical-to-temperate zonations developed for the northwest Pacific [31] and southwest Pacific [14,18]. We excluded taxa from this study that occurred at less than three sites, which were mainly species used in the tropical zonation as secondary datums.

3. Results

3.1. Late Neogene Western Pacific Planktic Foraminiferal Biostratigraphy

Using our updated planktic foraminiferal occurrence data and biostratigraphic zonations from the Leg 90 sites in the southwest Pacific, we directly correlated the biozones developed for the northwest Pacific, western equatorial Pacific, and tropical ocean (Figure 2). We made minor adjustments to the southwest Pacific planktic foraminiferal biostratigraphic zonations as necessary due to updates in taxonomy, discontinuous ranges of species previously employed as datums, and the addition of zones utilized in the northwest Pacific. Our biostratigraphic framework highlights how the diachroneity of datums used to construct biozones affects first-order age interpretations and the need for regionally calibrated da-

tums and biozones. We adopted the zone nomenclature as presented by Wade et al. [12], and refer the reader to this publication for a more detailed discussion of zone definitions.

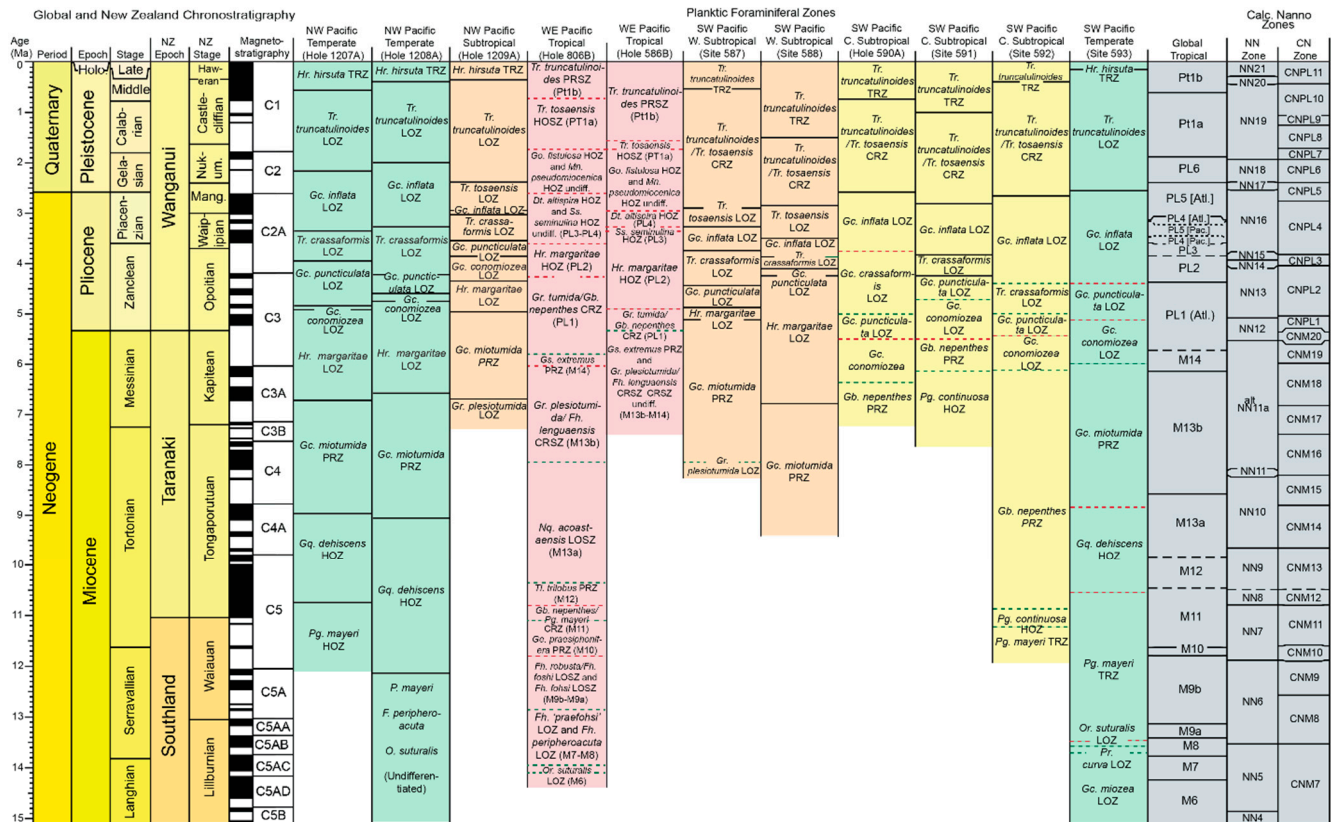


Figure 2. Global and New Zealand chronostratigraphy and magnetostratigraphy with major chrons and subchrons, plotted against the northwest, western equatorial, and southwest Pacific planktic foraminiferal biozones, and correlated with the global tropical planktic foraminiferal and calcareous nannofossil zones (in grey). Sites that utilize the tropical zonation (western equatorial Holes 806B and 586B) are in red, the warm subtropical (southwest Pacific Sites 587 and 588) and subtropical (northwest Pacific Hole 1209A) zonations are in orange, the cool subtropical (southwest Pacific Sites 590A, 591, and 592) zonations are in yellow, and the temperate (northwest Pacific Holes 1207A and 1208A, southwest Pacific Site 593) zonations are in green. Green dashed zone boundaries indicate a calcareous nannofossil or bolboform datum based on a species’ first occurrence, whereas red dashed zone boundaries indicate a datum based on a species’ last occurrence. Black solid zone boundaries indicate age constrained by magnetostratigraphy. Chronostratigraphy, tropical planktic foraminiferal, and calcareous nannofossil zones are from the GTS 2020 [68].

3.1.1. Tropical Holes 806B and 586B

At tropical holes 806B and 586B, we applied the tropical planktic foraminiferal zonation [13]; however, not all Late Neogene zones could be identified. Within the Pliocene at Hole 806B, the *Globigerinoidesella fistulosa* highest occurrence zone (HOZ; Indo-Pacific PL6) and *Menardella pseudomiocenica* HOZ (PL5) are undifferentiated, as the last occurrence of *Mn. pseudomiocenica* (which defines the base of zone PL6 and the top of PL5) occurs at 4.80 Ma—well below the last occurrence of *Dentoglobigerina altispira* (which defines the base of zone PL5). In other words, the last occurrences of *Mn. pseudomiocenica* and *Dt. altispira* are switched relative to their order of occurrence in the study of King et al. [13]. The *Sphaeroidinellopsis seminulina* HOZ (PL3) is undifferentiated from the *Dt. altispira* HOZ (PL4), due to the last occurrence of *Hirsutella margaritae* (which defines the base of zone PL3) occurring stratigraphically and temporally above the last occurrence of *Ss. seminulina* (this datum defines the base of the *Dt. altispira* HOZ; PL4).

In the Miocene section of Hole 806B, the *Fohsella fohsi* lowest occurrence subzone (LOSZ; M9a) and *Fh. robusta/Fh. fohsi* concurrent range subzone (CRSZ; M9b) are undifferentiated, as not all morphospecies in the *Fohsella* lineage were differentiated in the planktic foraminiferal occurrence conducted by Chaisson and Leckie [43]. The bottom of the *Orbulina suturalis* lowest occurrence zone (LOZ; M6) is based on the first occurrence of the nominate taxon; however, the base of this species occurs above the anomalous base of *Or. universa* [43]. Thus, we defined the base of Zone M6 by the first occurrence of *Orbulina* spp.

Hole 586B is located close to Hole 806B in the western equatorial Pacific (Figure 1). In the Pliocene section of Hole 586B, the *Go. fistulosa* HOZ (Indo-Pacific zone PL6) and *Mn. pseudomiocenica* HOZ (PL5) were undifferentiated, as *Mn. pseudomiocenica* was not recognized [18]. In the Miocene sections of Hole 586B, the *Globigerinoides extremus* partial range zone (PRZ; M14) and *Globorotalia plesiotumida/Fohsella linguaensis* CRSZ (M13b) were undifferentiated, as *Fh. linguaensis* was not recognized.

3.1.2. Warm Subtropical Sites 587 and 588

Southwest Pacific Sites 587 and 588 are located in subtropical water masses, between the southern tropical divergence and the Tasman Front, at latitudes 21.2° S and 26.3° S, respectively (Figure 1). The warm subtropical zonation [18] was applied at these sites (Figure 2) with amendments made for the northwest Pacific [31], with all zones from both zonations identified except for the *Globoconella conomiozea* LOZ, as this species was absent (Site 587; Supplementary Table S3) or rare and sporadic (Site 588; Supplementary Table S4). Specifically, we were able to identify the late Miocene *Globoconella miotumida* partial range zone (PRZ) first defined for subtropical Hole 1209A in the northwest Pacific [31]. This new zone adds additional biostratigraphic age control to the Upper Miocene, as it subdivides the *Gr. plesiotumida* LOZ.

3.1.3. Cool Subtropical Sites 590, 591, and 592

Sites 590, 591, and 592 lie between 31° S and 37° S, just south of subtropical sites 587 and 588 in the Tasman Sea (Figure 1). The cool subtropical zonation scheme [14] was applied at these sites.

Originally, the biostratigraphic zonation scheme implemented at Hole 590A was the warm subtropical scheme [18]. However, we found that the cool subtropical zonation scheme works best at this site, for several reasons. The Late Miocene to Early Pliocene *Gc. miotumida* PRZ—first created for the subtropical northwest Pacific Hole 1209A [31]—could not be identified because *Globoquadrina dehiscens*, the last occurrence of which defines the base of the zone, was not recognized at Hole 590A. The absence of this species at the hole also made it problematic to employ the temperate zonation scheme [18], as the last occurrence of *Gq. dehiscens* is used for Late Miocene stratigraphic control. The first occurrence of *Gr. plesiotumida* is used to define the base of the Late Miocene *Gr. plesiotumida* LOZ in the warm subtropical scheme. However, at Hole 590A, this species is highly discontinuous throughout its range, invalidating it as a useful and reliable datum at such latitudes in the southwest Pacific. For all of the aforementioned reasons, we chose to employ the cool subtropical scheme first developed for southwest Pacific Leg 21 Site 207 [14], without the modifications that were later made for the Late Miocene for Leg 90 sites [18]. We chose not to use the modified cool subtropical scheme of Jenkins and Srinivasan [18], as their Late Miocene zone ‘*Gc. sphericomiozea*’ is named after a species that has been synonymized with *Globoconella puncticulata* [42] for Hole 590A.

At Sites 591 and 592, the unmodified cool subtropical zones of Kennett [14] developed for Leg 21 Site 207 were applied, with all zones identified (Figure 2).

3.1.4. Temperate Site 593

Site 593 is the highest southern latitude site in this study, and is located in the central Tasman Sea in the temperate (transitional) province (subtropical frontal zone) at 40° S and 167° E (Table 1). The temperate southwest Pacific zonation of Jenkins and Srinivasan [18]

was employed at this site, with modifications. The scheme differs from the temperate northwest Pacific zonation, which has additional biostratigraphic markers [31].

We applied the zones of Jenkins and Srinivasan [18] for the youngest sections at Site 593, with modifications. We added the *Hr. hirsuta* total range zone (TRZ) at Site 593—a zone that is also defined at northwest Pacific Sites 1207A, 1208A, and 1209A (Figure 2; [31]). We also implemented Jenkins and Srinivasan's [18] *Tr. truncatulinoides* LOZ, *Gc. inflata* LOZ, *Gc. puncticulata* LOZ, *Gc. conomiozea* LOZ, and *Gc. miotumida* PRZ. The dextral *Tr. truncatulinoides* coiling zone is entirely within the *Tr. truncatulinoides* TRZ, ranging from the base of the *Tr. truncatulinoides* TRZ to 0.284 Ma (Supplementary Table S8). For the *Gc. puncticulata* LOZ, we used the base of *Gc. puncticulata* s.s. rather than the first appearance of *Gc. puncticulata* s.l., in accordance with the population concept adapted by the New Zealand Geological Timescale [77], and because the earliest morphospecies are rare. Below the *Gc. miotumida* PRZ, the *Gq. dehiscens* highest occurrence zone is defined by the last occurrence of *Pg. mayeri* at its base, and the last occurrence of the nominate taxon at the top of the zone.

We defined the *Pg. mayeri* TRZ as being below the *Gq. dehiscens* HOZ. However, it should be noted that in New Zealand, the first and last occurrences of *Pg. mayeri* are not used as regional biostratigraphic markers, as this species becomes rare and sporadic at the beginning and end of its local range. Instead, New Zealand biostratigraphers implement the highest common occurrence and lowest common occurrence for this taxon. We retained the use of the last occurrence of *Pg. mayeri* in this scheme, as the focus of this study is on diachroneity, and how the first and last occurrences of key species used to define datums can lead to diachronous zones in the mid-latitudes.

Below the *Pg. mayeri* TRZ lies the newly defined *Orbulina suturalis* lowest occurrence zone, *Praeorbulina curva* LOZ, *Gc. miozea* LOZ, and *Gr. praescitula* LOZ. The coiling shift in *Gc. miozea* (20% dextral) at 395.21 mbsf is a proxy for the base of the *Pr. curva* LOZ. The base of the Site 593 section used in this study (45X-7, 32 cm to 45-CC, 18.044–18.049 mbsf) remains unzoned (Supplementary Table S8).

3.2. Western Pacific Plankton Biogeographic Patterns

When the first and last occurrences of planktic foraminiferal species used as primary and secondary datums in tropical and mid-latitude zonations are plotted through time and across space, striking biogeographic patterns emerge (Table 2). Diachroneity had been noted previously for southwest Pacific planktic foraminiferal species (e.g., [26]), but such patterns become even more apparent when compared to northwest Pacific evolutionary events. For those interested in a more detailed discussion of species-specific biogeographic patterns, we summarize such patterns in the following Sections 3.2.1–3.2.16.

3.2.1. *Globigerinella* Biogeographic Patterns

Planktic foraminifera species belonging to the genus *Globigerinella* include thermocline and symbiont-bearing mixed-layer dwellers that lived within subtropical-to-tropical water masses (e.g., [53,78]). Specifically, the first occurrence of *Globigerinella calida* is a secondary marker used in the tropical zonation [12,13] to subdivide the Late Pleistocene. The first appearance of *Ge. calida*, which was calibrated to the geomagnetic polarity timescale by Chaproniere et al. [79] from sediments drilled within the Lau Basin of the southwest Pacific Ocean, is highly diachronous across the western Pacific.

Table 2. Species and their evolution (base) and/or extinction (top) events with age error, as calibrated from magnetostratigraphy or calcareous microfossil biostratigraphy from the northwest Pacific (Holes 1207A, 1208A, and 1209A), the western equatorial Pacific (Holes 806B and 586B), and the southwest Pacific (Sites 587, 588, 590, 591, 592, and 593), and dates of datums from the global tropical planktic foraminiferal biozonation of King et al. [13] (tropical). All ages and age errors are reported in millions of years.

Species	Evolutionary Event	1207A Age	1208A Age	1209A Age	806B Age	586B Age	587 Age	588 Age	590 Age	591 Age	592 Age	593 Age	Tropical Age
<i>Globigerinella calida</i>	Base	3.870 ± 0.088	1.589 ± 0.018	3.139 ± 0.102	4.062 ± 0.072	1.369 ± 0.035	0.795 ± 0.041	1.801 ± 0.056	2.178 ± 0.253	2.509 ± 0.160	-	-	0.22
<i>Globigerinoides subquadratus</i>	Top	8.470 ± 0.213	8.443 ± 0.178	6.480 ± 0.043	11.056 ± 0.011	-	-	9.010 ± 0.041	-	-	11.963 ± 0.017	8.130 ± 0.165	11.57
<i>Globigerinoides extremus</i>	Top	2.093 ± 0.097	1.625 ± 0.018	1.583 ± 0.032	2.172 ± 0.092	1.921 ± 0.010	2.458 ± 0.018	2.671 ± 0.035	2.917 ± 0.155	2.825 ± 0.018	3.945 ± 0.140	2.662 ± 0.269	1.97
	Base	6.054 ± 0.101	5.777 ± 0.036	6.209 ± 0.008	8.438 ± 0.040	-	8.147 ± 0.103	8.342 ± 0.049	-	-	11.746 ± 0.079	3.170 ± 0.238	8.83
<i>Globigerinoides conglobatus</i>	Base	7.203 ± 0.009	6.561 ± 0.091	6.299 ± 0.048	5.953 ± 0.014	-	-	5.849 ± 0.161	7.042 ± 0.093	6.882 ± 0.143	0.397 ± 0.094	-	6.21
<i>Globigerinoides obliquus</i>	Top	0.293 ± 0.011	1.668 ± 0.024	1.328 ± 0.033	1.821 ± 0.064	2.978 ± 0.051	3.964 ± 0.118	3.891 ± 0.008	6.238 ± 0.030	-	-	-	1.3
<i>Globigerinoidesella fistulosa</i>	Top	-	-	-	1.736 ± 0.019	1.736 ± 0.052	2.093 ± 0.134	1.632 ± 0.113	1.765 ± 0.161	-	-	-	1.88
	Base	-	-	-	2.801 ± 0.086	3.740 ± 0.354	3.266 ± 0.091	3.866 ± 0.016	2.917 ± 0.155	-	-	-	3.33
<i>Pulleniatina primalis</i>	Top	0.900 ± 0.001	1.906 ± 0	1.583 ± 0.032	2.042 ± 0.036	1.866 ± 0.007	3.266 ± 0.091	3.515 ± 0.056	3.577 ± 0.056	3.596 ± 0.072	5.177 ± 0.024	-	3.66
	Base	5.095 ± 0.297	2.335 ± 0.023	1.678 ± 0.160	6.587 ± 0.015	6.998 ± 0.040	7.138 ± 0.023	6.154 ± 0.145	5.547 ± 0.015	5.680 ± 0.124	5.223 ± 0.022	-	6.57
<i>Globoquadrina dehiscens</i>	Top	8.972 ± 0.791	9.053 ± 0.097	6.747 ± 0.149	5.686 ± 0.040	5.345 ± 0.015	7.941 ± 0.103	7.964 ± 0.285	-	6.882 ± 0.143	9.557 ± 0.184	8.861 ± 0.015	5.91
<i>Sphaeroidinella dehiscens</i>	Base	3.732 ± 0.126	3.490 ± 0.022	3.718 ± 0.181	4.585 ± 0.400	4.904 ± 0.013	3.964 ± 0.118	3.745 ± 0.025	3.970 ± 0.081	3.515 ± 0.008	-	-	5.54
<i>Sphaeroidinellopsis kochi</i>	Top	4.471 ± 0.031	4.324 ± 0.024	3.058 ± 0.058	4.987 ± 0.072	-	-	-	-	-	-	-	4.49
<i>Sphaeroidinellopsis seminulina</i>	Top	3.487 ± 0.033	3.762 ± 0.028	2.913 ± 0.010	3.625 ± 0.032	3.270 ± 0.029	2.899 ± 0.099	3.177 ± 0.208	3.243 ± 0.171	3.151 ± 0.187	3.463 ± 0.341	12.250 ± 0.256	3.59
<i>Globoconella conomiozea</i>	Top	3.434 ± 0.008	3.490 ± 0.022	3.281 ± 0.022	-	-	-	5.532 ± 0.156	5.475 ± 0.058	4.898 ± 0.021	5.277 ± 0.032	5.145 ± 0.105	-
	Base	4.915 ± 0.063	4.753 ± 0.033	4.341 ± 0.034	-	-	-	6.807 ± 0.012	6.371 ± 0.104	5.498 ± 0.058	7.198 ± 0.141	6.650 ± 0.343	-
<i>Globoconella puncticulata</i>	Base	4.821 ± 0.025	4.632 ± 0	3.862 ± 0.036	-	-	4.885 ± 0.094	4.245 ± 0.021	5.475 ± 0.058	4.705 ± 0.019	5.420 ± 0.048	5.730 ± 0.006	-
<i>Globoconella inflata</i>	Base	3.364 ± 0.016	3.289 ± 0.029	3.018 ± 0.007	0.978 ± 0.085	-	3.758 ± 0.087	3.832 ± 0.018	3.770 ± 0.015	3.827 ± 0.007	4.412 ± 0.092	4.395 ± 0.247	-
<i>Globoturborotalita nepenthes</i>	Top	4.498 ± 0.022	4.889 ± 0.012	4.025 ± 0.072	4.276 ± 0.021	4.904 ± 0.013	4.203 ± 0.121	3.891 ± 0.008	3.837 ± 0.052	4.215 ± 0.006	5.341 ± 0.032	5.043 ± 0.003	4.38
	Base	11.967 ± 0.096	12.371 ± 0.110	-	11.112 ± 0.043	-	-	-	-	-	10.506 ± 0.090	10.619 ± 0.133	11.67

Table 2. Cont.

Species	Evolutionary Event	1207A Age	1208A Age	1209A Age	806B Age	586B Age	587 Age	588 Age	590 Age	591 Age	592 Age	593 Age	Tropical Age
<i>Globoturbotalita decoraperta</i>	Top	3.163 ± 0.114	4.926 ± 0.025	3.535 ± 0.023	2.399 ± 0.007	1.892 ± 0.019	3.758 ± 0.087	1.476 ± 0.042	3.243 ± 0.171	1.002 ± 0.025	3.463 ± 0.341	1.929 ± 0.172	2.74
	Base	8.972 ± 0.791	9.178 ± 0.028	-	11.408 ± 0.047	-	-	-	-	-	11.564 ± 0.286	13.356 ± 0.181	11.51
<i>Globoturbotalita apertura</i>	Top	2.873 ± 0.035	2.517 ± 0.018	2.372 ± 0.281	1.821 ± 0.064	3.206 ± 0.035	-	2.671 ± 0.035	2.198 ± 0.155	-	-	-	1.64
	Base	10.74 ± 0.061	9.354 ± 0.148	-	11.056 ± 0.011	7.094 ± 0.056	-	4.689 ± 0.231	5.318 ± 0.100	-	-	-	11.24
<i>Globoturbotalita woodi</i>	Top	0.914 ± 0.027	0.427 ± 0.018	0.708 ± 0.035	2.172 ± 0.092	1.921 ± 0.010	2.568 ± 0.091	3.422 ± 0.037	3.681 ± 0.048	2.948 ± 0.016	2.461 ± 0.126	2.247 ± 0.146	2.3
<i>Neogloboquadrina acostaensis</i>	Top	0.914 ± 0.027	3.289 ± 0.029	0.451 ± 0.035	5.213 ± 0.039	4.904 ± 0.013	3.964 ± 0.118	4.193 ± 0.030	4.176 ± 0.124	4.368 ± 0.062	-	-	1.58
	Base	11.156 ± 0.064	7.205 ± 0.004	4.970 ± 0.041	10.355 ± 0.039	-	-	9.010 ± 0.041	6.525 ± 0.050	7.538 ± 0.087	-	-	9.81
<i>Fohsella lenguaensis</i>	Top	5.629 ± 0.614	11.469 ± 0.107	-	6.018 ± 0.050	-	-	-	-	5.971 ± 0.166	-	-	6.14
<i>Hirsutella margaritae</i>	Top	3.969 ± 0.022	4.009 ± 0.029	3.473 ± 0.041	3.075 ± 0.111	3.343 ± 0.029	3.758 ± 0.087	3.745 ± 0.025	2.918 ± 0.155	3.720 ± 0.053	3.945 ± 0.140	4.671 ± 0.029	3.83
	Base	6.707 ± 0.183	6.561 ± 0.091	4.970 ± 0.041	5.686 ± 0.040	5.082 ± 0.004	5.119 ± 0.029	6.779 ± 0.016	5.547 ± 0.015	5.680 ± 0.124	5.341 ± 0.032	4.793 ± 0.093	6.09
<i>Hirsutella cibaensis</i>	Top	3.732 ± 0.126	2.747 ± 0.018	3.862 ± 0.036	5.118 ± 0.032	-	0.431 ± 0.005	4.088 ± 0.013	3.970 ± 0.081	3.875 ± 0.007	5.341 ± 0.032	4.671 ± 0.029	4.61
	Base	7.773 ± 0.522	8.120 ± 0.017	4.970 ± 0.041	8.013 ± 0.039	-	-	8.256 ± 0.007	7.193 ± 0.058	6.550 ± 0.189	8.100 ± 0.186	8.972 ± 0.207	9.44
<i>Hirsutella hirsuta</i>	Base	1.123 ± 0.046	0.755 ± 0.027	0.673 ± 0.035	-	-	0.582 ± 0.026	-	-	-	2.216 ± 0.119	0.115 ± 0.007	0.45
<i>Truncorotalia crassaformis</i>	Base	3.969 ± 0.022	4.224 ± 0.021	3.535 ± 0.023	3.675 ± 0.17	3.740 ± 0.354	4.440 ± 0.115	5.148 ± 0.228	4.982 ± 0.071	4.239 ± 0.018	5.003 ± 0.028	4.671 ± 0.029	4.3
<i>Truncorotalia tosaensis</i>	Top	0.293 ± 0.011	0.586 ± 0.032	0.417 ± 0.035	0.735 ± 0.084	1.539 ± 0.035	0.530 ± 0.026	1.476 ± 0.042	0.736 ± 0.249	1.002 ± 0.025	0.397 ± 0.094	-	0.61
	Base	2.150 ± 0.018	3.328 ± 0.009	2.947 ± 0.019	3.075 ± 0.111	3.270 ± 0.029	3.266 ± 0.091	3.515 ± 0.056	3.578 ± 0.056	3.935 ± 0.052	2.663 ± 0.076	-	3.35
<i>Truncorotalia truncatulinoides</i>	Base	2.150 ± 0.018	1.994 ± 0.019	2.372 ± 0.281	2.332 ± 0.067	2.262 ± 0.002	2.899 ± 0.099	2.869 ± 0.100	2.597 ± 0.165	2.825 ± 0.018	2.663 ± 0.076	2.556 ± 0.004	1.92
<i>Globorotalia tumida</i>	Base	5.629 ± 0.614	5.383 ± 0.036	4.474 ± 0.101	5.806 ± 0.050	5.345 ± 0.015	5.257 ± 0.061	5.849 ± 0.161	4.852 ± 0.058	5.035 ± 0.116	5.177 ± 0.024	-	5.57
<i>Globorotalia plesiotumida</i>	Top	4.036 ± 0.022	3.025 ± 0.026	3.473 ± 0.041	4.370 ± 0.072	4.339 ± 0.030	4.885 ± 0.094	5.532 ± 0.156	3.578 ± 0.056	4.215 ± 0.006	-	-	3.72
	Base	8.972 ± 0.791	6.561 ± 0.091	7.151 ± 0.019	7.924 ± 0.050	-	-	7.583 ± 0.096	5.902 ± 0.100	-	-	-	8.77
<i>Menardella multicamerata</i>	Top	-	-	-	6.653 ± 0.050	1.921 ± 0.010	2.333 ± 0.107	2.273 ± 0.107	2.179 ± 0.253	2.509 ± 0.160	-	-	2.97
<i>Menardella limbata</i>	Top	2.595 ± 0.020	4.372 ± 0.024	2.082 ± 0.300	1.126 ± 0.114	-	-	-	-	-	-	-	2.37
<i>Dentoglobigerina altispira</i>	Top	3.348 ± 0.016	3.074 ± 0.022	2.928 ± 0.020	2.603 ± 0.111	2.978 ± 0.051	2.568 ± 0.091	2.869 ± 0.100	3.243 ± 0.171	3.151 ± 0.187	4.412 ± 0.092	7.002 ± 0.180	3.47

The first occurrence of *Ge. calida* occurs at 4.06 Ma in the mid-Pliocene of western equatorial Pacific Hole 806B (Table 2)—a much older datum than that recorded for the Lau Basin sites. In fact, based on our analysis, this is the first occurrence of *Ge. calida* in the western Pacific. From Hole 806B, the species then appears in the northwest Pacific at Holes 1207A and 1209A at 3.87 and 3.13 Ma, respectively, before appearing in the southwest Pacific at 2.50 Ma at Site 591 (Figure 3). The first appearance of this species can then be traced from south to north, from Sites 591 to 587, in the southwest Pacific. From this study, it is apparent that *Ge. calida* is likely not a reliable marker for the Late Pleistocene and, in the mid-latitude regions, could mark the Pliocene in the northwest Pacific, and the low-to-mid-Pleistocene in the southwest Pacific.

3.2.2. *Globigerinoides* Biogeographic Patterns

Planktic foraminifera species in the genus *Globigerinoides* are generally classified as photosymbiont-bearing, tropical-to-subtropical, mixed-layer dwellers. Because of their affinity for warmer waters, the first and last occurrences of *Globigerinoides* spp. are used extensively as primary and secondary markers in the tropical zonation [12,13]. The bases of *Globigerinoides extremus* and *Globigerinoides conglobatus* are used as secondary datums to constrain the age of Late Miocene deposits. The last occurrence of *Gs. extremus* is also used in the tropical zonation to constrain the age of Late Pliocene sections [12,13]. The last occurrences of *Globigerinoides obliquus* and *Globigerinoides subquadratus* are both secondary markers in the tropical zonations, with the former subdividing the Pleistocene, and the latter subdividing the Miocene. Due to their paucity at higher latitudes, *Globigerinoides* species are not employed in temperate zonations.

The last occurrence of *Gs. subquadratus* is used to subdivide the tropical Late Miocene biozone M11 (*Gb. nepenthes*/*Pg. mayeri* CRZ; [12]). This extinction event in the tropical zonation is reported at 11.57 Ma, but occurs at western tropical Pacific Hole 806B at 11.05 Ma—a difference of over 0.5 Myr (Table 2). In the mid-latitude regions of the northwest and southwest Pacific, this datum is highly diachronous, first going extinct at southwest Pacific Site 592 (11.96 Ma), and becoming extinct much later at northwest Pacific Hole 1209A (6.48 Ma; Figure 4).

Globigerinoides extremus first appears at southwest Pacific Site 592 at 11.74 Ma. It subsequently disperses into the tropics at 8.43 Ma (Table 2), and appears in the mid-latitudes of the northwest Pacific more than 2 Myr later, at 6.20 Ma (Figure 3). In contrast, the first appearance of *Gs. extremus* at Site 593—the highest southern latitude site in our dataset—occurs after its appearance in the northwest Pacific, at 3.17 Ma. The range expansion of *Gs. extremus* in the western Pacific occurs in a clear Southern-to-Northern Hemisphere pattern (with the exception of its very late first occurrence at Site 593), and its range contraction exhibits the same pattern (Figures 3 and 4). *Globigerinoides extremus* first disappears from the mid-latitudes of the southwest Pacific, then the tropics, and finally the northwest Pacific mid-latitudes, with its latest last occurrence at Hole 1209A at 1.58 Ma (Figure 4).

Globigerinoides conglobatus first appears in the northwest Pacific at Hole 1207A at 7.20 Ma, and then in the southwest Pacific at Site 590 at 7.04 Ma (Table 2). This pattern indicates that *Gs. conglobatus* evolved first in the mid-latitudes of the northwest Pacific, and then relatively quickly (within 160 kyr) dispersed into and established a notable population in the southwest Pacific (Figure 3). The majority of the lowest occurrence dates for *Gs. conglobatus* all occur within the Messinian Stage, making this secondary datum reliable from the tropics to the mid-latitudes to constrain Late Miocene deposits. The exception to this is at Site 592, where the species first appears much later at 0.39 Ma.

In the western Pacific, *Gs. obliquus* first disappears from the mid-latitudes in the southwest Pacific at 6.23 Ma, with a pattern of extirpation from this region of the Pacific to the northwest Pacific mid-latitudes (Figure 4). From the tropics to Hole 1208A, the last appearance of this species is relatively stable, with a difference in events at each hole and

as recorded in the tropical zonation [12,13] of 0.52 Myr. *Globigerinoides obliquus* has its latest extirpation event in the northwest Pacific at Hole 1207A at 0.29 Ma.

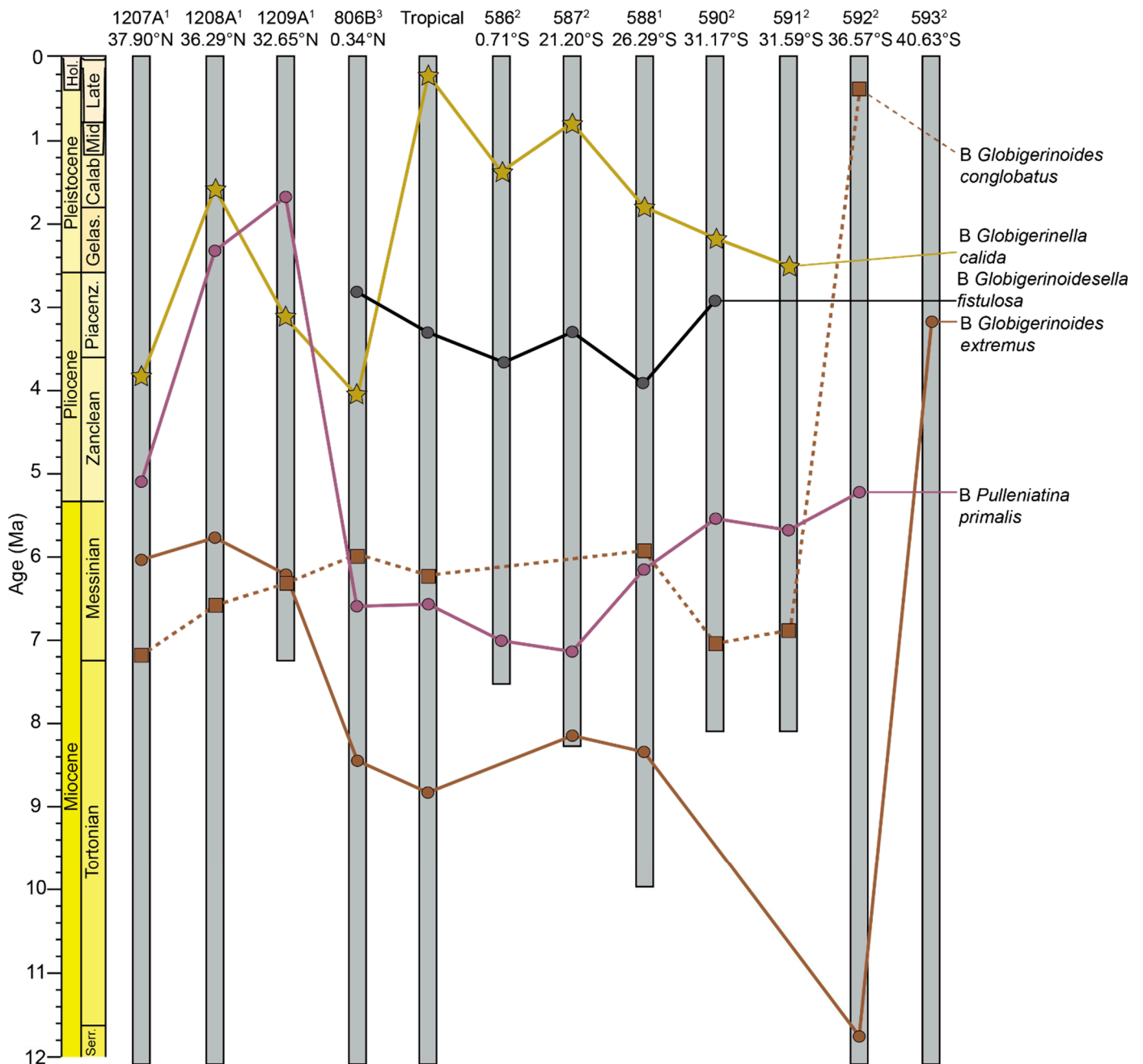


Figure 3. First occurrences of species used as primary and secondary datums in tropical-to-mid-latitude biostratigraphic zonations belonging to the genera *Globigerinoides*, *Globigerinella*, *Globigerinoidesella*, and *Pulleniatina*. Sites are ranked 1–3, as denoted by the superscript number beside each site number. A ranking of 1 indicates that the sites’ age model is based solely on magnetostratigraphy, a ranking of 2 indicates that the sites’ age model is a mix of magnetostratigraphy and biostratigraphy, and a ranking of 3 indicates that the sites’ age model is based solely on biostratigraphy (Supplementary Table S1).

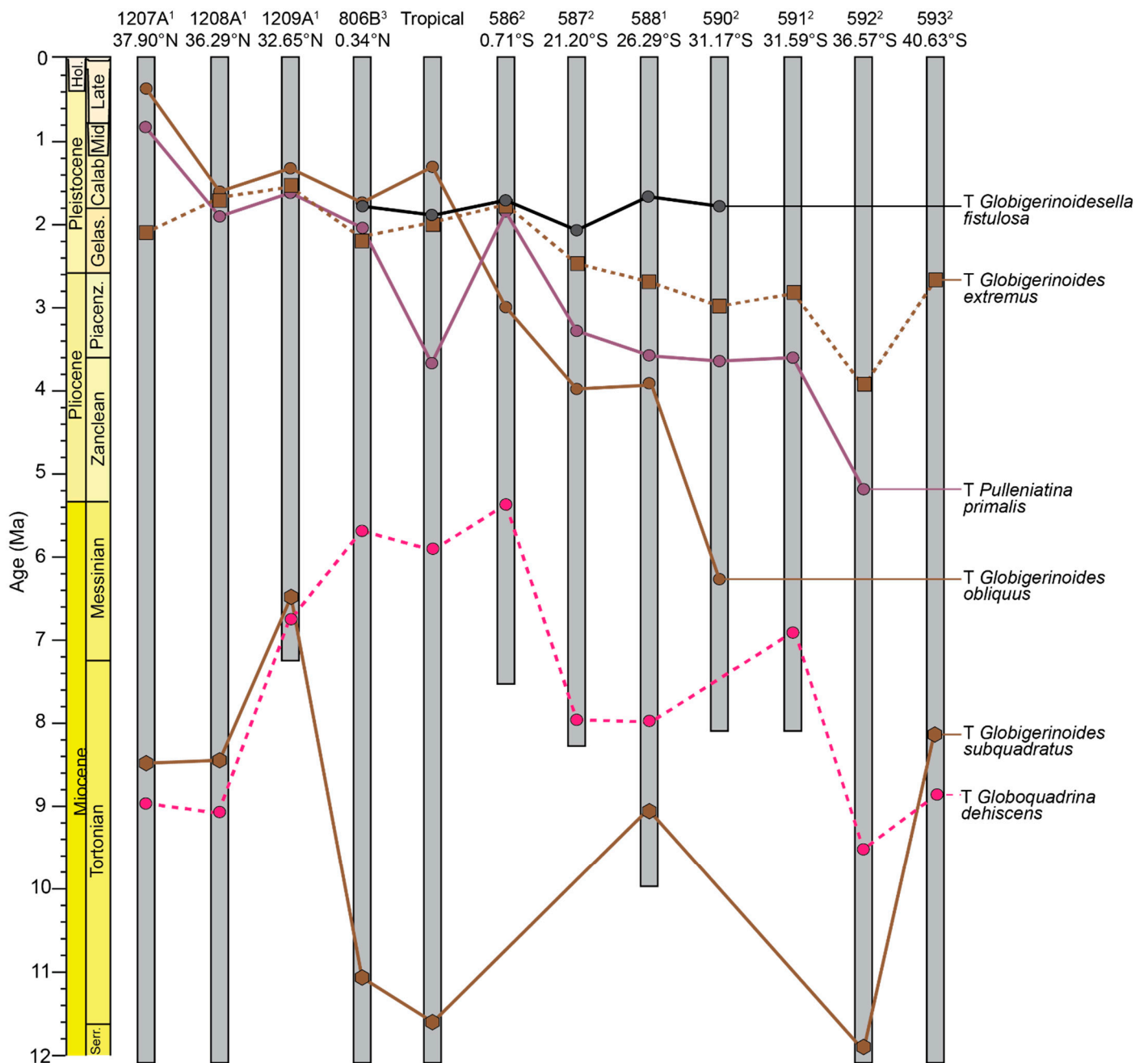


Figure 4. Last occurrences of species used as primary and secondary datums in tropical-to-mid-latitude biostratigraphic zonations belonging to the genera *Globigerinoides*, *Globigerinoidesella*, *Pulleniatina*, and *Globoquadrina*. Sites are ranked 1–3, as denoted by the superscript number beside each site number. A ranking of 1 indicates that the sites’ age model is based solely on magnetostratigraphy, a ranking of 2 indicates that the sites’ age model is a mix of magnetostratigraphy and biostratigraphy, and a ranking of 3 indicates that the sites’ age model is based solely on biostratigraphy (Supplementary Table S1).

3.2.3. *Globigerinoidesella* Biogeographic Patterns

The only species in its genus, *Globigerinoidesella fistulosa* was a symbiont-bearing mixed-layer dweller common in the subtropics to tropics. The extinction event of this species marks the top of Zone PL6 (*Go. fistulosa* HOZ Indo-Pacific), and denotes the boundary between the Pliocene and Pleistocene [12,13]. Its first appearance is used as a secondary datum in the tropical zonations to subdivide the Upper Pliocene.

The first and last occurrences of *Go. fistulosa* in the western Pacific are confined to the tropics and subtropics of the southwest Pacific (Sites 806B to 590). This species first appears at subtropical Site 588, and generally disperses north towards the Equator (Figure 3). Its first appearances from the southwest Pacific to the tropics are relatively stable, with a total difference in first appearance dates of 1.07 Myr. The last appearance of *Go. fistulosa* is more stable, with a difference in last appearance dates of only 0.46 Myr (Figure 4). Refinement of the last occurrence of this species in the southwest Pacific, in which age errors at Sites 587, 588, and 590 exceed 100 kyr (Table 2), could reveal reduced diachroneity for the extinction event of *Go. fistulosa*.

3.2.4. *Pulleniatina* Biogeographic Patterns

The genus *Pulleniatina* is used extensively in the tropical zonation for the Neogene [12,13], based on *Pu. primalis*' evolutionary events, disappearances and reappearances, and coiling changes. Coiling changes in the genus have been quantified for the western equatorial Pacific and eastern equatorial Indian Ocean, further highlighting the utility of coiling changes in these regions as tools for correlation [43,80]. Here, we focus on *Pulleniatina primalis*, as this species was identified at most sites in our study. The first occurrence of *Pu. primalis* is a secondary marker used to subdivide the tropical biozone M13b (*Gr. plesiotumida*/*Fh. linguaensis* CRSZ; [13]). The last occurrence of the species is used as a secondary marker to subdivide biozone PL4 (*Dt. altispira* HOZ) in the Late Pliocene [13]. The species was a thermocline-dweller in tropical-to-warm-subtropical water masses.

The tropical first appearance dates for *Pu. primalis* are very stable (Hole 806B and age recorded in [13]), but diachroneity is apparent in the subtropics and mid-latitude regions of the northwest and southwest Pacific. This species first appears in the western Pacific at Site 587, and then disperses to Site 586, before moving to the equatorial region (Figure 3). The species exhibits a more gradual dispersal from low to high latitudes in the Southern Hemisphere, but appears latest in the northwest Pacific (Figure 3). In the northwest Pacific, *Pu. primalis* first appears at Hole 1207A at 5.09 Ma—the site located on the northern edge of the Kuroshio Current Extension—before dispersing into nearby Holes 1208A and 1209A, at 2.33 Ma and 1.67 Ma, respectively (Table 2).

The last appearance dates for *Pu. primalis* exhibit a range contraction in the western Pacific from the southwest to the northwest (Figure 4), with the species going extinct first at Site 592 at 5.17 Ma, and last at Hole 1207A at 0.90 Ma—a difference of 4.27 Myr (Table 2). In the tropics of the western Pacific, at Holes 806B and 586B, *Pu. primalis* has extirpation dates of 2.04 Ma and 1.86 Ma, respectively—a difference of 0.18 Ma. However, the extinction date for this species reported by King et al. [13] is 3.66 Ma. Thus, our study indicates that the last occurrences for *Pu. primalis* in the equatorial western Pacific are vastly different from its last occurrence dates as recorded from sediments in the eastern equatorial Pacific and Atlantic [13,81].

3.2.5. *Globoquadrina* Biogeographic Patterns

Globoquadrina dehiscens was a thermocline-dwelling species, and is widely distributed from the tropics to higher latitudes. Its first appearance date is a primary marker datum in the tropical zonation [12,13], and denotes the base of biozone M1b (*Gq. dehiscens*/*Pg. kugleri* CRSZ) in the Early Miocene. Similarly, this datum was found to denote the Early Miocene in land-based sections of New Zealand [82]. Its last appearance is a secondary datum used to subdivide the earliest Pliocene zone PL1 (*Gr. tumida*/*Gb. nepenthes* CRZ), and approximates the top of the Miocene in the tropical zonation. The first occurrence of this species is also used in the temperate and subtropical planktic foraminiferal biozones for the northwest Pacific [31]. The last occurrence of *Gq. dehiscens* is utilized in the warm subtropical and temperate zonations for southwest Pacific Sites 587 and 593, respectively.

The last occurrences for *Gq. dehiscens* across the western Pacific are highly diachronous (Figure 4). This species first goes extinct at southwest Pacific Site 592 (9.55 Ma), and later at Hole 1208A in the northwest Pacific (9.05 Ma). *Globoquadrina dehiscens* experiences its

latest extirpation events at western equatorial Pacific Hole 806B (5.68 Ma), and then Hole 586B (5.34 Ma). In short, *Gq. dehiscens* experiences a range contraction from high to low latitudes, and persists longest in the tropics prior to its extinction. Further, Hodell and Kennett [25] found the last occurrence of *Gq. dehiscens* to occur in the Late Miocene in the South Atlantic, indicating large diachroneity between the Pacific and Atlantic. Thus, in the mid-latitude regions of the Pacific, the last occurrence of *Gq. dehiscens* is not a reliable species to approximate the Late Miocene.

3.2.6. *Sphaeroidinella* Biogeographic Patterns

The first occurrence of *Sphaeroidinella dehiscens*—a tropical-to-warm-subtropical species [17]—is used as a secondary marker in the tropical zonation to subdivide zone PL1 (*Gr. tumida*/*Gb. nepenthes* CRZ; [12]), which identifies the Early Pliocene. The first appearance of *Sphaeroidinella dehiscens* is closest to the Miocene/Pliocene boundary in the tropics only. However, the datum is diachronous away from the tropics in the western Pacific. The first appearance of *Sa. dehiscens*, as recorded at Site 925 in the western equatorial Atlantic at the Ceara Rise [83] and reported by King et al. ([13]; 5.54 Ma), occurs much earlier compared to its first appearances at western equatorial Pacific Holes 806B (4.58 Ma) and 586B (4.90 Ma; Table 2). Across the mid-latitudes of the western Pacific (Holes 1207A–1209A in the northwest; Sites 587–591 in the southwest), the first appearances of *Sa. dehiscens* in these regions are diachronous within 0.48 Myr in the Southern and Northern Hemispheres (Figure 5).

In the warm-subtropical-to-temperate regions of the western Pacific, the first appearance of *Sa. dehiscens* best approximates the Middle Pliocene, rather than the Miocene/Pliocene boundary as it does in the tropical Atlantic Ocean.

3.2.7. *Sphaeroidinellopsis* Biogeographic Patterns

The *Sphaeroidinellopsis* lineage first evolved in the Early Miocene, with subsequent evolution of new species through the Late Neogene [84,85]. The last occurrences of two species in this lineage—*Sphaeroidinellopsis kochi* and *Sphaeroidinellopsis seminulina*—are used in the global tropical zonation. The top of *Ss. kochi* is used as a secondary marker to subdivide the Early Pliocene biozone PL1 (*Gr. tumida*/*Gb. nepenthes* CRZ), whereas the last occurrence of *Ss. seminulina* is used as a primary marker to define the top of biozone PL4 (*Dt. altispira* HOZ) in the Pacific and Atlantic oceans [12,13].

Sphaeroidinellopsis kochi was not recorded in the southwest Pacific by Jenkins and Srinivasan [18], and may have been lumped in with *Ss. disjuncta*; however, the species was recorded in the western equatorial to mid-latitudes of the northwest Pacific (Figure 6). *Sphaeroidinellopsis kochi* experiences its last occurrence in this region at western equatorial Pacific Hole 806B at 4.98 Ma, and in the western equatorial Atlantic (Ceara Rise Site 925; [83]) at 4.49 Ma [13]—an age that differs by nearly half a million years (0.49 Myr; Table 2). In the mid-latitudes of the northwest Pacific, *Ss. kochi* experiences extirpation from the low-to-high latitudes, first going extinct at Hole 806B, and lastly at Hole 1209A (Figure 6). *Sphaeroidinellopsis kochi* persists in the subtropics of the northwest Pacific for approximately 1.9 Myr longer after it disappears from the western equatorial Pacific.

In the southwest Pacific, the last occurrence dates of *Ss. seminulina* from Sites 592–588 differ by 0.31 Myr (Figure 6; Table 2). At northwest Pacific Sites 1207A and 1208A, *Ss. seminulina* goes extinct within 0.28 Myr between the two sites. In the tropical western Pacific, this species goes extinct at 3.62 Ma—an age that differs by 0.57 Myr compared to the age reported by King et al. [13] for the Atlantic Ocean (3.05 Ma), and by 0.03 Myr compared to dates reported from Site 846 in the eastern equatorial Pacific (3.59 Ma). The diachroneity of *Ss. seminulina* between ocean basins is well known; thus, the different ages for this species between the Atlantic and eastern equatorial Pacific oceans are accounted for in the tropical zonations of Wade et al. [12] and King et al. [13]. Perhaps of most interest is the later last occurrence of *Ss. seminulina* that is apparent at subtropical Hole 1209A in the northwest Pacific and Site 587 in the southwest Pacific (Figure 6). At Site 587, *Ss. seminulina*

goes extinct at 2.89 Ma, whereas at Hole 1209A it goes extinct at 2.91 Ma; taking error at both sites into account, this datum is isochronous in the subtropics of each hemisphere.

3.2.8. *Globoconella* Biogeographic Patterns

The genus *Globoconella* is a prominent lineage in temperate mid-latitude waters [17], in most cases being among the dominant genera in the planktic foraminiferal assemblages from these areas of the world ocean (e.g., [39,42,86,87]). Species belonging to this genus first evolved in the Early Miocene [88], making this lineage valuable for subdividing Neogene strata of the mid-latitudes (e.g., [14,18,20,31,76,88–92]). Specifically, the first occurrences of *Globoconella* species are used to define mid-latitude planktic foraminiferal biozones. From our analysis, it is apparent that there can be high diachroneity among globoconellid datums between regions, but reduced diachroneity within regions. These species likely originated in the Southern Hemisphere.

Globoconella conomiozea is a short-ranging species that is used in the temperate zonation for the northwest Pacific [31], and in the cool subtropical, temperate, and subarctic zonations for the southwest Pacific [14,18]. Importantly, *Gc. conomiozea* is used in the southwest Pacific to subdivide and identify Upper Miocene strata, but in the northwest Pacific this species is used to delineate Lower Pliocene strata. *Globoconella conomiozea* first appears in the southwest Pacific at Site 592 at 7.19 Ma (Figure 5). It has later first occurrences at southwest Pacific Sites 588, 590, 592, and 593. This species is not recorded at tropical western Pacific Hole 806B. In the northwest Pacific, *Gc. conomiozea* has less diachronous first appearance dates compared to the southwest Pacific, ranging from 4.91 at Hole 1207A to 4.34 Ma at Hole 1209A—a difference of 0.57 Myr (Table 2). From these data, it is clear that after first appearing in the Southern Hemisphere, *Gc. conomiozea* took at least 0.58 Myr to disperse into the mid-latitudes of the Northern Hemisphere. The last occurrence dates of *Gc. conomiozea* are much less diachronous within their respective hemispheres compared to this species' overall first occurrence dates (Figure 6). *Globoconella conomiozea* first disappears from southwest Pacific Sites 588 and 590 around 5.5–5.4 Ma, experiencing a complete extirpation from the southwest Pacific by 4.89 Ma. This species persists in the northwest Pacific, disappearing from this region between 3.49 and 3.28 Ma.

Globoconella puncticulata exhibits a similar biogeographic pattern to that of *Gc. conomiozea* with respect to its first appearance dates; this species first appears in the southwest Pacific, before appearing in the northwest Pacific (Figure 5). Interestingly, the first appearance dates for *Gc. puncticulata* and *Gc. conomiozea* in the northwest Pacific converge more closely, indicating that there may be some abiotic or biotic factors at work that allowed for these globoconellid species to disperse into the northwest from the southwest Pacific during the Early Pliocene.

The first appearance of *Globoconella inflata*—the last species in the lineage to evolve—is used in the mid-latitude biozonations to subdivide the Pliocene (e.g., [14,18,31]). This species' datum in the southwest is quite stable; at Sites 592 and 593, the species first appears at 4.41 Ma and 4.39 Ma, respectively. Considering the age error at these sites, these dates are isochronous (Table 2). In the northwest Pacific, *Gc. inflata* first appears at Holes 1207A (3.36 Ma) and 1208A (3.28 Ma), before appearing at subtropical Hole 1209A (3.01 Ma). At western equatorial Pacific Hole 806B, *Gc. inflata* does not appear until much later, at 0.97 Ma (Figure 5), but with very rare occurrences [43].

3.2.9. *Globoturborotalita* Biogeographic Patterns

The *Globoturborotalita* lineage, which is mainly categorized as a tropical-to-warm-subtropical genus [17], has its roots in the Early Eocene [93], with several new species evolving in the Neogene. Specifically, the first and last occurrences of *Globoturborotalita nepenthes*, *Globoturborotalita decoraperta*, *Globoturborotalita apertura*, and *Globoturborotalita woodi* are used as primary and secondary datums in the tropical planktic foraminiferal zonation [12,13].

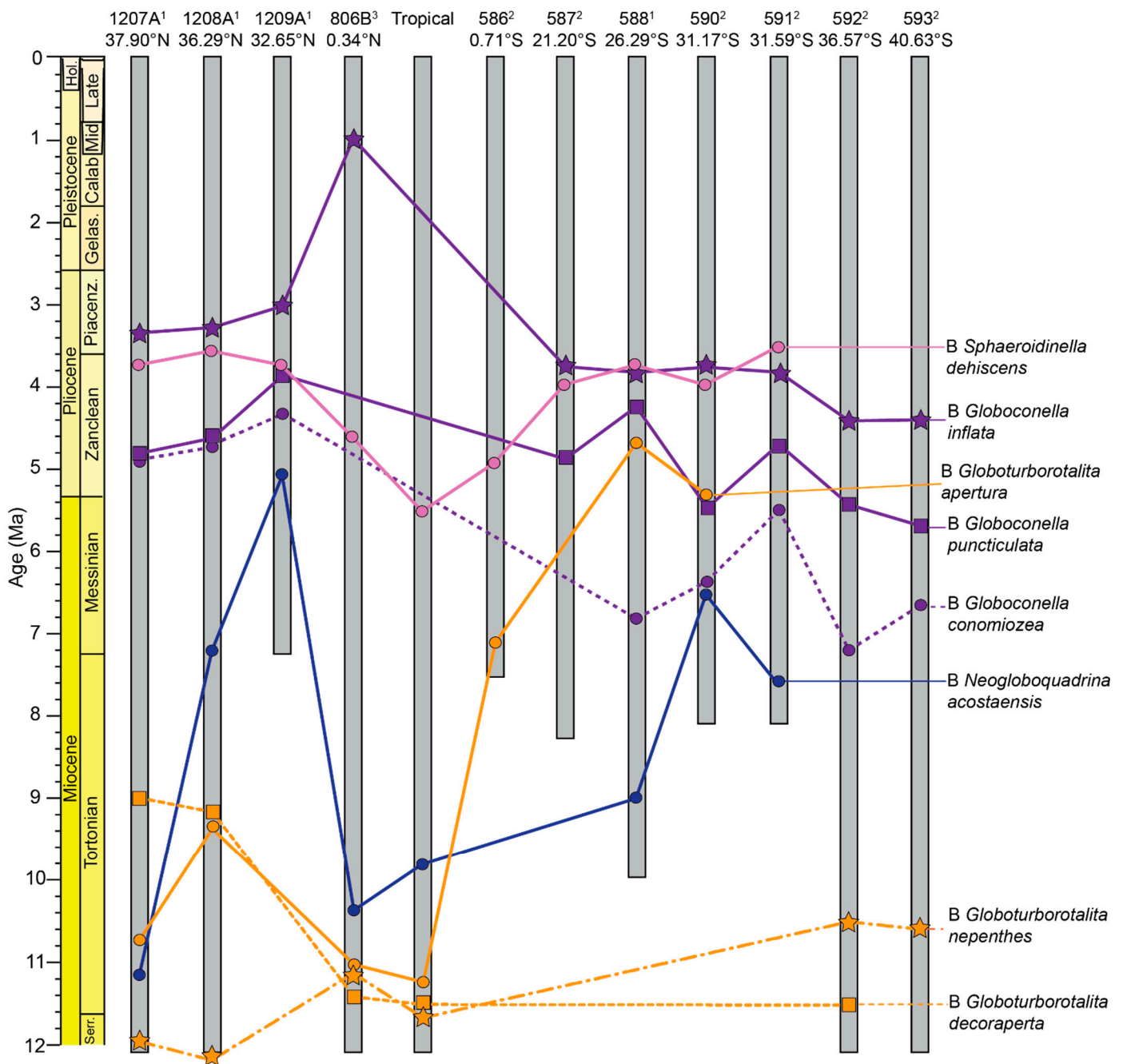


Figure 5. First occurrences of species used as primary and secondary datums in tropical-to-mid-latitude biostratigraphic zonations belonging to the genera *Sphaeroidinella*, *Globoconella*, *Globoturborotalita*, and *Neogloboquadrina*. Sites are ranked 1–3, as denoted by the superscript number beside each site number. A ranking of 1 indicates that the sites’ age model is based solely on magnetostratigraphy, a ranking of 2 indicates that the sites’ age model is a mix of magnetostratigraphy and biostratigraphy, and a ranking of 3 indicates that the sites’ age model is based solely on biostratigraphy (Supplementary Table S1).

The first occurrence of *Gb. nepenthes* defines the base of tropical biozone M11 (*Gb. nepenthes*/*Pg. mayeri* CRZ) of the Late Miocene, whereas the last occurrence of this species defines the top of the tropical zone PL1 (*Gr. tumida*/*Gb. nepenthes* CRZ) in the Early Pliocene [12,13]. Kennett [14] used the first occurrence of *Gb. nepenthes* to define the base of his Late Miocene *Paragloborotalia continua* zone. However, this zone was amended by Jenkins and Srinivasan [18] so that *Gb. nepenthes* was no longer implemented as a primary

marker, and the species was not used in the temperate and subtropical biozones of Lam and Leckie [31]. From our dataset, it is apparent that *Gb. nepenthes* first appeared in the northwest Pacific Hole 1208A (12.37 Ma), 0.76 Myr prior to its first appearance date as recorded in the tropical zonation (11.61 Ma; [13]). The first appearance of *Gb. nepenthes* in the southwest Pacific is only recorded at Sites 592 and 593, as the records from these two sites extend into the Middle Miocene. The first appearance dates of *Gb. nepenthes* in the southwest Pacific occur after its appearance in the northwest Pacific, but this observation may be the consequence of the lack of Late-to-Middle Miocene strata at Sites 586–591.

The last occurrences of *Gb. nepenthes* across the western Pacific indicate that this species had the shortest range at the highest latitudes (e.g., Site 592 in the southwest Pacific), but persisted longest in the mid-latitudes—specifically, at Site 590 in the southwest Pacific (3.83 Ma) and Hole 1209A in the northwest Pacific (4.02 Ma; Figure 6). The last appearance date for this species in the tropical zonation (4.38 Ma; [13]) is close to the last appearance date at western equatorial Pacific Hole 806B (4.27 Ma), indicating that this datum may be nearly isochronous between the tropical Atlantic and western Pacific oceans (Table 2).

The first appearance of *Gb. decoraperta* is used in the tropical biozonation as a secondary marker to subdivide the Late Miocene zone M11 (*Gb. nepenthes*/*Pg. mayeri* CRZ), whereas the last occurrence of this species is used as a secondary datum to subdivide biozone PL5 (*Mn. miocenica* HOZ) in the Atlantic Ocean [13]. Similar to its ancestor *Gb. nepenthes*, the base of *Gb. decoraperta* is recorded at two sites in the southwest Pacific (Figure 5). The earliest first appearance date for *Gb. decoraperta* is in this region, at Site 593 (13.35 Ma)—a much earlier first occurrence date than that recorded for this species in the tropical zonation (11.51; [13]; Table 2). The last appearance dates for *Gb. decoraperta* in our dataset are highly diachronous, even for sites in close proximity (Figure 6). From our dataset, it appears as though *Gb. decoraperta* goes extinct first in the northwest Pacific (Hole 1208A; 4.92 Ma), and persists longest in the southwest Pacific (Site 591; 1.00 Ma).

The first occurrence of *Gb. apertura* is used as a secondary marker in the tropical zonation to subdivide the Late Miocene zone M11 (*Gb. nepenthes*/*Pg. mayeri* CRZ), and the last occurrence is also a secondary marker used to subdivide the Early Pleistocene zone PT1a (*Tr. tosaensis* HOSZ; [12,13]). It is very apparent the earliest occurrence for this species is in the tropics (Figure 5)—specifically, its evolution in the western equatorial Atlantic at Site 925, at the Ceara Rise [83]. This species appears in the western equatorial Pacific only 0.18 Myr after its first appearance in the equatorial Atlantic, meaning that this datum exhibits lower diachroneity between these ocean basins at a time when the Central American Seaway was still open [94]. In the western Pacific, *Gb. apertura* appears in the northwest Pacific after its earliest appearances in the tropics, and then appears much later in the southwest Pacific mid-latitudes (4.68 Ma at Site 588; 5.31 at Site 590). The extirpation events across the western Pacific for *Gb. apertura* exhibit a clear pattern of extinction from the mid-latitudes to the tropics (Figure 6), where this species persists longest at western equatorial Pacific Hole 806B (1.82 Ma) and in the western equatorial Atlantic (1.64 Ma; [13,83]).

The last occurrence of *Globoturborotalita woodi* is used as a secondary marker to subdivide tropical Pleistocene zone PT1a (*Tr. tosaensis* HOSZ; [12,13]). The last occurrence of *Gb. woodi* at western tropical Pacific Hole 806B occurs at 2.17 Ma, just 0.13 Myr after its recorded extinction in the western equatorial Atlantic [13,83]. Thus, this datum is likely nearly isochronous between the Atlantic and the Pacific. The biogeographic pattern for the last occurrences of *Gb. woodi* across the western Pacific is very clear: this species disappears first from the southwest Pacific, then the tropics, and persists longest in the northwest Pacific—specifically at Hole 1208A (0.42 Ma), for 1.75 Myr longer compared to its last occurrence in the western equatorial Pacific (Figure 6).

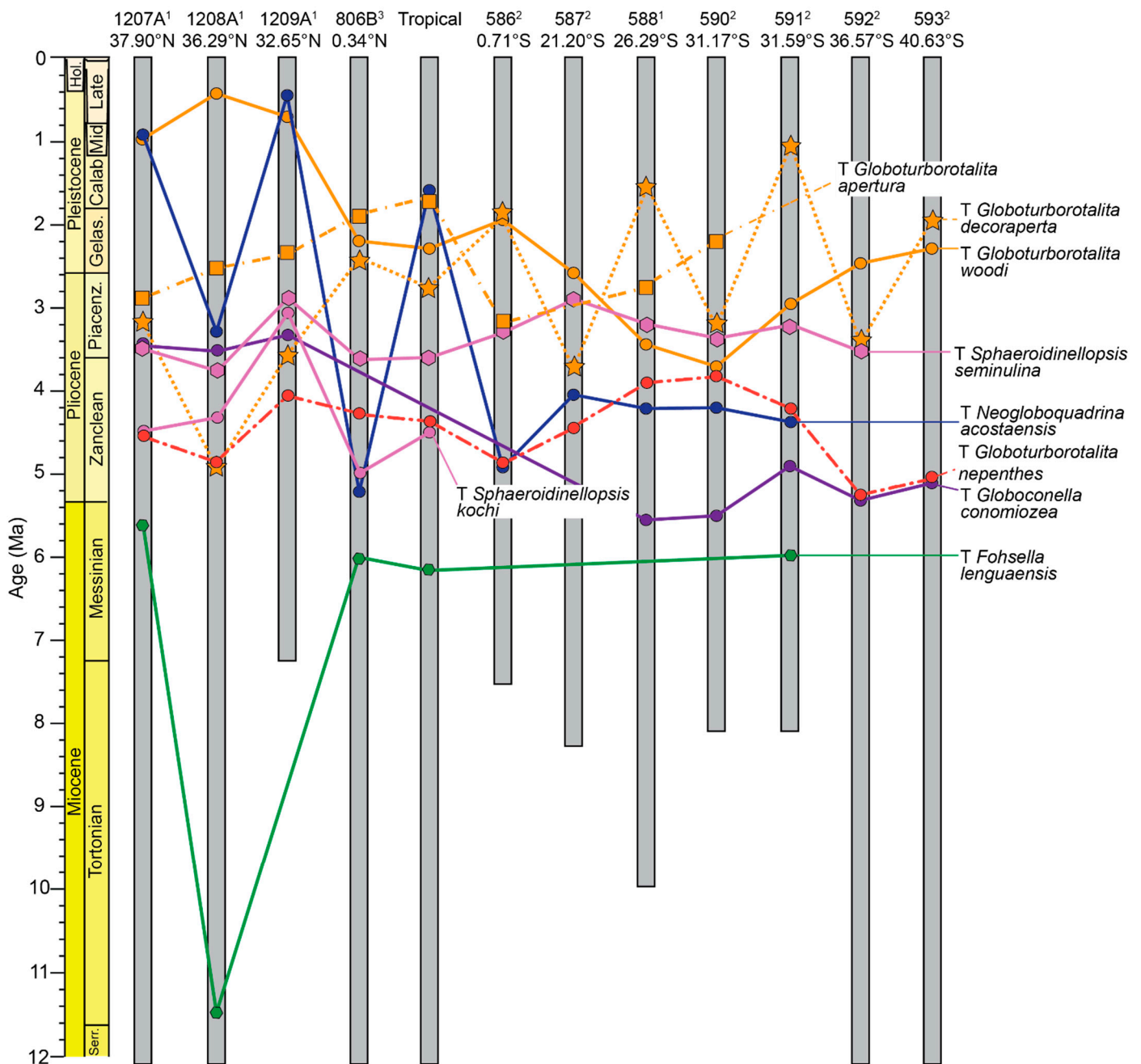


Figure 6. Last occurrences of species used as primary and secondary datums in tropical-to-mid-latitude biostratigraphic zonations belonging to the genera *Globoturbortalita*, *Sphaeroidinellopsis*, *Neogloboquadrina*, *Globoconella*, and *Fohsella*. Sites are ranked 1–3, as denoted by the superscript number beside each site number. A ranking of 1 indicates that the sites’ age model is based solely on magnetostratigraphy, a ranking of 2 indicates that the sites’ age model is a mix of magnetostratigraphy and biostratigraphy, and a ranking of 3 indicates that the sites’ age model is based solely on biostratigraphy (Supplementary Table S1).

3.2.10. *Neogloboquadrina* Biogeographic Patterns

The tropical-to-warm-subtropical [17] species *Neogloboquadrina acostaensis* is used extensively in the tropical zonation [12,13]. Its first appearance datum is a primary marker for the base of the Late Miocene zone M13 (*Nq. acostaensis* LOSZ), with coiling changes used as secondary datums to further subdivide the Miocene strata. The last occurrence of *Nq. acostaensis* further subdivides tropical Pleistocene zone PT1a (*Tr. tosaensis* HOSZ; [13]).

Across the western Pacific, the first and last occurrences of *Nq. acostaensis* are highly diachronous (Figures 5 and 6). The earliest first appearance date in our dataset for this species occurs at northwest Pacific Hole 1207A at 11.15 Ma, and then appears at tropical Hole 806B at 10.35 Ma—approximately 0.54 Myr earlier than its recorded age in the tropical zonation ([13]; Table 2) as recorded from the equatorial western Atlantic at Site 925, at the Ceara Rise [83]. Interestingly, the first occurrences of *Nq. acostaensis* in the mid-latitude regions, at northwest Pacific Hole 1209A and southwest Pacific Site 590, are much delayed compared to sites to the north and south of them (Figure 5). Compared to western equatorial Pacific Hole 806B, *Nq. acostaensis* appears 5.38 Myr later at Hole 1209A, and 3.83 Myr later at Site 590.

In the southwest Pacific, the last occurrences of *Nq. acostaensis* are much less diachronous compared to the northwest Pacific, where they are highly diachronous (Figure 6). *Neogloboquadrina acostaensis* first disappears from western equatorial Pacific Hole 806B (5.21 Ma), and then from Hole 586B (4.90 Ma). Both of these last occurrence dates are much earlier than the date of 1.58 Ma given in the tropical zonation [13] (Table 2). This species persists the longest in the northwest Pacific subtropics at Hole 1209A, where it experiences its extirpation event at 0.45 Ma.

3.2.11. *Fohsella* Biogeographic Patterns

Fohsella linguaensis was a thermocline-dwelling protist most prominent in tropical-to-warm-subtropical water masses [17]. The last occurrence of this species is a primary marker that denotes the top of Late Miocene biozone M13b (*Gr. plesiotumida*/*Fh. linguaensis* CRSZ). This species is not used as a marker species in the mid-latitude regions, as it occurs at few sites outside of the tropics.

In the western Pacific, *Fh. linguaensis* goes extinct first in the northwest Pacific, at Hole 1208A at 11.46 Ma (Figure 6). This species then goes extinct at western equatorial Pacific Hole 806B, and then in the southwest Pacific at Site 591, with a difference of only 0.04 Myr (Table 2). However, taking error into account, the extinction of *Fh. linguaensis* in the western tropical Pacific and southwest Pacific mid-latitudes is isochronous. Interestingly, this species persists the longest in the northwest Pacific at Hole 1207A—a site that is located close to Hole 1208A. The last recorded occurrence dates of this species in the tropical zonation (6.14 Ma; [13]) and at tropical western Pacific Hole 806B (6.01 Ma) differ by 0.13 Myr.

3.2.12. *Hirsutella* Biogeographic Patterns

The hirsutellids include species that are generally regarded as occurring in tropical-to-temperate water masses and inhabiting sub-thermocline depths [17,84]. Three of these species—*Hirsutella margaritae*, *Hirsutella cibaoensis*, and *Hirsutella hirsuta*—are used in both the global tropical zonation [12,13] and zonations for the western Pacific subtropics to mid-latitudes [14–16,18,31].

In the global tropical zonation [13], the first occurrence of *Hr. margaritae* is used as a secondary marker to subdivide the Late Miocene biozone M14 (*Gs. extremus* PRZ). In the northwest Pacific, this datum is used to define the base of the Late Miocene to Early Pliocene biozone *Hr. margaritae* HOZ in the temperate zonation, as well as the base of the Early Pliocene *Hr. margaritae* LOZ in the warm subtropical [18] and subtropical [31] zonations.

The first occurrence of *Hr. margaritae* in the western equatorial Pacific (Hole 806B; 5.68 Ma) is later than this species' first appearance date in the western equatorial Atlantic (Site 925; 6.09 Ma; [13,83]) by 0.41 Myr (Table 2). The earliest first appearance for this species in our dataset occurs in the southwest Pacific (Site 588) at 6.77 Ma; the second earliest first occurrence is at northwest Pacific Hole 1207A at 6.70 Ma. Taking age error into account, it is difficult to determine whether this species first evolved or appeared in the southwest or northwest Pacific, or entered the western Pacific mid-latitude regions at the same time in

the Late Miocene. From these sites, *Hr. margaritae* then dispersed towards the tropics and in the southwest Pacific, towards higher latitudes (Figure 7).

The last occurrence of *Hr. margaritae* is used as a primary marker to denote the base of Late Pliocene biozone PL3 (*Ss. seminulina* HOZ) in the global tropical zonation [12,13]. This datum is not used as a marker in the mid-latitude zonations, but in the northwest Pacific temperate scheme, the last occurrence of *Hr. margaritae* approximates the base of the *Gc. puncticulata* HOZ [31]. Across the western Pacific, the last occurrence of *Hr. margaritae*, like its first occurrence, is diachronous. The species goes extinct first at the highest latitude sites in our study (Figure 8), with a general range contraction towards the tropics. The species' latest last occurrences are in the western equatorial Pacific (Hole 806B; 3.07 Ma) and southwest Pacific (Site 590; 2.91 Ma). The last occurrence date for *Hr. margaritae* in the western equatorial Pacific (Hole 806B; 3.07 Ma) occurs 0.76 Myr later than its recorded extinction event in the tropical zonation (3.83 Ma; [13]), as recorded from the Ceara Rise, Site 925, in the western equatorial Atlantic.

The first occurrence of *Hirsutella cibaoensis* is used in the tropical zonation as a secondary marker within the Late Miocene biozone M13a (*Nq. acostaensis* LOZ; [12,13]). The first appearance of this species was recorded at all of our northwest Pacific sites, but only a few of the study sites in the southwest Pacific, due to hiatuses in the Miocene (Figure 7). Regardless, it is very apparent that this species exhibits high diachroneity across the western Pacific and between the tropics of the western Pacific and Atlantic. At Ceara Rise Site 925, *Hr. cibaoensis* is recorded as first appearing at 9.44 Ma [13,83]—a date that occurs 1.43 Myr earlier than its first appearance in the western equatorial Pacific (Hole 806B; 8.01 Ma). The earliest first occurrence of *Hr. cibaoensis* in our dataset is at Site 593 in the high latitudes of the southwest Pacific at 8.97 Ma. From here, this species then migrated to nearby southwest Pacific sites and appeared in the northwest Pacific at 8.12 Ma (Table 2). These data indicate that *Hr. cibaoensis* likely appeared at higher latitudes first—probably in the Southern Hemisphere—before dispersing to lower latitudes.

The last occurrence of *Hr. cibaoensis* is used as a secondary marker in the tropical zonation to denote the Early Pliocene biozone PL1 [13]. Like its first occurrence, the last occurrence of this species is highly diachronous in our dataset (Figure 8). It disappears at western equatorial Pacific Hole 806B approximately 0.5 Myr before it goes extinct in the mid-latitudes of the South Atlantic Ocean at 4.61 Ma [13,95]. The disappearance of *Hr. cibaoensis* in the South Atlantic occurs prior to its disappearance from the highest latitude southwest Pacific Site 593 (4.67 Ma). This finding suggests that even within the mid-latitude regions of the Pacific and Atlantic, there is diachroneity. The latest last occurrence for *Hr. cibaoensis* occurs at southwest Pacific Site 587 at 0.43 Ma; however, because other last occurrences for this species are confined to the Pliocene, we believe that this late last occurrence may be an identification error or reworking.

The first appearance of *Hirsutella hirsuta* is used in the tropical zonation scheme as a secondary marker to denote the Late Pleistocene zone PT1b (*Tr. truncatulinoides* PRSZ; [12,13]). In the temperate and subtropical zonation schemes for the northwest Pacific, this datum is used to define the base of the Pleistocene biozone *Hr. hirsuta* TRZ [31]. With our new data, we also identified and defined the *Hr. hirsuta* TRZ at southwest Pacific temperate Site 593 (Figure 2). Although this species is used in the tropical-to-subtropical zonation scheme, its occurrence is recorded from the southwest Atlantic Ocean [96]. The species' absence from tropical Pacific regions (Figure 7) may be an indication that this datum is not appropriate for tropical regions and, thus, its use in the tropical-to-subtropical zonation may require re-evaluation.

Hirsutella hirsuta was not recorded at southwest Pacific Sites 588–591 (Figure 7). However, its first occurrence dates at southwest Pacific Site 587 and in the southwest Atlantic, as recorded in King et al. [13], are moderately diachronous when taking age error into account. The first occurrence for this species as recorded by Jenkins and Srinivasan [18] at Site 592 is vastly different to the revised first occurrence date that we recorded for *Hr. hirsuta*, by a difference of 2.10 Myr (Table 2). Such a drastic difference in first appearance dates for this

species at Sites 592 and 593 may be due to differences in taxonomic concepts between the authors of this paper and Jenkins and Srinivasan [18].

Our data indicate that *Hr. hirsuta* may have evolved in the southwest Pacific Ocean prior to migrating to the southwest Atlantic (Table 2). This is supported by the early first appearance date for the species at southwest Pacific Site 592 (2.21 Ma); however, this is a tentative finding, as the first appearance of *Hr. hirsuta* at Site 593 occurs much later. This species first appears in the northwest Pacific at 1.12 Ma. The biogeographic pattern of dispersal for *Hr. hirsuta* from our study indicates that it first appeared in the higher latitudes, before migrating towards lower latitudes (Figure 7).

3.2.13. *Truncorotalia* Biogeographic Patterns

The truncorotaliid planktic foraminifera lineage evolved throughout the Late Miocene, and underwent a radiation in the Pliocene, with species still extant today. Generally, species within this group inhabit warm-subtropical-to-temperate water masses, and dwell within the sub-thermocline [17,84,97,98]. Three species are used in the tropical zonation and the mid-latitude zonations of the northwest and southwest Pacific Ocean in this study: *Truncorotalia crassaformis*, *Truncorotalia tosaensis*, and *Truncorotalia truncatulinoides*.

The first occurrence of *Truncorotalia crassaformis* is used as a secondary marker in the tropical zonation to further subdivide the Early Pliocene biozone PL2 (*Hr. margaritae* HOZ; [12,13]). In the northwest Pacific, the first occurrence of *Tr. crassaformis* is used to denote the Mid-to-Late Pliocene *Tr. crassaformis* HOZ biozone in the temperate zonation, as well as the *Tr. crassaformis* LOZ biozone in the subtropical zonation [31]. In the southwest Pacific in this paper, based on the findings of Kennett [14] and Jenkins and Srinivasan [18], the base of *Tr. crassaformis* is used in the warm and cool subtropical zonations to denote the base of the Pliocene *Tr. crassaformis* LOZ biozone (Figure 2, Supplementary Tables S3–S8).

The first occurrences of *Tr. crassaformis* across the western Pacific exhibit a clear pattern, indicating that the species evolved or entered in the southwest Pacific and subsequently migrated to the northwest Pacific (Figure 7). Specifically, the species occurs earliest at the highest latitude southwest Pacific sites (excluding Site 591), before then appearing in more subtropical-to-tropical regions of the Southern Hemisphere. There is, of course, diachroneity of the first occurrence of *Tr. crassaformis* between the western equatorial Pacific (Hole 806B; 3.67 Ma) and the western equatorial Atlantic (Site 925; 4.3 Ma; [13,83]), where the species occurs first in the equatorial Atlantic, 0.63 Myr prior to the western equatorial Pacific.

The lowest occurrence of *Truncorotalia tosaensis* is used in the tropical zonation as a secondary datum to denote the Late Pliocene biozone PL5 (*Mn. (pseudo)miocenica* HOZ; [12,13]). In the northwest Pacific, this datum event is used to define the base of the *Tr. tosaensis* LOZ in the subtropical zonation [31]. In the southwest Pacific, the base of *Tr. tosaensis* is used to denote the bottom of the *Tr. tosaensis* LOZ in the warm subtropical zonation [14]. In our dataset, the appearance of *Tr. tosaensis* in the western Pacific is diachronous, but like *Tr. crassaformis* it has a clear pattern of appearing first in the southwest Pacific, and later migrating to lower latitudes, before finally appearing in the northwest Pacific (Figure 7). Compared to the base of *Tr. tosaensis* at 3.35 Ma from King et al. [13], this species appears in the equatorial Pacific (Hole 806B, 3.07 Ma) 0.28 Myr later than its first appearance at other sites in the equatorial Pacific [99].

The last occurrence of *Tr. tosaensis* is a primary marker that defines the base of Late Pleistocene biozone PT1b (*Tr. truncatulinoides* PRSZ; [12,13]). In the southwest Pacific, this datum denotes the base of the *Tr. truncatulinoides* TRZ biozone in the warm and cool subtropical zonations ([14,18]; Figure 2). Our data indicate that the extirpation events of *Tr. tosaensis* are diachronous across the western Pacific (Figure 8), and the species likely first disappeared in this ocean basin in the Southern Hemisphere at Sites 588 (1.47 Ma) and 586 (1.53 Ma). It then exhibits a bipolar range contraction towards higher latitudes, and its latest last occurrences are recorded at northwest Pacific Hole 1207A (0.29) and southwest Pacific Site 592 (0.39 Ma). *Truncorotalia tosaensis* disappears first from the western equatorial

Pacific (Hole 806B; 0.73 Ma), and 0.12 Myr later from the eastern equatorial Pacific ([13,100]; 0.61 Ma). The differences in this datum event on the western and eastern side of the equatorial Pacific provide further evidence for diachroneity in equatorial regions.

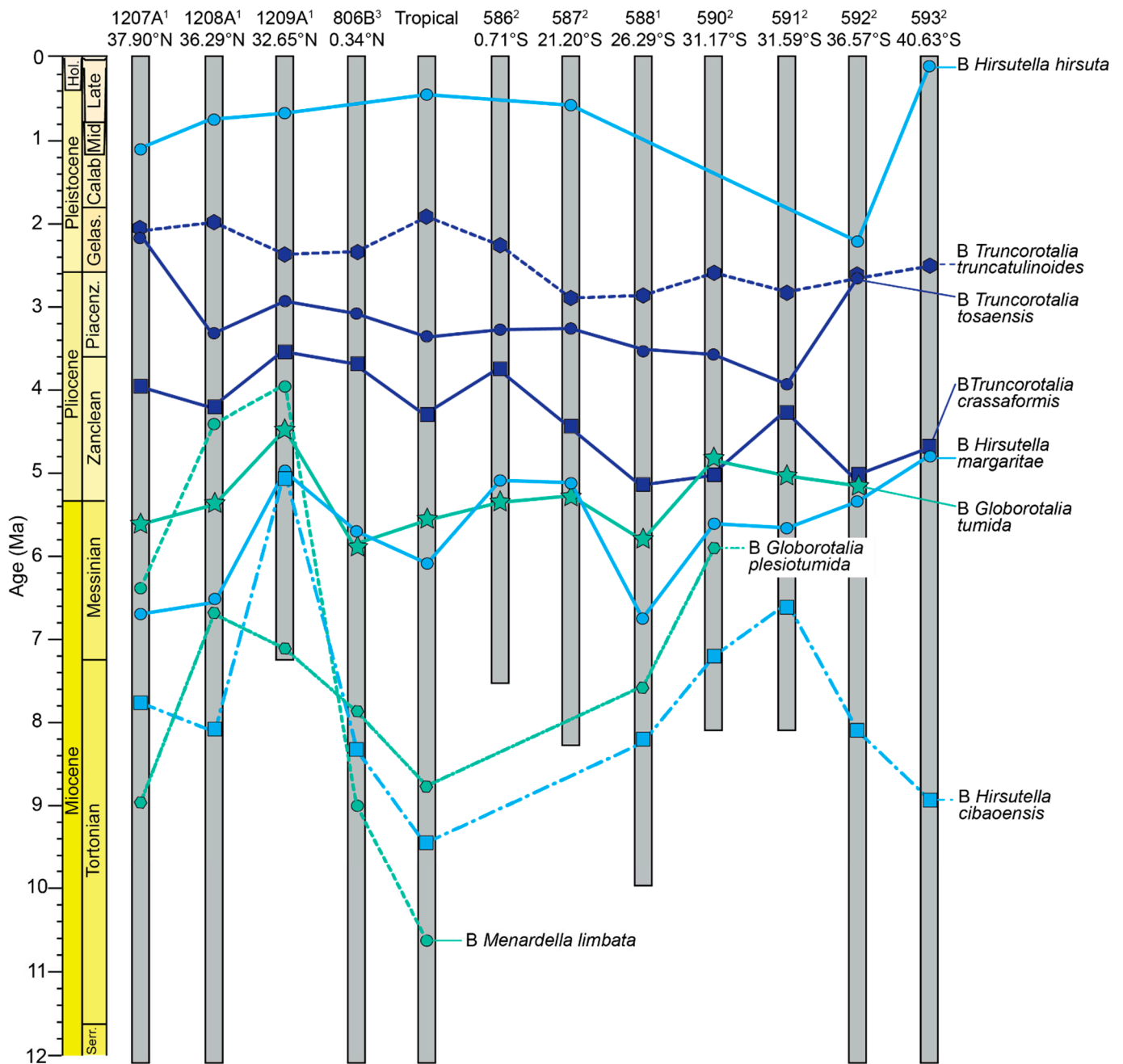


Figure 7. First occurrences of species used as primary and secondary datums in tropical-to-mid-latitude biostratigraphic zonations belonging to the genera *Truncorotalia*, *Hirsutella*, *Globorotalia*, and *Menardella*. Sites are ranked 1–3, as denoted by the superscript number beside each site number. A ranking of 1 indicates that the sites’ age model is based solely on magnetostratigraphy, a ranking of 2 indicates that the sites’ age model is a mix of magnetostratigraphy and biostratigraphy, and a ranking of 3 indicates that the sites’ age model is based solely on biostratigraphy (Supplementary Table S1).

The first appearance of *Tr. truncatulinoides* is a secondary marker in the global tropical zonation to further denote Late Pliocene biozone PL6 (*Go. fistulosa* HOZ; [12,13]). In the northwest Pacific, this datum event defines the base of the Pleistocene *Tr. truncatulinoides*

LOZ in the temperate and subtropical zonation schemes [31]. In the southwest Pacific, the first occurrence of *Tr. truncatulinoides* defines the base of the *Tr. truncatulinoides*/*Tr. tosaensis* CRZ in the warm and cool subtropical zonation scheme, along with the *Tr. truncatulinoides* LOZ in the temperate zonation scheme at Site 593 [14,18] (Figure 2).

Like *Tr. crassaformis* and *Tr. tosaensis*, the first appearance of *Tr. truncatulinoides* is diachronous in the western Pacific, with a clear pattern of earliest first occurrences in the southwest Pacific, with subsequent dispersal into the northwest Pacific (Figure 7). In the southwest Pacific mid-latitudes, the base of *Tr. truncatulinoides* exhibits diachroneity across such latitudes, with a difference of 0.34 Myr between the sites where it appears the earliest (Site 587; 2.89 Ma) and the latest (Site 593; 2.55 Ma). From the southwest Pacific, *Tr. truncatulinoides* disperses into the northwest Pacific by 2.37 Ma—approximately 0.52 Myr after its first appearance in the southwest Pacific (Table 2). *Truncorotalia truncatulinoides* first appears in the western equatorial Pacific, before its recorded first appearance in the western equatorial Atlantic (Site 925, Ceara Rise; [83]) at 1.92 Ma, as reported in King et al. [13] in the global tropical planktic foraminiferal zonation—a difference of 0.41 Myr.

3.2.14. *Globorotalia* Biogeographic Patterns

Globorotalia tumida is an extant thermocline-dwelling species common to tropical waters [17,101]. The first occurrence of this species is a primary marker in the tropical zonation [12,13] that marks the base of the Early Pliocene biozone PL1 (*Gr. tumida*/*Gb. nepenthes* CRZ). The diachronous first occurrence of *Gr. tumida* between the Pacific and Atlantic oceans is well known; thus, the base of zone PL1 differs between these ocean basins [12].

The first occurrence of *Gr. tumida* in the eastern equatorial Pacific (Site 846) is recorded at 5.57 Ma [13,100], and in the western equatorial Pacific (Hole 806B) at 5.80 Ma. This difference of 0.23 Myr further highlights the diachroneity of the first and last occurrences of planktic foraminiferal species between the eastern and western equatorial regions of the Pacific.

Across the western Pacific, the earliest first occurrence of *Gr. tumida* is recorded at southwest Pacific Site 588 and western equatorial Pacific Hole 806B (Figure 7). This species' latest first appearances are recorded in the subtropical mid-latitudes of each hemisphere—4.85 Ma at southwest Pacific Site 590, and northwest Pacific Hole 1209A at 4.47 Ma (Table 2).

Globorotalia plesiotumida is the ancestor of *Gr. tumida* [17,84,102], and was a thermocline-dwelling species that inhabited tropical-to-warm-subtropical waters. The first occurrence of this species is a primary marker that denotes the base of the Late Miocene biozone M13b (*Gr. plesiotumida*/*Fh. linguaensis* CRZ; [12,13]). The last occurrence of this species is used as a secondary marker in the global tropical zonation to subdivide the Late Pliocene biozone PL3 (*Ss. seminulina* HOZ; [12,13]).

The earliest occurrence of *Gr. plesiotumida* is recorded at two sites in the southwest Pacific, and is missing at some sites due to hiatuses (Figure 7). From the data we do have, however, the datum is highly diachronous across the western Pacific, and between the western equatorial Pacific and the tropical age presented by King et al. [13]. The first occurrence of *Gr. plesiotumida*, as reported in the tropical zonation, is recorded from western equatorial Atlantic Site 925, at the Ceara Rise [83], at 8.77 Ma. At western equatorial Pacific Hole 806B, the first occurrence of this species is recorded to occur at 7.92 Ma—a much later first occurrence compared to Site 925, by 0.84 Myr.

The first occurrence of *Gr. plesiotumida* in the northwest Pacific at Hole 1207A (8.97 Ma; Table 2) is closest to the date recorded at western equatorial Atlantic Site 925, and accounting for age error, these datums may be isochronous. The latest first occurrences for *Gr. plesiotumida* occur in the mid-latitude regions, at northwest Pacific Hole 1208A (6.56 Ma) and southwest Pacific Site 590 (5.90 Ma), where this datum best approximates the Late Miocene Messinian Stage.

The last occurrence of *Gr. plesiotumida* across the western Pacific is also diachronous within our Pliocene sections (Figure 8). Its last occurrence in the western equatorial

Pacific (Hole 806B; 4.37 Ma) and the date recorded in the tropical zonation (3.72 Ma; [13]) differ by 0.65 Myr. This indicates that *Gr. plesiotumida* disappeared from the equatorial Pacific before the equatorial Atlantic. In the southwest Pacific, the last occurrence of *Gr. plesiotumida* occurs first at Site 588, and then sequentially at Site 586 (Figure 8). From here, *Gr. plesiotumida* then goes extinct at northwest Pacific Hole 1207A, then Hole 1209A, and lastly Hole 1208A, which is located between the former two sites. It is here, at Hole 1208A, that the species persists the longest.

3.2.15. *Menardella* Biogeographic Patterns

Menardella multicamerata was a thermocline-dwelling species that was common in tropical-to-subtropical water masses [17,84]. The last occurrence of *Mn. multicamerata* is used as a secondary marker to further identify and subdivide the Late Pliocene zone PL5 (*Mn. (pseudo)miocenica* HOZ) in the global tropical planktic foraminiferal zonation [12,13].

In our dataset, the last occurrence of *Mn. multicamerata* is highly diachronous between the western equatorial Pacific and the western equatorial Atlantic; at Hole 806B (6.65 Ma) the datum occurs 3.68 Myr earlier than it does at Ceara Rise Site 925 (2.97 Ma; [83]), as reported by King et al. [13] (Figure 8). This is another indication that equatorial Atlantic and Pacific datum dates differ between these ocean basins, perhaps in part because the species is always rare. In the southwest Pacific mid-latitudes, the last occurrences of *Mn. multicamerata* from Sites 591–587 are diachronous by 0.33 Myr (Table 2; Figure 8). The less diachronous nature of this species in the southwest Pacific indicates that it may be a good datum to approximate the Early Pliocene Gelasian Stage (Figure 8). The last occurrences for *Mn. multicamerata* at western equatorial Holes 806B and 586B differ by 4.73 Myr, perhaps indicating that such large differences in this species' first occurrences in the western equatorial Pacific could be due to misidentification errors and/or unstable taxonomic concepts. This species was not recorded from Late Neogene sediments in the northwest Pacific Ocean [31].

The ancestor of *Mn. multicamerata*, *Menardella limbata*, was also a thermocline-dwelling species typical of tropical-to-warm-subtropical waters [17,84,102]. The last occurrence of *Mn. limbata* is used as a secondary marker in the tropical zonation [13] to denote Late Pliocene zone PL5 (*Mn. (pseudo)miocenica* HOZ). The extinction of *Mn. limbata* between the western equatorial Pacific (Hole 806B) and the western equatorial Atlantic (Site 925, Ceara Rise; [83]) is diachronous by 1.25 Myr, with this species first going extinct in the Atlantic [13].

Menardella limbata was not reported by Jenkins and Srinivasan [18] in the southwest Pacific; thus, we cannot assess its biogeographic patterns in the Southern Hemisphere. In the Northern Hemisphere, the last occurrence of this species is highly diachronous (Figure 8), perhaps due to being synonymized with *Mn. menardii* by some authors. The earliest last occurrence is at Hole 1208A (4.37 Ma), and occurs 1.78 Myr later at Hole 1207A (2.59 Ma), and approximately 0.51 Myr later still at Hole 1209A (2.08 Ma). In the Northern Hemisphere, this species seems to constrict its range towards the western equatorial Pacific through the Late Pliocene to the Middle Pleistocene (Figure 8).

3.2.16. *Dentoglobigerina* Biogeographic Patterns

Dentoglobigerina altispira was likely a mixed-layer species most common in tropical-to-warm-subtropical water masses [17,103]. The last occurrence of *Dt. altispira* is used as a primary datum to indicate the base of the Late Pliocene biozone PL5 (*Dt. altispira* HOZ). The timing of datums differs between the Atlantic and the Pacific [12,13].

The last occurrence of *Dt. altispira* between the western equatorial Pacific (Hole 806B) and Site 846 in the eastern equatorial Pacific [13] is quite diachronous. In the western equatorial Pacific, *Dt. altispira* goes extinct at 2.60 Ma, whereas its last occurrence in the eastern equatorial Pacific is recorded as occurring at 3.47 Ma [100]—a difference of 0.87 Myr. This datum event, like that of *Gr. tumida*, indicates that even in the equatorial regions of the

Pacific Ocean, the timing of planktic foraminifera’s first and last occurrences may differ significantly.

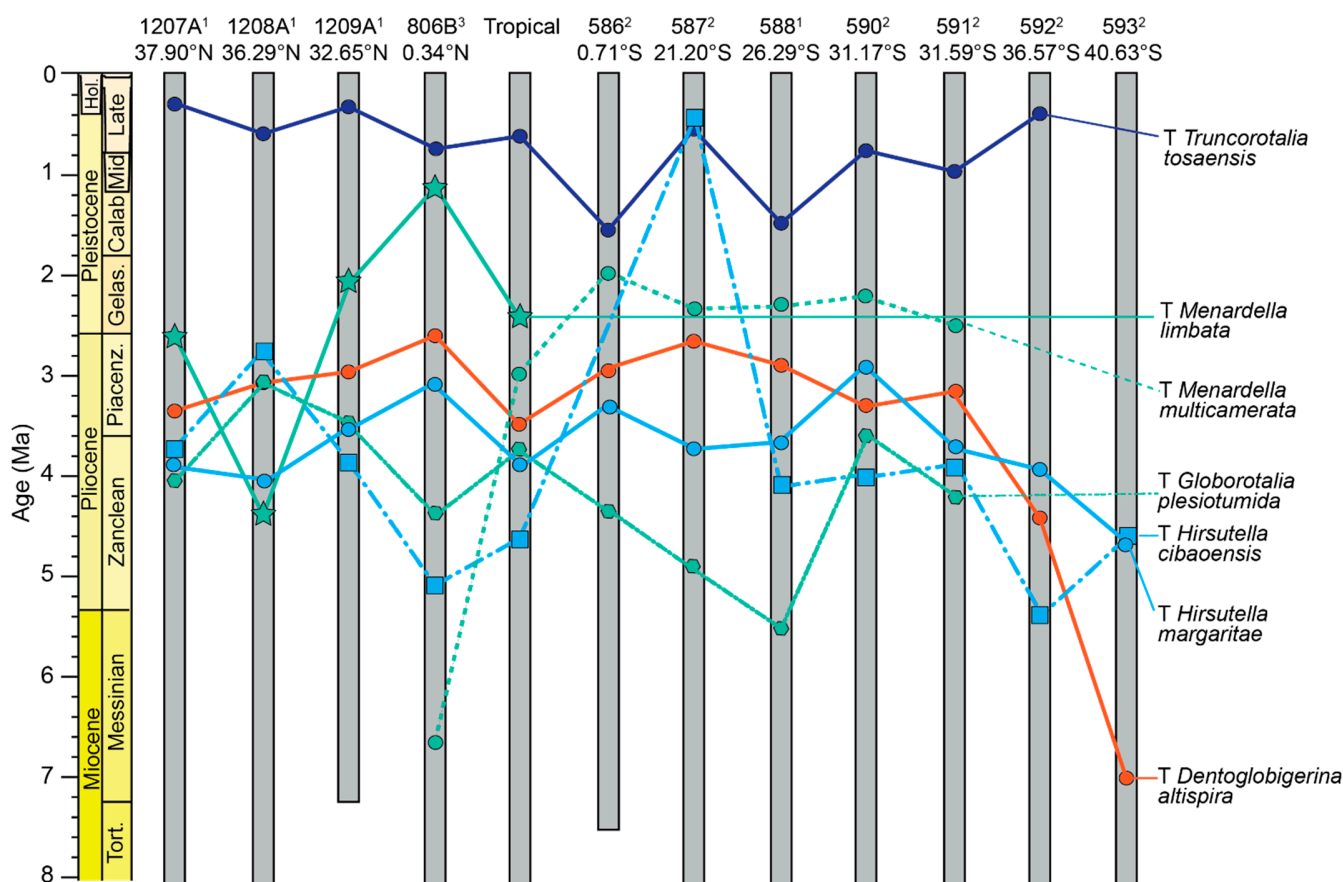


Figure 8. Last occurrences of species used as primary and secondary datums in tropical-to-mid-latitude biostratigraphic zonations belonging to the genera *Globorotalia*, *Hirsutella*, *Truncorotalia*, *Menardella*, and *Dentoglobigerina*. Sites are ranked 1–3, as denoted by the superscript number beside each site number. A ranking of 1 indicates that the sites’ age model is based solely on magnetostratigraphy, a ranking of 2 indicates that the sites’ age model is a mix of magnetostratigraphy and biostratigraphy, and a ranking of 3 indicates that the sites’ age model is based solely on biostratigraphy (Supplementary Table S1).

In the western Pacific, the last occurrence of *Dt. altispira* is slightly diachronous across the sites examined in this study, except in the higher latitudes of the southwest Pacific (Figure 8). The species first goes extinct at southwest Pacific Site 593—our highest latitude site—at 7.00 Ma. It is clear this species persists longest in the tropical-to-warm-subtropical regions (Holes 806B and 587B), where its last occurrence event approximates the boundary between the Pliocene and the Pleistocene. However, in the mid-latitude regions, the extinction of *Dt. altispira* is more indicative of the Late-Middle-to-Late Pliocene.

4. Discussion

4.1. Sources of Error

Several sources can contribute to the accuracy of dating that is used to assess the diachroneity of the first and last occurrences of planktic foraminifera. One major source of error that underlies this study and hinders more precise calculation of diachroneity among datums is the lack of robust age models that are either orbitally tuned or based on well-constrained magnetic reversal boundaries. In this study, none of the age models for the western Pacific sites are orbitally tuned, although some intervals have been tuned in prior studies (e.g., Hole 1208A [104]). Four of our sites (Sites 1207A, 1208A, 1209A, and 588) have

age models that are based solely on magnetostratigraphy, one (Hole 806B) is based solely on calcareous nannofossil biostratigraphy, four are based on a mix of magnetostratigraphy and nannofossil biostratigraphy, and two have age models constructed from magnetic reversal boundaries, calcareous nannofossils, and bolboform biostratigraphy (Supplementary Table S1). However, previous studies [26] have highlighted the diachroneity of calcareous nannofossil datums in the southwest Pacific using Leg 90 sites in the Neogene to Quaternary. For example, the last occurrence of *Reticulofenestra pseudoumbilicus* was found to be diachronous to a degree of 0.31 Myr across the southwest Pacific [26]. Such diachroneity among datums used to construct age models can significantly affect the measurement of synchrony among other fossil groups. It can also adversely affect the interpretation of binary magnetostratigraphic signals and orbital tuning if cycles are not aligned precisely.

At Sites 592 and 593 in the southwest Pacific Ocean, we applied the Miocene bolboform datums of Grützmacher [75] and Crundwell and Nelson [76], respectively. For Site 593, the bolboform datums were calibrated to the magnetostratigraphic age model of Site 1123 on the Chatham Rise, which has an almost complete Late Neogene and Quaternary magnetostratigraphic record [105]. Discrepancies exist between the bolboform and calcareous nannofossil datums recorded at Site 593 [74]. Specifically, the first (base) and last (top) occurrences of *Discoaster hamatus*, along with the last occurrence (top) of *Coccolithus miopelagicus*, were removed from the Site 593 age model, as they were in conflict with bolboform datums (Supplementary Table S1). Bolboforms hold great promise as biostratigraphic datums in the Miocene; however, the discrepancy between calcareous nannofossil and bolboform datums further highlights the need for a robust refinement of such datums in the southwest Pacific and across latitudes.

Another major source of error that may be contributing to diachroneity is the resolution of sampling at which biostratigraphic studies are conducted. For many of the DSDP Leg 90 sites, specifically, sampling resolution was lower compared to the sites in the northwest and western equatorial Pacific. The biostratigraphic analyses at Leg 90 Sites 586, 587, and 588 were conducted on core section and core-catcher samples. Assuming linear sedimentation rates, the sample resolution for these sites is 0.05 Myr (Site 586), 0.12 Myr (Site 587), and 0.13 Myr (Site 588). Biostratigraphic analyses at Sites 590–593 were conducted mainly on core-catcher samples, with minimal core section samples utilized originally by Jenkins and Srinivasan [18]. Thus, average sample resolutions at these sites are generally lower compared to Sites 586–588: 0.49 Myr at Site 590, 0.13 Myr at Site 591, 0.30 Myr at Site 592, and 0.33 Myr at Site 593 (0.22 Myr with our additional samples added to this study). For comparison, the resolution of sampling in the northwest Pacific (Leg 198 Sites; [31,42]) is 0.09 Myr (Hole 1207A), 0.07 Myr (Hole 1208A), and 0.07 Myr (Hole 1209A); at western equatorial Pacific Hole 806B, the average sample resolution is 0.03 Myr [43]. Thus, increased sampling resolution to constrain species' first and last occurrences will decrease age errors and potentially lower diachroneity.

Differences in taxonomic concepts and species identifications among micropaleontologists no doubt also contribute to diachroneity. In our dataset, one author (R. M. Leckie) supervised the biostratigraphic investigations at Holes 1207A, 1208A, and 1209A in the northwest Pacific [31,42], and at Hole 806B in the western equatorial Pacific [43]. For the southwest Pacific sites, taxonomic assignments were made by the same team of micropaleontologists [18] and one of the authors of this study (M. P. Crundwell). Jenkins and Srinivasan's [18] work, however, was based on low-resolution shipboard sampling that is unlikely to identify short-lived influxes and rare occurrences of key species. Misidentification by different researchers and research groups and/or poorly constrained taxonomy may be the cause of some of the diachroneity that is recorded in this study. For example, the last occurrence of *Hr. cibaoensis* occurs at all sites within the Pliocene, except at Site 587, where it last occurs in the Pleistocene (0.43 Ma; Figure 8). The very late extirpation of this species at Site 587 suggests that it is likely to be an artifact of misidentification (or reworking), rather than a real signal. Similarly, the very late first occurrence of the temperate species *Gc. inflata* at Hole 806B is an exceptionally rare occurrence outside its expected range. Such

anomalous occurrences may add another dimension of error and diachroneity. We have been completely transparent about the species' first and last occurrences reported here.

Several studies have examined the factors that contribute to the misidentification of species by students and more experienced micropaleontologists. Key factors include the size of the species being identified, with students and professionals more likely to identify larger species more consistently and correctly compared to smaller species, with the duration of training in taxonomic concepts also being important [106,107]. Boltovskoy [108] suggested that an increased number of high-quality planktic foraminiferal images in taxonomic literature could reduce taxonomic uncertainty. Thus, increased taxonomic training and the inclusion of more SEM and high-quality light microscope images in publications that showcase the acceptable range of morphological variability of species (e.g., [109]) will help to stabilize taxonomic concepts and reduce instances of misidentification. The availability of open-access online taxonomic atlases (e.g., pforams@mikrotax [110]; Endless-Forams.org [5]), as well as planktic foraminiferal taxonomic atlases and detailed taxonomic publications [42,70,111–113], has led to increased access for learners of taxonomy, and provides a more rigorous framework for the identification of planktic foraminiferal species. These resources and others like them (e.g., atlases of 3D foraminifera species, such as The Foraminarium 3D Project [114]) will undoubtedly benefit research areas where taxonomy underpins the recovered signals (e.g., paleobiogeography, geochemistry).

4.2. Biostratigraphy across the Western Pacific

Keller [115] applied some of the biozones of Kennett [14] to correlate north–central Pacific Site 310 with southwest Pacific sites based on the same lineages present in the mid-latitude regions in both the Northern and Southern hemispheres. Keller [115] applied a modified version of the tropical zonation of Blow [116] at Site 310, supplemented with southwest Pacific biozones based on the temperate genus *Globoconella*. Keller's [115] study and ours indicate that temperate biozones, like those of the northwest Pacific [31], can be used in both the Northern and Southern hemispheres. Furthermore, since similar lineages are present in the Northern and Southern hemispheres, there could be great promise in the use of event-based biostratigraphy to refine biozones, even if the biozones are diachronous between regions but nearly isochronous within regions.

Unlike the tropical–subtropical zonations [12,13], the mid-latitude zonations do not include secondary markers and event-based biostratigraphic markers, such as coiling changes. The use of such event-based biostratigraphy in the southwest Pacific has proven useful to correlate onshore sections with deep-sea sections, even though this technique has been noted as being less reliable compared to the evolutionary first and last appearances of species [117]. For example, Jenkins [89,90] erected several planktic foraminiferal subzones for the Pliocene and Quaternary based on coiling direction changes in *Neogloboquadrina pachyderma*. It was noted that the subzones based on coiling changes created by Jenkins [89,90], which were erected from assemblages recovered from the east coast of New Zealand, are not widely applicable to other sections [91]. Additional biostratigraphic studies (e.g., [20,72,76,80,91,92,118,119]) have further investigated the use of planktic foraminiferal coiling changes in the western Pacific, but few studies to date have tried to correlate such coiling changes across latitudes. As several mid-latitude biozones are of considerable length (e.g., the *Gq. dehiscens* HOZ at northwest Pacific Hole 1208A extends from 12.61 to 9.05 Ma, Figure 2), the use of coiling direction changes may hold great promise to subdivide such extensive biozones and increase the precision of sediment dating using biostratigraphy. For example, the coiling shift to 20% dextral *Gc. miozea* within the *Gc. miozea* LOZ at Site 593 is an approximation for the base of the *Pr. curva* LOZ (Supplementary Table S8). More recently, Crundwell and Woodhouse [120] implemented planktic foraminifera coiling zones and identified sequences of short-lived influxes of species unique to Quaternary marine isotope stages at ODP Site 1123.

Our data highlight how the diachroneity of datums affects the position of biozone boundaries, which in some cases is so extreme that similar biozones in different hemi-

spheres indicate different stages and epochs. The *Gc. conomiozea* LOZ at southwest Pacific Site 592 corresponds to the Late Miocene Messinian Stage (7.19–5.42 Ma), whereas the same biozone at northwest Pacific Hole 1208A spans the Early Pliocene Zanclean Stage (4.75–4.63 Ma). A less severe example is the placement of the *Gc. inflata* LOZ at southwest Pacific Site 587, which indicates the Middle–Late Pliocene Zanclean–Piacenzian Stage (3.75–3.26 Ma), whereas at northwest Pacific Hole 1209A this same zone indicates the Late Pliocene Piacenzian Stage (3.01–2.94 Ma). As biozones are used for first-order age control, such large differences in biozones, if not based on regionally calibrated datums, can lead to misinterpretations of magnetostratigraphy and orbital cycles.

Thus, our dataset indicates the importance of region-specific planktic foraminiferal biozones for use as first-order age control in sedimentary sections—especially for mid-latitude sedimentary sequences.

4.3. Diachroneity of Planktic Foraminiferal Datums

Regional diachroneity (northwest Pacific, southwest Pacific, western equatorial Pacific) among our sites for datums investigated in this study varies in the range of 0 to 9.35 Myr (Table 3). Our study highlights the high degree of diachroneity (1) between the equatorial Atlantic and the western equatorial Pacific, (2) between sites located in the same regions of the western Pacific, (3) between the northwest and southwest Pacific, and (4) between the western and eastern equatorial Pacific (Table 3).

4.3.1. Diachroneity between the Western Equatorial Pacific and Equatorial Atlantic Oceans

There is a high degree of diachroneity between the first occurrences of planktic foraminiferal species in the western Pacific and the Atlantic. Of the 31 species and 43 datums investigated (Table 2), only 2 datums have been shown to be isochronous or nearly isochronous between the global tropical zonation of King et al. [13] and the western equatorial Pacific: the last occurrences of *Gb. nepenthes* and *Gb. woodi*. Other studies have also noted differences in the timing of the first and last occurrences of planktic foraminifera between the Pacific and the Atlantic (e.g., [121]), and between the Pacific and the Mediterranean (e.g., [122]). The species of focus in the aforementioned studies (*Gc. inflata*, *Gc. puncticulata*) are used as primary markers in subtropical and temperate zonations (Figure 2).

Importantly, this study highlights diachroneity among planktic foraminiferal datums recorded from Ceara Rise Site 925 in the western equatorial Atlantic, and the western Pacific. Such datums calibrated at the Ceara Rise are included in the tropical zonation [13]; however, these events may not be appropriate for other ocean basins outside of the Atlantic. The diachroneity of datums between Hole 806B in the tropical western equatorial Pacific and Site 925 in the tropical western Atlantic ranges from 0.18 Myr to 3.86 Myr. Instances of marked diachroneity between these sites include the last occurrence of *Mn. multicamerata* (3.86 Myr), the first occurrence of *Hr. ciboensis* (1.43 Myr), the last occurrence of *Mn. limbata* (1.25 Myr), and the last occurrence of *Sa. dehiscens* (0.96 Myr). As noted above, *Mn. multicamerata* is rare everywhere, and *Mn. limbata* may be synonymized with *Mn. menardii*, contributing significantly to their perceived diachroneity between the tropical western Pacific and eastern Pacific. *Hirsutella ciboensis* can be confused with *Hr. scitula* and early forms of *Hr. margaritae*.

The high diachroneity between the western equatorial Atlantic and Pacific can be attributed to several factors: (1) local oceanographic factors, such as seasonality and surface ocean currents; (2) regional to inter-basin oceanographic and/or tectonic events (e.g., gateway closures) that caused the datums at either site to not be representative of the western equatorial Pacific and western equatorial Atlantic region; (3) taxonomic inconsistencies attributed to different operators; (4) the spacing of samples constraining datums; and (5) the criteria used to develop the age models (e.g., the Site 925 age model is orbitally-tuned [123], whereas the age model at Hole 806B is based on calcareous nannofossil datums [42]). The high degree of diachroneity between our two western equatorial Pacific sites (Holes 806B and 586B; Table 3) supports points (3) and (4) above, as the biostratigraphic analyses were

conducted by different teams of micropaleontologists, and Hole 806B was sampled at a higher resolution compared to Hole 586B. Additional work remains to create robust, orbitally tuned age models for the western equatorial Pacific sites, so as to better constrain the source(s) of such diachroneity between the western equatorial Pacific and western equatorial Atlantic sites.

Table 3. Degree of diachroneity of planktic foraminiferal evolutionary events (latest occurrence of datum subtracted from earliest occurrence) across the northwest Pacific (Holes 1207A, 1208A, and 1209A), the southwest Pacific (Sites 587, 588, 589, 590, 591, 592, and 593), the western equatorial Pacific (Holes 806B and 586B), and the entire western Pacific (all western Pacific sites, excluding the datum dates from [13]). NW = northwest; SW = southwest; WE = western equatorial.

Species	Evolutionary Event	NW Pacific Diachroneity (Myr)	SW Pacific Diachroneity (Myr)	WE Pacific Diachroneity (Myr)
<i>Globigerinella calida</i>	Base	2.281	1.714	2.693
<i>Globigerinoides subquadratus</i>	Top	1.990	3.883	-
<i>Globigerinoides extremus</i>	Top	0.510	1.487	0.251
	Base	0.432	8.576	-
<i>Globigerinoides conglobatus</i>	Base	0.904	6.645	-
<i>Globigerinoides obliquus</i>	Top	1.375	2.274	1.157
<i>Globigerinoidesella fistulosa</i>	Top	-	0.461	0.000
	Base	-	0.949	0.939
<i>Pulleniatina primalis</i>	Top	1.006	0.311	0.176
	Base	3.417	1.915	0.411
<i>Globoquadrina dehiscens</i>	Top	2.306	2.675	0.341
<i>Sphaeroidinella dehiscens</i>	Base	0.242	0.455	0.319
<i>Sphaeroidinellopsis kochi</i>	Top	1.413	-	-
<i>Sphaeroidinellopsis seminulina</i>	Top	0.574	9.351	0.355
<i>Globoconella conomiozea</i>	Top	0.209	0.634	-
	Base	0.574	1.700	-
<i>Globoconella puncticulata</i>	Base	0.959	1.485	-
<i>Globoconella inflata</i>	Base	0.346	0.654	-
<i>Globoturborotalita nepenthes</i>	Top	0.864	1.504	0.628
	Base	0.404	0.113	-
<i>Globoturborotalita decoraperta</i>	Top	1.763	2.756	0.507
	Base	0.206	1.792	-
<i>Globoturborotalita apertura</i>	Top	0.501	0.473	1.385
	Base	1.386	0.629	3.962
<i>Globoturborotalita woodi</i>	Top	0.487	1.434	0.251
<i>Neogloboquadrina acostaensis</i>	Top	2.838	0.404	0.309
	Base	6.186	2.485	-
<i>Fohsella linguaensis</i>	Top	5.840	-	-
<i>Hirsutella margaritae</i>	Top	0.536	1.753	0.268
	Base	1.737	1.986	0.604
<i>Hirsutella cibaoensis</i>	Top	1.115	4.910	-
	Base	3.150	2.422	-
<i>Hirsutella hirsuta</i>	Base	0.450	2.101	-
<i>Truncorotalia crassaformis</i>	Base	0.689	0.764	0.065
<i>Truncorotalia tosaensis</i>	Top	0.293	1.079	0.804
	Base	1.178	1.272	0.195
<i>Truncorotalia truncatulinooides</i>	Base	0.378	0.343	0.070
<i>Globorotalia tumida</i>	Base	1.155	0.997	0.461
<i>Globorotalia plesiotumida</i>	Top	1.011	1.307	0.031
	Base	2.411	1.681	-
<i>Menardella multicamerata</i>	Top	-	0.330	4.732
<i>Menardella limbata</i>	Top	2.290	-	-
<i>Dentoglobigerina altispira</i>	Top	0.420	4.434	0.375
Average diachroneity		1.396	2.052	0.819

4.3.2. Diachroneity within the Northwest and Southwest Pacific

Within the northwest and southwest Pacific, diachroneity is apparent among sites that are located close to one another. In the southwest Pacific, the last occurrence of *Dt. altispira* occurs in the Early Messinian Stage at Site 593 (7.00 Ma), in the Zanclean Stage at Site 592 (4.41 Ma), and in the Piacenzian Stage at Site 591 (3.15 Ma; Figure 8)—sites that lie within 10° latitude of one another (Figure 1). In the northwest Pacific, the first occurrence of *Nq. acostaensis* occurs in the Early Tortonian Stage at Hole 1207A (11.15 Ma), in the Early Messinian Stage at Hole 1208A (7.20 Ma), and in the Early Zanclean Stage at Hole 1209A (4.97 Ma)—sites that lie within about 5° of latitude of one another. In the northwest Pacific (Holes 1207A–1209A), the average diachroneity of datums is 1.39 Myr, while in the southwest Pacific (Sites 587–593) the average diachroneity is slightly higher, at 2.05 Myr (Table 3).

However, this study also reveals that datums may be diachronous between regions (e.g., the southwest Pacific and northwest Pacific), but less diachronous within regions (Figure 9). From our data, some datums with reduced diachroneity disperse into the northwest Pacific in a stepwise fashion across the tropics (e.g., top of *Gc. conomiozea*, base of *Gc. inflata*, base of *Gs. extremus*), whereas other patterns of dispersal from the southwest Pacific into the northwest Pacific occur more gradually (e.g., top of *Tr. truncatulinoidea*, top of *Gs. extremus*; Figure 9).

4.3.3. Diachroneity between the Northwest and Southwest Pacific

We found that very few species have isochronous or nearly isochronous first or last appearances between the northwest and southwest Pacific (e.g., the last appearance of *Ss. seminulina* at Sites 1209A and 597). There are several instances where a species first occurs in one region, and later in another. Sometimes, the diachroneity exhibited by a species between the northwest and southwest Pacific can also be quite extreme. For example, *Pu. primalis* first occurs in the southwest Pacific in the Miocene, and migrates into the northwest Pacific during the Early Pliocene (Figure 3); *Gs. obliquus* last occurs in the southwest Pacific in the Miocene, and in the northwest Pacific it last occurs during the Pleistocene (Figure 4); and the last occurrence of *Gb. woodi*, which occurs in the southwest Pacific in the Pliocene and later in the northwest Pacific in the Pleistocene (Figure 6). The persistent and sometimes high diachroneity between these regions further highlights the need for separate regional planktic foraminiferal biostratigraphic zonations within mid-latitude regions. In addition, continued work on taxonomic atlases is essential; we suspect that some of the diachroneity in the Late Neogene planktic foraminifera record of the western Pacific is due to human subjectivity in the application of taxonomic concepts.

4.3.4. Diachroneity between the Western Equatorial and Eastern Equatorial Pacific, and the Eastern Equatorial Indian Ocean

Between the western and eastern equatorial Pacific, there are a few species that exhibit differences in the timing of their evolutionary and dispersal events. For example, the last occurrence of *Tr. tosaensis* in the western equatorial Pacific at Hole 806B (0.73 Ma) occurs 0.12 Myr prior to that in the eastern equatorial Pacific at sites 846 and U1338 (0.61 Ma; [124]). The first occurrence of *Gr. tumida* in the western equatorial Pacific at Hole 806B (5.80 Ma) is 0.23 Myr prior to the eastern equatorial Pacific at Sites 846 and U1338 (5.57 Ma; [100,124–126]). The last occurrence of *Dt. altispira* in the eastern equatorial Pacific at Site 846 (3.47 Ma; [100,125]) is 0.87 Myr prior to that in the western equatorial Pacific at Hole 806B (2.60 Ma).

The last occurrences of *Dt. altispira*, *Dt. baroemoenensis*, and *Dt. globosa* were recently calibrated at eastern equatorial Pacific Site U1338 [10], located just west of Site 846. The last occurrence of *Dt. altispira* at Site U1338 (3.03 Ma) occurs 0.43 Myr later compared to nearby Site 846 (3.47 Ma), and occurs 0.43 Myr earlier compared to western equatorial Pacific Hole 806B (2.60 Ma). The diachroneity of the last occurrence of *Dt. altispira* is the same between the two eastern equatorial Pacific sites as it is between Site U1338 and the

western equatorial Pacific. The extirpation of *Dt. baroemoenensis* in the equatorial Pacific occurs first in the east and last towards the west. Very few specimens of *Dentoglobigerina globosa* were identified at Hole 806B, so they were included in *Dt. altispira* by Chaisson and Leckie [43]. Consequently, this may have contributed to the diachroneity of this datum.

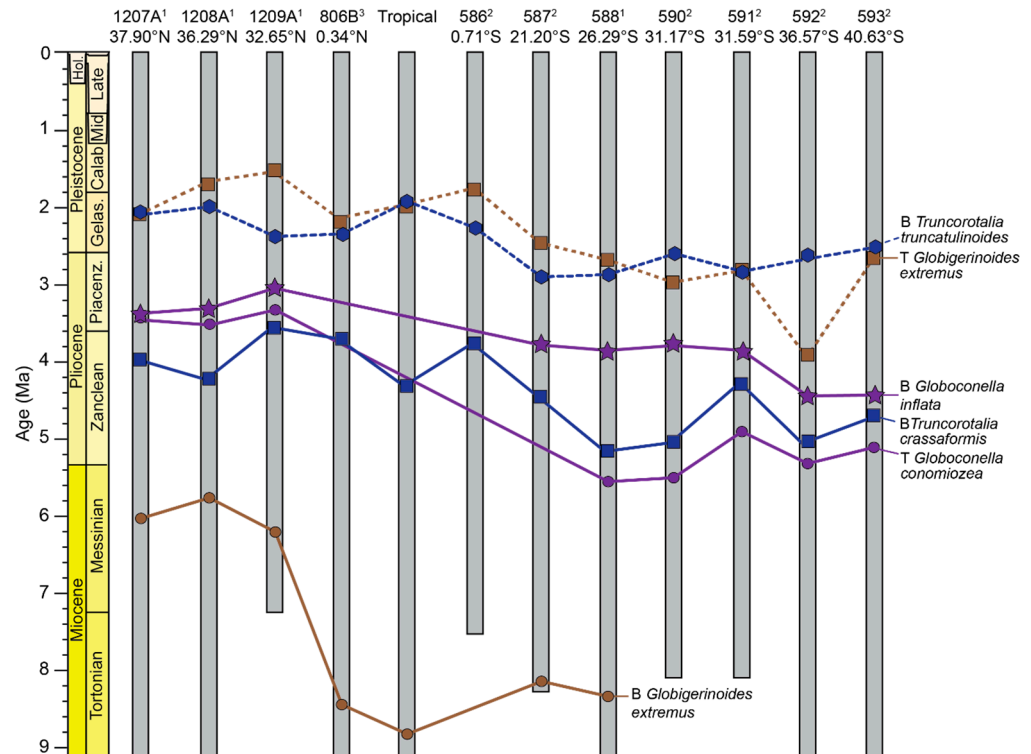


Figure 9. Select datums that exhibit diachroneity between regions, but reduced diachroneity within regions. Of note are the two styles of dispersal: more gradual dispersal from south to north (base of *Tr. truncatulinoides*, top of *Gs. extremus*, base of *Tr. crassaformis*), and dispersal from the southwest Pacific into the northwest Pacific that occurs in a stepwise fashion across the tropics (base of *Gc. inflata*, top of *Gc. conomiozea*, base of *Gs. extremus*). We have left out the base of *Gc. inflata* at Hole 806B, as these specimens were very rare, and also removed the bases of *Gs. extremus* at Sites 592 and 593, as we suspect that these are anomalous datums.

Comparison of the first occurrences of planktic foraminifera in the Pacific and Indian oceans is critical, as these ocean basins are linked by the Indonesian Throughflow, which has affected the shallow-to-deep ocean connectivity between these oceans through the Neogene (reviewed by [127]). There have been numerous Neogene planktic foraminiferal biostratigraphic studies in the Indian Ocean (e.g., [128–130]). Recent orbitally tuned and calibrated planktic foraminiferal bioevents from the northwest coast of Australia, at Site U1463 [131], have been compared to datums from Hole 806B in the western equatorial Pacific and the ages of datums reported by King et al. [13] (Table 4).

The average diachroneity of planktic foraminiferal datums between the western equatorial Pacific [43] and the northwest coast of Australia [131] is 0.49 Myr, and the diachroneity ranges from 0.01 Myr to 1.85 Myr (Table 4). The average diachroneity between datums on the northwest coast of Australia and those of King et al. [13] is 0.39 Myr, and ranges from 0.003 Myr to 1.35 Myr (Table 4). Thus, some datums are isochronous (or nearly so) between the eastern equatorial Indian Ocean and the tropical zonation of King et al. [13], and possibly between the Indian and western Pacific oceans. As noted by Groeneweld et al. [131], the diachroneity between datums in the Indian Ocean and those in the Atlantic and Pacific oceans affects the reliability of biostratigraphic and magnetostratigraphic interpretations. Groeneweld et al. [131] also found diachroneity between Site U1463 and nearby Site 763 [130].

Thus, rigorous paleobiogeographic analyses of key planktic foraminiferal biohorizons using tuned age models for comparison to other geochemically dated, orbitally tuned, and magnetostratigraphically dated sites may be necessary to create a robust biostratigraphic zonation (or zonations) for the Indian Ocean.

Table 4. Ages of evolutionary events and degree of diachroneity of planktic foraminiferal evolutionary events (latest occurrence of datum subtracted from earliest occurrence of datum) between eastern equatorial Indian Ocean Site U1463 [131] and western equatorial Pacific Hole 806B (IO-WEP), and between Site U1463 and the datum dates from the global tropical planktic foraminiferal zonation [13] (IO-Tropical). IO = Indian Ocean; WEP = western equatorial Pacific. All ages reported in millions of years.

Species	Evolutionary Event	U1463 (IO) Age	806B (WEP) Age	Tropical Age	IO-WEP Diachroneity (Myr)	IO-Tropical Diachroneity (Myr)
<i>Globigerinoides extremus</i>	Top	1.973	2.172	1.97	0.199	0.003
<i>Globigerinoidesella fistulosa</i>	Top	1.685	1.736	1.88	0.051	0.195
	Base	3.155	2.801	3.33	0.354	0.175
<i>Pulleniatina primalis</i>	Top	3.358	2.042	3.66	1.316	0.302
<i>Sphaeroidinellopsis kochi</i>	Top	3.131	4.987	4.49	1.856	1.359
<i>Sphaeroidinellopsis seminulina</i>	Top	3.335	3.625	3.59	0.290	0.255
<i>Globoconella inflata</i>	Base	1.908	0.978	-	0.930	-
<i>Globoturbotalita nepenthes</i>	Top	4.200	4.276	4.38	0.076	0.180
<i>Globoturbotalita woodi</i>	Top	2.512	2.172	2.3	0.340	0.212
<i>Hirsutella margaritae</i>	Top	3.131	3.075	3.83	0.056	0.699
<i>Truncorotalia tosaensis</i>	Base	3.059	3.075	3.35	0.016	0.291
<i>Truncorotalia truncatulinoides</i>	Base	2.159	2.332	1.92	0.173	0.239
<i>Globorotalia plesiotumida</i>	Top	3.358	4.37	3.72	1.012	0.362
<i>Menardella limbata</i>	Top	1.837	1.126	2.37	0.711	0.533
<i>Dentoglobigerina altispira</i>	Top	2.697	2.603	3.47	0.094	0.773
Average diachroneity					0.498	0.398

5. Major Biogeographic Patterns and Their Oceanographic Drivers

Planktic foraminifera are passive floaters that are transported widely in surface and subsurface ocean currents [132–137]). Foraminifera, however, only establish viable populations when oceanographic conditions are favorable for reproduction [138]. Several studies have highlighted temperature as a dominant control on planktic foraminifera distribution and diversity patterns through the Cenozoic (e.g., [53,135,138–143]). Other oceanographic factors, such as nutrient availability and the depths of the mixed layer and thermocline, also influence distribution and diversity patterns [144]. As the mid-latitude regions are areas defined by strong seasonality and sharp latitudinal gradients in water temperature, salinity, and nutrients—specifically due to the presence of western boundary currents and their ecotones, such as the Kuroshio Current and Extension in the northwest Pacific and the East Australian Current and Tasman Front in the southwest Pacific—these features may be the leading reason for planktic foraminiferal provinciality and diachroneity.

The above observations related to evolution, dispersal, and factors that control plankton distribution have major implications for two major biogeographic patterns highlighted by the data in this study: (1) conditions in the southwest Pacific were viable for reproduction and establishment of populations prior to conditions becoming suitable in the northwest Pacific, and (2) when conditions in the northwest Pacific were suitable for species to establish regional populations, these conditions may have first been established at Holes 1207A or 1208A, and later at Hole 1209A.

A number of species in this study seem to first occur in the southwest Pacific, which may hint that they first evolved in this region. These include species such as *Pu. primalis* (Figure 3), *Gc. conomiozea* (Figure 5), *Tr. crassaformis* (Figure 7), *Tr. tosaensis* (Figure 7), and *Tr. truncatulinoides* (Figure 7). Several of the aforementioned species are diachronous between regions, but exhibit reduced diachroneity within regions—some dispersing across the tropical Pacific in a stepwise manner (e.g., top of *Gc. conomiozea*, base of *Gc. inflata*; Figure 9). The hypothesis that some Late Neogene species first evolved in the Southern Hemisphere prior to dispersing into the Northern Hemisphere was proposed by Jenkins [29], who found that several species of planktic foraminifera evolved in the southwest Pacific between 12°–56° S from 10.4 Ma to the present. Previous research has confirmed this finding for the evolution of *Gc. inflata* from its ancestor *Gc. puncticulata* [145]. As the Southern Hemisphere experienced oceanic cooling and the development of oceanic fronts [46] due to Antarctic ice sheet growth [146], it is likely that such increased Equator-to-pole temperature gradients led to new habitats and niches that promoted planktic foraminiferal evolution in the Southern Hemisphere [147,148].

The second major biogeographic pattern to emerge from our data is that several species seem to migrate into the northwest Pacific via the highest-latitude sites prior to migrating southward. Species that exhibit such a pattern enter to the northwest Pacific via the highest-latitude sites (Holes 1207A or 1208A), and later migrate to the lowest-latitude site (Hole 1209A) after entering the western Pacific or migrating into the northwest Pacific from the southwest Pacific. Species that exhibit such a dispersal pattern include *Gc. inflata*, *Gc. puncticulata*, *Gc. conomiozea*, *Nq. acostaensis*, *Gb. apertura*, *Gb. decoraperta*, and *Gb. nepenthes* (Figure 5), as well as *Mn. limbata*, *Gr. tumida*, *Hr. cibaoensis*, *Hr. margaritae*, and *Hr. hirsuta* (Figure 7). The aforementioned include species that are common in temperate waters (e.g., *Gc. inflata*, *Gc. puncticulata*, *Gc. conomiozea*, *Hr. cibaoensis*, *Hr. margaritae*, *Hr. hirsuta*), subtropical waters (e.g., *Nq. acostaensis*, *Gb. apertura*, *Gb. decoraperta*, *Gb. nepenthes*), and tropical waters (e.g., *Mn. tumida*; [17]).

The northwest Pacific Sites 1207A–1209A represent a transect across the modern-day position of the Kuroshio Current Extension (KCE). Across the KCE today, annual average upper mixed-layer ocean (0–50 m) temperatures differ by 4.06 °C across 5.25° of latitude (Holes 1207A to 1209A; [52])—a distance of approximately 600 km (Table 1). Within the permanent thermocline (254–582 m; [149]) of the KCE region, averaged temperatures differ by 4.94 °C across Holes 1207A to 1209A. The KCE region today is dominated by tropical/subtropical species south of the current and temperate-to-subpolar species within the current and to the north [138]. The presence of tropical species at our higher-latitude sites through the Late Neogene indicates that tropical waters associated with the KCE may have reached higher latitudes during periods of warmer global temperatures in the Miocene and Pliocene. Previous studies have indicated that during warm periods of the Neogene, the North Pacific Subtropical Gyre (NPSG) was likely expanded, with warmer subtropical waters reaching higher latitudes via the Kuroshio Current and Extension [34,42,48,150]. Northward migration of the KCE under increased warming and CO₂ concentrations has also been observed over anthropogenic timescales [151]. Thus, northward expansion of the NPSG and KCE may partially explain why some species first migrated into the highest-latitude northwest Pacific Hole 1207A prior to dispersing south; under expanded gyre scenarios, species were carried northward via the warm Kuroshio Current, with subsequent dispersal events southward. However, this phenomenon requires further research and exploration to more fully explain the biogeographic patterns that this study has uncovered in the northwest Pacific.

6. Conclusions and Future Directions

This study builds on previous studies (e.g., [14,18,26,27]) that investigated planktic foraminiferal biostratigraphy and diachroneity across the southwest Pacific. Here, we quantify diachroneity from the mid-latitudes of the northwest Pacific to the mid-latitudes of the southwest Pacific, and correlate the western Pacific Ocean using existing planktic

foraminiferal zonations. Specifically, we used published occurrence data and biostratigraphic zonations for ODP Leg 198 Holes 1207A, 1208A, and 1209A in the northwest Pacific [31,42], ODP Hole 806B and DSDP Leg 90 Hole 586B in the western equatorial Pacific [18,43], and DSDP Leg 90 Sites 587–593 in the southwest Pacific [18].

For the first time, Late Neogene planktic foraminiferal biozones created for the northwest Pacific are correlated with the southwest Pacific. However, these biostratigraphic zones should be viewed as preliminary, and are applied here to show how diachroneity affects zonations in different mid-latitude regions. Several biostratigraphic zones are similar between the northwest and southwest Pacific, with few modifications between hemispheres. For the sites that we studied, the tropical planktic foraminiferal zonation [12,13] was not applicable in the mid-latitudes of the northwest or southwest Pacific. However, Matsui et al. [152] identified most of the tropical biozones at DSDP Site 296 (29° N, 133° E) in the northwest Pacific. These results indicate that for the western Pacific Ocean, the tropical zonation may not be applicable north of 29° N in the northwest Pacific and south of 21° S in the southwest Pacific, based on the fact that we implemented the warm subtropical zonation scheme at Site 587, which lies at 21° S. Based on our results, it is clear that the mid-latitude regions of each ocean basin require their own biostratigraphic frameworks, due to oceanic fronts partitioning planktic foraminiferal assemblages into distinct biogeographic provinces.

We systematically documented the biogeographic patterns of planktic foraminifera across the western Pacific, and provided updated ages for the earliest occurrences and dispersals of species, with age errors for comparison. Only two datums are isochronous or nearly isochronous between the global tropical zonation [13] and the western equatorial Pacific: the last occurrences of *Gb. nepenthes* and *Gb. woodi*. Inter-regional diachroneity is also recorded within the Pacific. At the three northwest Pacific sites in our study, diachroneity ranges from 0.21 Myr to 6.18 Myr; at the six southwest Pacific sites, diachroneity ranges from 0.11 to 9.35 Myr; and between our two western equatorial sites, diachroneity ranges from 0 to 4.73 Myr. Our data also indicate diachroneity between the mid-latitudes of the northwest and southwest Pacific. Brief comparison of our datums to those in the eastern equatorial Pacific and eastern Indian Ocean also reveals diachroneity between ocean basins, and the need for a more in-depth analysis of datums and biostratigraphic review.

Of particular note, we found that two major biogeographic patterns emerged from our data. First, we found that several species first occurred in the southwest Pacific, indicating that several Neogene species may have first evolved in the Southern Hemisphere prior to migrating to the Northern Hemisphere. In some cases, species that exhibit this pattern have greatly reduced diachroneity within a region, such as the base of *Tr. truncatulinoides*, the base of *Gc. inflata*, and the top of *Gc. conomiozea*, with the former species dispersing gradually from south to north, and the latter two species exhibiting a 'step' from the southwest Pacific to the northwest Pacific. This phenomenon was hypothesized by Jenkins [29], and may be related to Antarctic glaciation and the development of oceanic fronts [147,148]. Second, we found that when species do enter the North Pacific, they do so through the higher-latitude sites prior to migrating to the lower-latitude sites. This may indicate that through the Pliocene and Miocene, the North Pacific Subtropical Gyre was generally expanded, which allowed for warm-water species to disperse into higher latitudes.

Certainly, there are factors affecting the biogeographic patterns in this study and diachroneity within species. Robust age models available for sites that are either orbitally tuned or based on well-constrained magnetic reversal boundaries are generally lacking for the sites used in this study. The resolution of sampling at each site may also affect diachroneity, especially when sites are sampled at a low resolution (e.g., mainly core-catcher samples are used). Differences in taxonomic concepts among micropaleontologists may also contribute to diachroneity. Currently, taxonomic atlases exist for most of the Cenozoic [17,70,111,112], without a robust update to the Neogene atlas of Kennett and Srinivasan [17]. Stabilized Neogene taxonomy of planktic foraminifera, in addition to

open-access resources and high-quality light and SEM images, is certainly required to further interpret robust patterns of biogeography over time.

This study highlights that there is definitely a dire need for more detailed micropaleontological studies of mid-latitude sites with robust age models to further constrain planktic foraminifera evolutionary events and the timing of dispersal and extirpation events. With improved age models, robust taxonomy, and higher-resolution sampling, the micropaleontological community can begin to best quantify diachroneity and patterns of species' dispersal within regions, between hemispheres in the same ocean basin, and between ocean basins. With such detailed regional information, we can further harness the power of paleobiogeography to investigate deep-time abiotic processes that govern plankton dispersal patterns and speciation modes in the open ocean.

Supplementary Materials: The following supporting information can be downloaded at: <https://doi.org/10.6084/m9.figshare.19063532.v1> (accessed on 11 February 2021), Table S1: Age models for Deep Sea Drilling Project Leg 90 sites, Table S2: Deep Sea Drilling Project Leg 90 Hole 586B biostratigraphy, Table S3: Deep Sea Drilling Project Leg 90 Site 587 biostratigraphy, Table S4: Deep Sea Drilling Project Leg 90 Site 588 biostratigraphy, Table S5: Deep Sea Drilling Project Leg 90 Hole 590A biostratigraphy, Table S6: Deep Sea Drilling Project Leg 90 Site 591 biostratigraphy, Table S7: Deep Sea Drilling Project Leg 90 Site 592 biostratigraphy, Table S8: Deep Sea Drilling Project Leg 90 Site 593 biostratigraphy.

Author Contributions: Conceptualization, A.R.L., R.M.L. and M.P.C.; methodology, A.R.L., J.A. and J.P.U.; data curation, A.R.L.; writing—original draft preparation, A.R.L.; writing—review and editing, A.R.L., R.M.L., M.P.C., J.A. and J.P.U.; visualization, A.R.L. All authors have read and agreed to the published version of the manuscript.

Funding: This research received no external funding.

Institutional Review Board Statement: Not applicable.

Informed Consent Statement: Not applicable.

Data Availability Statement: Not applicable.

Acknowledgments: The authors thank four anonymous reviewers and the editors for their very thorough and thoughtful reviews that greatly improved an earlier version of this manuscript. This work is dedicated to M.S. Srinivasan, whose biostratigraphic work in the southwest Pacific, and significant planktic foraminiferal taxonomic revisions, greatly furthered the field of micropaleontology. Several of M.S. Srinivasan's ideas and publications inspired and provided the foundation for this study.

Conflicts of Interest: The authors declare no conflict of interest.

References

1. Leckie, R.M. Seeking a better life in the plankton. *Proc. Natl. Acad. Sci. USA* **2009**, *106*, 14183–14184. [[CrossRef](#)] [[PubMed](#)]
2. Fraass, A.J.; Kelly, D.C.; Peters, S.E. Macroevolutionary history of the planktic foraminifera. *Annu. Rev. Earth Planet. Sci.* **2015**, *43*, 139–166. [[CrossRef](#)]
3. Gradstein, F.; Waskowska, A.; Glinskikh, L. The First 40 Million Years of Planktonic Foraminifera. *Geosciences* **2021**, *11*, 85. [[CrossRef](#)]
4. Lam, A.R.; Bauer, J.E.; Fraass, S.; Sheffield, S.; Limbeck, M.R.; Borden, R.M.; Bryant, R. Time Scavengers: An Educational Website to Communicate Climate Change and Evolutionary Theory to the Public through Blogs, Web Pages, and Social Media Platforms. *J. STEM Outreach* **2019**, *7*, 1–8. [[CrossRef](#)]
5. Hsiang, A.Y.; Brombacher, A.; Rillo, M.C.; Mleneck-Vautravers, M.J.; Conn, S.; Lordsmith, S.; Hull, P.M. Endless Forams: >34,000 modern planktonic foraminiferal images for taxonomic training and automated species recognition using convolutional neural networks. *Paleoceanogr. Paleoclimatol.* **2019**, *34*, 1157–1177. [[CrossRef](#)]
6. Pearson, P.N.; Shackleton, N.J.; Hall, M.A. Stable isotopic evidence for the sympatric divergence of *Globigerinoides trilobus* and *Orbulina universa* (planktonic foraminifera). *J. Geol. Soc.* **1997**, *154*, 295–302. [[CrossRef](#)]
7. Darling, K.F.; Wade, C.M.; Stewart, I.A.; Kroon, D.; Dingle, R.; Brown, A.J.L. Molecular evidence for genetic mixing of Arctic and Antarctic subpolar populations of planktonic foraminifera. *Nature* **2000**, *405*, 43–47. [[CrossRef](#)]
8. Norris, R.D.; de Vargas, C. Evolution all at sea. *Nature* **2000**, *405*, 23–24. [[CrossRef](#)]
9. Brombacher, A.; Wilson, P.A.; Bailey, I.; Ezard, T.H. The breakdown of static and evolutionary allometries during climatic upheaval. *Am. Nat.* **2017**, *190*, 350–362. [[CrossRef](#)]

10. Woodhouse, A.; Jackson, S.; Jamieson, R.; Newton, R.; Sexton, P.; Aze, T. Adaptive Ecological Niche Migration does not Negate Extinction Susceptibility. *Sci. Rep.* **2021**, *11*, 1–10. [[CrossRef](#)]
11. Boscolo-Galazzo, F.; Jones, A.; Dunkley Jones, T.; Crichton, K.A.; Wade, B.S.; Pearson, P.N. Late Neogene evolution of modern deep-dwelling plankton. *Biogeosciences* **2022**, *19*, 743–762. [[CrossRef](#)]
12. Wade, B.S.; Pearson, P.N.; Berggren, W.A.; Pälike, H. Review and revision of Cenozoic tropical planktonic foraminiferal biostratigraphy and calibration to the geomagnetic polarity and astronomical time scale. *Earth-Sci. Rev.* **2011**, *104*, 111–142. [[CrossRef](#)]
13. King, D.J.; Wade, B.S.; Liska, R.D.; Miller, C.G. A review of the importance of the Caribbean region in Oligo-Miocene low latitude planktonic foraminiferal biostratigraphy and the implications for modern biogeochronological schemes. *Earth-Sci. Rev.* **2020**, *202*, 102968. [[CrossRef](#)]
14. Kennett, J.P. Middle and late Cenozoic planktonic foraminiferal biostratigraphy of the south-west Pacific- DSDP Leg 21. In *Initial Reports of the Deep Sea Drilling Project*; Burns, R.E., Andrews, J.E., van der Lingen, G.J., Churkin, M., Jr., Galehouse, J.S., Packham, G.H., Davies, T.A., Kennett, J.P., Dumitrica, P., Edwards, A.R., et al., Eds.; U.S. Government Printing Office: Washington, DC, USA, 1973; Volume 21, pp. 575–639.
15. Srinivasan, M.S.; Kennett, J.P. Neogene planktonic foraminiferal biostratigraphy and evolution: Equatorial to subantarctic, South Pacific. *Mar. Micropaleontol.* **1981**, *6*, 499–533. [[CrossRef](#)]
16. Srinivasan, M.S.; Kennett, J.P. *A Review of Neogene Planktonic Foraminiferal Biostratigraphy Applications in the Equatorial and South Pacific*; SEPM Special Publications: Tulsa, AK, USA, 1981; Volume 32, pp. 395–432.
17. Kennett, J.P.; Srinivasan, M.S. *Neogene Planktonic Foraminifera a Phylogenetic Atlas*; Hutchinson Ross Publishing Co.: Hutchinson, KS, USA, 1983.
18. Jenkins, D.G.; Srinivasan, M.S. Cenozoic Planktonic Foraminifers from the Equator to the sub-Antarctic of the Southwest Pacific. In *Initial Reports of the Deep Sea Drilling Project*; Kennett, J.P., von der Borch, C.C., Baker, P.A., Barton, C.E., Boersma, A., Caulet, J.P., Dudley, W.C., Jr., Gardner, J.V., Jenkins, D.G., Lohman, W.H., et al., Eds.; U.S. Government Printing Office: Washington, DC, USA, 1986; Volume 90, pp. 795–834.
19. Cifelli, R.; Scott, G. Stratigraphic record of the Neogene globorotalid radiation (Planktonic Foraminiferida). *Smithson. Contrib. Paleobiol.* **1986**, *58*. [[CrossRef](#)]
20. Scott, G.H. Planktonic foraminiferal biostratigraphy (Altonian-Tongaporutuan Stages, Miocene) at DSDP Site 593, Challenger Plateau, Tasman Sea. *N. Z. J. Geol. Geophys.* **1992**, *35*, 501–513. [[CrossRef](#)]
21. Keller, G. Planktonic foraminiferal biostratigraphy and paleoceanography of the Japan trench, Leg 57, Deep Sea Drilling Project. In *Initial Reports of the Deep Sea Drilling Project*; von Huene, R., Nasu, N., Arthur, M.A., Barron, J.A., Bell, G.D., Cadet, J.-P., Carson, B., Fujioka, K., Honza, E., Keller, G., et al., Eds.; U.S. Government Printing Office: Washington, DC, USA, 1980; Volume 57, pp. 809–833.
22. Weaver, P.P.E.; Clement, B.M. Magnetobiostratigraphy of planktonic foraminiferal datums: Deep Sea Drilling Project Leg 94, North Atlantic. In *Initial Reports of the Deep Sea Drilling Project*; Ruddiman, W.F., Kidd, R.B., Baldauf, J.G., Clement, B.M., Dolan, J.F., Eggers, M.R., Hill, M.R., Keigwin, L.D., Jr., Mitchell, M., Philipps, I., et al., Eds.; U.S. Government Printing Office: Washington, DC, USA, 1986; Volume 94, pp. 815–829.
23. Fraass, A.J.; Leckie, R.M.; Lowery, C.M.; DeConto, R. Precision in Biostratigraphy: Evidence for a temporary flow reversal in the Central American Seaway during or after the Oligocene-Miocene transition. *J. Foraminifer. Res.* **2019**, *49*, 357–366. [[CrossRef](#)]
24. Scott, G.H. Divergences and phyletic transformations in the history of the *Globorotalia inflata* lineage. *Paleobiology* **1983**, *9*, 422–426. [[CrossRef](#)]
25. Hodell, D.A.; Kennett, J.P. Late Miocene–early Pliocene stratigraphy and paleoceanography of the South Atlantic and southwest Pacific Oceans: A synthesis. *Paleoceanography* **1986**, *1*, 285–311. [[CrossRef](#)]
26. Dowsett, H.J. Diachrony of late Neogene microfossils in the southwest Pacific Ocean: Application of the graphic correlation method. *Paleoceanography* **1988**, *3*, 209–222. [[CrossRef](#)]
27. Dowsett, H.J. Improved dating of the Pliocene of the eastern South Atlantic using graphic correlation: Implications for paleobiogeography and paleoceanography. *Micropaleontology* **1989**, *35*, 279–292. [[CrossRef](#)]
28. Srinivasan, M.S.; Sinha, D.K. Improved correlation of the late Neogene planktonic foraminiferal datums in the equatorial to cool subtropical DSDP sites, southwest Pacific: Application of the graphic correlation method. *Mem. Geol. Soc. India* **1991**, *20*, 55–93.
29. Jenkins, D.G. The paleogeography, evolution and extinction of Late Miocene-Pleistocene planktonic foraminifera from the southwest Pacific. *Centen. Jpn. Micropaleontol.* **1992**, *27*, 1–35.
30. Spencer-Cervato, C.; Thierstein, H.R.; Lazarus, D.B.; Beckmann, J.P. How synchronous are Neogene marine plankton events? *Paleoceanography* **1994**, *9*, 739–763. [[CrossRef](#)]
31. Lam, A.R.; Leckie, R.M. Subtropical to temperate late Neogene to Quaternary planktic foraminiferal biostratigraphy across the Kuroshio Current Extension, Shatsky Rise, northwest Pacific Ocean. *PLoS ONE* **2020**, *15*, e0234351. [[CrossRef](#)]
32. Lam, A.R.; Stigall, A.L. Pathways and mechanisms of Late Ordovician (Katian) faunal migrations of Laurentia and Baltica. *Est. J. Earth Sci.* **2015**, *64*, 62–67. [[CrossRef](#)]
33. Lam, A.R.; Stigall, A.L.; Matzke, N.J. Dispersal in the Ordovician: Speciation patterns and paleobiogeographic analyses of brachiopods and trilobites. *Palaeogeogr. Palaeoclimatol. Palaeoecol.* **2018**, *489*, 147–165. [[CrossRef](#)]

34. Lam, A.R.; Leckie, R.M.; Patterson, M.O. Illuminating the Past to See the Future of Western Boundary Currents. *Oceanography* **2020**, *33*, 65–67. [CrossRef]
35. Zheng, H.; Sun, X.; Wang, P.; Chen, W.; Yue, J. Mesozoic tectonic evolution of the Proto-South China Sea: A perspective from radiolarian paleobiogeography. *J. Asian Earth Sci.* **2019**, *179*, 37–55. [CrossRef]
36. Bauer, J.E. Paleobiogeography, paleoecology, diversity, and speciation patterns in the Eublastoidea (Blastozoa: Echinodermata). *Paleobiology* **2021**, *47*, 221–235. [CrossRef]
37. Lam, A.R.; Sheffield, S.L.; Matzke, N.J. Estimating dispersal and evolutionary dynamics in diploporan blastozoans (Echinodermata) across the great Ordovician biodiversification event. *Paleobiology* **2021**, *47*, 198–220. [CrossRef]
38. Petruzzo, M.R.; Huber, B.T.; Falzoni, F.; MacLeod, K.G. Changes in biogeographic distribution patterns of southern mid-to high latitude planktonic foraminifera during the Late Cretaceous hot to cool greenhouse climate transition. *Cretac. Res.* **2020**, *115*, 104547. [CrossRef]
39. Brombacher, A.; Wilson, P.A.; Bailey, I.; Ezard, T.H. The Dynamics of Diachronous Extinction Associated with Climatic Deterioration near the Neogene/Quaternary Boundary. *Paleoceanogr. Paleoclimatol.* **2021**, *36*, e2020PA004205. [CrossRef]
40. Huber, B.T.; Tur, N.A.; Self-Trail, J.; MacLeod, K.G. Calcareous plankton biostratigraphic fidelity and species richness during the last 10 my of the Cretaceous at Blake Plateau, subtropical North Atlantic. *Cretac. Res.* **2022**, *131*, 105095. [CrossRef]
41. Sheffield, S.L.; Lam, A.R.; Philips, S.F.; Deline, B. *Morphological Dynamics and Response Following the Dispersal of Ordovician-Silurian Diploporan Echinoderms to Laurentia*; University of Michigan: Ann Arbor, MI, USA, 2022, in press.
42. Lam, A.R.; Leckie, R.M. Late Neogene and Quaternary diversity and taxonomy of subtropical to temperate planktic foraminifera across the Kuroshio Current Extension, northwest Pacific Ocean. *Micropaleontology* **2020**, *66*, 177–268. [CrossRef]
43. Chaisson, W.P.; Leckie, R.M. High-resolution Neogene planktonic foraminifer biostratigraphy of Site 806, Ontong Java Plateau (western equatorial Pacific). In *Proceedings of the Ocean Drilling Program Scientific Results*; Berger, W.H., Kroenke, L.W., Janecek, T.R., Backman, J., Bassinot, F., Corfield, R.M., Delaney, M.L., Hagen, R., Jansen, E., Krissek, L.A., et al., Eds.; Ocean Drilling Program: College Station, TX, USA, 1993; Volume 130, pp. 137–178.
44. Martini, E. Standard Tertiary and Quaternary calcareous nannoplankton zonation. *Proc. II Planktonic Conf. Rome Italy 1970 Tecnoscienza* **1971**, *2*, 739–785.
45. Backman, J.; Raffi, I.; Rio, D.; Fornaciari, E.; Pälke, H. Biozonation and biochronology of Miocene through Pleistocene calcareous nannofossils from low and middle latitudes. *Newsl. Stratigr.* **2012**, *45*, 221–244. [CrossRef]
46. Nelson, C.S.; Cooke, P.J. History of oceanic front development in the New Zealand sector of the Southern Ocean during the Cenozoic—A synthesis. *N. Z. J. Geol. Geophys.* **2001**, *44*, 535–553. [CrossRef]
47. Gallagher, S.J.; Kitamura, A.; Iryu, Y.; Itaki, T.; Koizumi, I.; Hoiles, P.W. The Pliocene to recent history of the Kuroshio and Tsushima Currents: A multi-proxy approach. *Prog. Earth Planet. Sci.* **2015**, *2*, 1–23. [CrossRef]
48. Lam, A.R.; MacLeod, K.G.; Schilling, S.H.; Leckie, R.M.; Fraass, A.J.; Patterson, M.O.; Venti, N.L. Pliocene to earliest Pleistocene (5–2.5 Ma) Reconstruction of the Kuroshio Current Extension Reveals a Dynamic Current. *Paleoceanogr. Paleoclimatol.* **2021**, *36*, e2021PA004318. [CrossRef]
49. Sutherland, R.; Dos Santos, Z.; Agnini, C.; Alegret, L.; Lam, A.R.; Asatryan, G. Neogene mass accumulation rate of carbonate sediment in Tasman Sea, southwest Pacific. *Paleoceanogr. Paleoclimatol.* **2022**, *37*, e2021PA004294. [CrossRef]
50. Hills, S.J.; Thierstein, H.R. Plio-Pleistocene calcareous plankton biochronology. *Mar. Micropaleontol.* **1989**, *14*, 67–96. [CrossRef]
51. Schlitzer, R. Ocean Data View. 2018. Available online: <https://odv.awi.de> (accessed on 11 February 2021).
52. Locarnini, R.A.; Mishonov, A.V.; Antonov, J.I.; Boyer, T.P.; Garcia, H.E.; Seidov, D. *World Ocean Atlas 2013, Volume 1: Temperature*; Levitus, S., Mishonov, A., Eds.; NOAA Atlas NESDIS 73; Department of Commerce: Silver Spring, MD, USA, 2013.
53. Bé, A.W. An ecological, zoogeographic and taxonomic review of recent planktonic foraminifera. *Ocean. Micropaleontol.* **1977**, *1*, 76–88.
54. Vincent, E.; Berger, W.H. Planktonic foraminifera and their use in paleoceanography. In *The Oceanic Lithosphere*; Emiliani, C., Ed.; Wiley-Interscience: New York, NY, USA, 1981; Volume 7, pp. 1–100.
55. Kučera, M. Planktonic foraminifera as tracers of past oceanic environments. *Dev. Mar. Geol.* **2007**, *1*, 213–262.
56. Reynolds, R.W.; Rayner, N.A.; Smith, T.M.; Stokes, D.C.; Wang, W. An improved in situ and satellite SST analysis for climate. *J. Clim.* **2002**, *15*, 1609–1625. [CrossRef]
57. National Geographic Society. Tropics. National Geographic Society. 9 October 2012. Available online: <https://www.nationalgeographic.org/encyclopedia/tropics/> (accessed on 3 April 2022).
58. American Meteorological Society. Subtropics—Glossary of Meteorology. 25 April 2012. Available online: <https://glossary.ametsoc.org/wiki/Subtropics> (accessed on 3 April 2022).
59. Bralower, T.J.; Silva, I.P.; Malone, M.J. *Proceedings of the Ocean Drilling Program, Initial Reports 198*; Ocean Drilling Program: College Station, TX, USA, 2002. [CrossRef]
60. Kroenke, L.W.; Berger, W.H.; Janecek, T.R.; Backman, J.; Bassinot, F.; Corfield, R.M.; Delaney, M.L.; Hagen, R.; Jansen, E.; Krissek, L.A.; et al. *Proceedings of the Ocean Drilling Program, Initial Reports*; Ocean Drilling Program: College Station, TX, USA, 1991; Volume 130. [CrossRef]
61. Kennett, J.P.; von der Borch, C.C.; Baker, P.A.; Barton, C.E.; Boersma, A.; Caulet, J.P.; Dudley, W.C.; Gardner, J.V.; Jenkins, G.; Lohman, W.H.; et al. *Initial Reports of the Deep Sea Drilling Project*; U.S. Government Printing Office: Washington, DC, USA, 1986; Volume 90. [CrossRef]

62. Cooke, P.J.; Nelson, C.S.; Crundwell, M.P. Miocene isotope zones, paleotemperatures, and carbon maxima events at intermediate water-depth, Site 593, Southwest Pacific. *N. Z. J. Geol. Geophys.* **2008**, *51*, 1–22. [[CrossRef](#)]
63. Sager, W.W.; Sano, T.; Geldmacher, J. Formation and evolution of Shatsky Rise oceanic plateau: Insights from IODP Expedition 324 and recent geophysical cruises. *Earth-Sci. Rev.* **2016**, *159*, 306–336. [[CrossRef](#)]
64. Sager, W.W.; Zhang, J.; Korenaga, J.; Sano, T.; Koppers, A.A.; Widdowson, M.; Mahoney, J.J. An immense shield volcano within the Shatsky Rise oceanic plateau, northwest Pacific Ocean. *Nat. Geosci.* **2013**, *6*, 976–981. [[CrossRef](#)]
65. Takayama, T. Notes on Neogene calcareous nannofossil biostratigraphy of the Ontong Java Plateau and size variations of Reticulofenestra coccoliths. In *Proceedings of the Ocean Drilling Program Scientific Results*; Berger, W.H., Kroenke, L.W., Janecek, T.R., Backman, J., Bassinot, F., Corfield, R.M., Delaney, M.L., Hagen, R., Jansen, E., Krissek, L.A., et al., Eds.; Ocean Drilling Program: College Station, TX, USA, 1993; Volume 130, pp. 179–229.
66. Kennett, J.P.; von der Borch, C.C.; Baker, P.A.; Barton, C.E.; Boersma, A.; Caulet, J.P.; Dudley, W.C.; Gardner, J.V.; Jenkins, G.; Lohman, W.H.; et al. (Eds.) Shipboard Scientific Party. Introduction and Objectives, Techniques, and Explanatory Notes. In *Initial Reports of the Deep Sea Drilling Program*; U.S. Government Printing Office: Washington, DC, USA, 1986; Volume 90, pp. 3–16.
67. Oke, P.R.; Pilo, G.S.; Ridgway, K.; Kiss, A.; Rykova, T. A search for the Tasman Front. *J. Mar. Syst.* **2019**, *199*, 103217. [[CrossRef](#)]
68. Gradstein, F.M.; Ogg, J.G.; Schmitz, M.D.; Ogg, G.M. *Geologic Time Scale 2020*; Elsevier: Amsterdam, The Netherlands, 2020.
69. Sutherland, R.; Dickens, G.R.; Blum, P.; Agnini, C.; Alegret, L.; Zhou, X. Expedition 371 methods. In *Proceedings of the International Ocean Discovery Program*; Sutherland, R., Dickens, G.R., Blum, P., Agnini, C., Alegret, L., Bhattacharya, J., Bordenave, A., Chang, L., Collot, J., Cramwinckel, M., et al., Eds.; International Ocean Discovery Program: College Station, TX, USA, 2019; Volume 371. [[CrossRef](#)]
70. Wade, B.S.; Olsson, R.K.; Pearson, P.N.; Huber, B.T.; Berggren, W.A. *Atlas of Oligocene Planktonic Foraminifera*; Cushman Foundation for Foraminiferal Research: Washington, DC, USA, 2018.
71. Crundwell, M.P. New Zealand Late Miocene Biostratigraphy and Biochronology: Studies of Planktic Foraminifers and Bolboforms at Oceanic Sites 593 and 1123, and Selected Onland Sections. Ph.D. Thesis, The University of Waikato, Hamilton, New Zealand, 2004. Available online: <https://hdl.handle.net/10289/13214> (accessed on 1 December 2021).
72. Scott, G.H. Coiling excursions in *Globorotalia miotumida*: High resolution bioevents at the middle-upper Miocene boundary in southern temperate water masses? *J. Foraminif. Res.* **1995**, *25*, 299–308. [[CrossRef](#)]
73. Barton, C.E.; Bloemendal, J. Paleomagnetism of sediments collected during Leg 90, southwest Pacific. In *Initial Reports of the Deep Sea Drilling Project*; Kennett, J.P., von der Borch, C.C., Baker, P.A., Barton, C.E., Boersma, A., Caulet, J.P., Dudley, W.C., Gardner, J.V., Jenkins, G., Lohman, W.H., et al., Eds.; U.S. Government Printing Office: Washington, DC, USA, 1986; Volume 90, pp. 1273–1316.
74. Lohman, W.H. Calcareous nannoplankton biostratigraphy of the southern Coral Sea, Tasman Sea, and southwestern Pacific Ocean, Deep Sea Drilling Project Leg 90: Neogene and Quaternary. In *Initial Reports of the Deep Sea Drilling Project*; Kennett, J.P., von der Borch, C.C., Eds.; U.S. Government Printing Office: Washington, DC, USA, 1986; Volume 90, pp. 763–793.
75. Grützmacher, U.J. Die Veränderungen der paläogeographischen Verbreitung von *Bolboforma*—ein Beitrag zur rekonstruktion und definition vor wassermassen in Tertiär. *GEOMAR Res. Cent. Mar. Geosci. Kiel Rep.* **1993**, *22*, 1–104.
76. Crundwell, M.P.; Nelson, C.S. A magnetostratigraphically-constrained chronology for late Miocene bolboformids and planktic foraminifers in the temperate Southwest Pacific. *Stratigraphy* **2007**, *4*, 1–34.
77. Raine, J.I.; Beu, A.G.; Boyes, A.F.; Campbell, H.J.; Cooper, R.A.; Crampton, J.S.; Crundwell, M.P.; Hollis, C.J.; Morgans, H.E.G. Revised Calibration of the New Zealand Geological Timescale: NZGT2015/1. *GNS Sci. Rep.* **2015**, *39*, 1–39.
78. Coxall, H.K.; Pearson, P.N.; Wilson, P.A.; Sexton, P.F. Iterative evolution of digitate planktonic foraminifera. *Paleobiology* **2007**, *33*, 495–516. [[CrossRef](#)]
79. Chaproniere, G.H.; Styzen, M.J.; Sager, W.W.; Nishi, H.; Quinterno, P.J. Late Neogene biostratigraphic and magnetostratigraphic synthesis, Leg 135. In *Proceedings of the Ocean Drilling Program, Scientific Results*; Hawkins, J., Parson, L., Allan, J., Abrahamsen, N., Bednarz, U., Blanc, G., Bloomer, S.H., Bøe, R., Bruns, T.R., Bryan, W.B., et al., Eds.; Ocean Drilling Program: College Station, TX, USA, 1994; Volume 135, pp. 857–877.
80. Pearson, P.N.; Penny, L. Coiling directions in the planktonic foraminifer *Pulleniatina*: A complex eco-evolutionary dynamic spanning millions of years. *PLoS ONE* **2021**, *16*, e0249113. [[CrossRef](#)]
81. Keigwin, L.D.; Prell, W.L.; Gardner, J.V. Neogene planktonic foraminifers from Deep Sea Drilling Project sites 502 and 503. In *Initial Reports of the Deep Sea Drilling Project*; Prell, W.L., Gardner, J.V., Adelseck, C.G., Jr., Blechschmidt, G., Fleet, A.J., Keigwin, L.D., Kent, D.V., Ledbetter, M.T., Mann, U., Mayer, L.A., et al., Eds.; U.S. Government Printing Office: Washington, DC, USA, 1982; Volume 68, pp. 269–288.
82. Morgans, H.E.; Edwards, A.R.; Scott, G.H.; Graham, I.J.; Kamp, P.J.; Mumme, T.C.; Wilson, G.S. Integrated stratigraphy of the Waitakian-Otaian Stage boundary stratotype, Early Miocene, New Zealand. *N. Z. J. Geol. Geophys.* **1999**, *42*, 581–614. [[CrossRef](#)]
83. Chaisson, W.P.; Pearson, P.N. Planktonic foraminifer biostratigraphy at Site 925: Middle Miocene-Pliocene. In *Proceedings of the Ocean Drilling Program Scientific Results*; Shackleton, N.J., Curry, W.B., Richter, C., Bralower, T.J., Eds.; Ocean Drilling Program: Station, TX, USA, 1997; Volume 154, pp. 3–31.
84. Aze, T.; Ezard, T.H.; Purvis, A.; Coxall, H.K.; Stewart, D.R.; Wade, B.S.; Pearson, P.N. A phylogeny of Cenozoic macroperforate planktonic foraminifera from fossil data. *Biol. Rev.* **2011**, *86*, 900–927. [[CrossRef](#)]

85. Fabbri, A.; Zaminga, I.; Ezard, T.H.; Wade, B.S. Systematic taxonomy of middle Miocene *Sphaeroidinellopsis* (planktonic foraminifera). *J. Syst. Palaeontol.* **2021**, *19*, 953–968. [[CrossRef](#)]
86. Wei, K.-Y.; Kennett, J.P. Phyletic gradualism and punctuated equilibrium in the Late Neogene planktic foraminiferal clade *Globoconella*. *Paleobiology* **1988**, *14*, 345–363. [[CrossRef](#)]
87. Chapman, M.R.; Funnell, B.M.; Weaver, P.P.E. Isolation, extinction and migration within Late Pliocene populations of the planktonic foraminiferal lineage *Globorotalia* (*Globoconella*) in the North Atlantic. *Mar. Micropaleontol.* **1998**, *33*, 203–222. [[CrossRef](#)]
88. Scott, G.H.; Bishop, S.; Burt, B.J. *Guide to some Neogene Globorotalids (Foraminiferida) from New Zealand*; New Zealand Geological Survey: Lower Hutt, New Zealand, 1990.
89. Jenkins, D.G. Planktonic foraminiferal zones and new taxa from the lower Miocene to the Pleistocene of New Zealand. *N. Z. J. Geol. Geophys.* **1967**, *10*, 1064–1078. [[CrossRef](#)]
90. Jenkins, D.G. New Zealand Cenozoic planktonic foraminifera. *Palaeont. Bull. N. Z. Geol. Surv.* **1971**, *42*, 1–278.
91. Hornibrook, N.D.B. *Globorotalia* (planktic Foraminiferida) in the late Pliocene and early Pleistocene of New Zealand. *N. Z. J. Geol. Geophys.* **1981**, *24*, 263–292. [[CrossRef](#)]
92. Hornibrook, N.D.B. Late Miocene to Pleistocene *Globorotalia* (Foraminiferida) from DSDP Leg 29, Site 284, Southwest Pacific. *N. Z. J. Geol. Geophys.* **1982**, *25*, 83–99. [[CrossRef](#)]
93. Olsson, R.K.; Hemleben, C.; Huber, B.T.; Berggren, W.A. Taxonomy, biostratigraphy, and phylogeny of Eocene *Globigerina*, *Globoturbotalita*, *Subbotina*, and *Turbotalita*. In *Atlas of Eocene Planktonic Foraminifera*; Pearson, P.N., Olsson, R.K., Huber, B.T., Hemleben, C., Berggren, W.A., Eds.; Cushman Foundation for Foraminiferal Research Special Publication: Washington, DC, USA, 2006; Volume 41, pp. 111–168.
94. Molnar, P. Closing of the Central American Seaway and the Ice Age: A critical review. *Paleoceanography* **2008**, *23*, PA22001. [[CrossRef](#)]
95. Poore, R.Z.; Tauxe, L.; Percival, S.F., Jr.; Labrecque, J.L.; Wright, R.; Petersen, N.P.; Hsü, K. Late Cretaceous—Cenozoic magnetostratigraphic and biostratigraphic correlations of the South Atlantic Ocean: DSDP Leg 73. *Palaeogeogr. Palaeoclimatol. Palaeoecol.* **1983**, *42*, 127–149. [[CrossRef](#)]
96. Pujol, C.; Duprat, J. Quaternary planktonic foraminifera of the southwestern Atlantic (Rio Grande Rise) Deep Sea Drilling Project Leg 72. In *Initial Reports of the Deep Sea Drilling Project*; Barker, P.F., Carlson, R.L., Johnson, D.A., Eds.; U.S. Government Printing Office: Washington, DC, USA, 1983; Volume 72, pp. 601–622.
97. Grazzini, C.V. Non-equilibrium isotopic compositions of shells of planktonic foraminifera in the Mediterranean Sea. *Palaeogeogr. Palaeoclimatol. Palaeoecol.* **1976**, *20*, 263–276. [[CrossRef](#)]
98. Shackleton, N.J.; Vincent, E. Oxygen and carbon isotope studies in recent foraminifera from the southwest Indian Ocean. *Mar. Micropaleontol.* **1978**, *3*, 1–13. [[CrossRef](#)]
99. Hays, J.D.; Saito, T.; Opdyke, N.D.; Burckle, L.H. Pliocene–Pleistocene sediments of the equatorial Pacific: Their paleomagnetic, biostratigraphic, and climatic record. *Geol. Soc. Am. Bull.* **1969**, *80*, 1481–1514. [[CrossRef](#)]
100. Mayer, L.; Pisias, N.; Janecek, T. (Eds.) Shipboard Scientific Party. Site 846. In *Proceedings of the Ocean Drilling Program Initial Reports*; Ocean Drilling Program: College Station, TX, USA, 1992; Volume 138, pp. 265–333.
101. Pearson, P.N.; Shackleton, N.J. Neogene multispecies planktonic foraminifer stable isotope record, Site 871, Limalok Guyot. In *Proceedings of the Ocean Drilling Program Scientific Results*; Silva, I.P., Haggerty, J., Rack, F., Arnaud-Vanneau, A., Bergersen, D.D., Bogdanov, Y., Bohrmann, H.W., Buchardt, B., Camoin, G., Christie, D.M., et al., Eds.; Ocean Drilling Program: College Station, TX, USA, 1995; Volume 144, pp. 401–410.
102. Stewart, D.R.M. Evolution of Neogene Globorotaliid Foraminifera and Miocene Climate Change. Ph.D. Thesis, University of Bristol, Bristol, UK, 2003.
103. Nathan, S.A.; Leckie, R.M. Early history of the Western Pacific Warm Pool during the middle to late Miocene (~13.2–5.8 Ma): Role of sea-level change and implications for equatorial circulation. *Palaeogeogr. Palaeoclimatol. Palaeoecol.* **2009**, *274*, 140–159. [[CrossRef](#)]
104. Venti, N.L.; Billups, K. Stable-isotope stratigraphy of the Pliocene–Pleistocene climate transition in the northwestern subtropical Pacific. *Palaeogeogr. Palaeoclimatol. Palaeoecol.* **2012**, *326*, 54–65. [[CrossRef](#)]
105. Carter, R.M.; McCave, I.N.; Richter, C.; Carter, L.; Aita, Y.; Buret, C.; Di Stefano, A.; Fenner, J.; Fothergill, F.; Gradstein, F.; et al. *Proceedings of the Ocean Drilling Program*; Initial Reports Volume 181; Ocean Drilling Program: College Station, TX, USA, 1999.
106. Al-Sabouni, N.; Fenton, I.S.; Telford, R.J.; Kučera, M. Reproducibility of species recognition in modern planktonic foraminifera and its implications for analyses of community structure. *J. Micropalaeontol.* **2018**, *37*, 519–534. [[CrossRef](#)]
107. Fenton, I.S.; Baranowski, U.; Boscolo-Galazzo, F.; Cheales, H.; Fox, L.; King, D.J.; Purvis, A. Factors affecting consistency and accuracy in identifying modern macroperforate planktonic foraminifera. *J. Micropalaeontol.* **2018**, *37*, 431–443. [[CrossRef](#)]
108. Boltovskoy, E. Twilight of foraminiferology. *J. Paleontol.* **1965**, *39*, 383–390.
109. Leckie, R.M.; Wade, B.S.; Pearson, P.N.; Fraass, A.J.; King, D.J.; Olsson, R.K.; Berggren, W.A. Taxonomy, biostratigraphy, and phylogeny of Oligocene and Early Miocene *Paragloborotalia* and *Parasubbotina*. In *Atlas of Oligocene Planktonic Foraminifera*; Wade, B.S., Olsson, P.N., Pearson, P.N., Huber, B.T., Berggren, W.A., Eds.; Cushman Foundation for Foraminiferal Research: Lawrence, KS, USA, 2018; Volume 46, pp. 125–178.
110. Huber, B.T.; Petrizzo, M.R.; Young, J.R.; Falzoni, F.; Gilardoni, S.E.; Bown, P.R.; Wade, B.S. Pforams@ microtax. *Micropaleontology* **2016**, *62*, 429–438. [[CrossRef](#)]

111. Olsson, R.K.; Berggren, W.A.; Hemleben, C.; Huber, B.T. *Atlas of Paleocene Planktonic Foraminifera*; Smithsonian Institution Press: Washington, DC, USA, 1999.
112. Pearson, P.N.; Olsson, R.K.; Huber, B.T.; Hemleben, C.; Berggren, W.A. *Atlas of Eocene Planktonic Foraminifera*; Cushman Foundation for Foraminiferal Research Special Publication: Washington, DC, USA, 2005.
113. Fraass, A.J.; Leckie, R.M. Oligocene Planktic Foraminiferal Taxonomy and Evolution: An Illustrated Revision of Ocean Drilling Program Site 803. *J. Foraminif. Res.* **2021**, *51*, 139–164. [[CrossRef](#)]
114. Fehrenbacher, J.; Fritz-Enders, T.; Schell, F.; Meyer, G.; Lane, M.K.; Kelly, J. Foraminarium. Available online: <https://www.foraminarium.com/> (accessed on 12 December 2021).
115. Keller, G. Late Neogene biostratigraphy and paleoceanography of DSDP Site 310 Central North Pacific and correlation with the Southwest Pacific. *Mar. Micropaleontol.* **1978**, *3*, 97–119. [[CrossRef](#)]
116. Blow, W.H. Late Middle Eocene to Recent planktonic foraminiferal biostratigraphy. In *Proceedings of the First International Conference Planktonic Microfossils 1967*; EJ Brill: Leiden, The Netherlands, 1969; Volume 1, pp. 199–242.
117. Jenkins, D.G. Planktonic foraminifera and Tertiary intercontinental correlations. *Micropaleontology* **1965**, *11*, 265–277. [[CrossRef](#)]
118. Saito, T. Geologic significance of coiling direction in the planktonic foraminifera *Pulleniatina*. *Geology* **1976**, *4*, 305–309. [[CrossRef](#)]
119. Hornibrook, N.D.B. Correlation of Pliocene biostratigraphy, magnetostratigraphy and O18 fluctuations in New Zealand and DSDP Site 284. *Newsl. Stratigr.* **1980**, *9*, 114–120. [[CrossRef](#)]
120. Crundwell, M.P.; Woodhouse, A. A detailed biostratigraphic framework for 0–1.2 Ma Quaternary sediments of north-eastern Zealandia. *N. Z. J. Geol. Geophys.* **2022**, 1–14. [[CrossRef](#)]
121. Scott, G.H.; Kennett, J.P.; Wilson, K.J.; Hayward, B.W. *Globorotalia puncticulata*: Population divergence, dispersal and extinction related to Pliocene–Quaternary water masses. *Mar. Micropaleontol.* **2007**, *62*, 235–253. [[CrossRef](#)]
122. Hornibrook ND, B. *Globorotalia* (planktic foraminifera) at the Miocene/Pliocene boundary in New Zealand. *Palaeogeogr. Palaeoclimatol. Palaeoecol.* **1984**, *46*, 107–117. [[CrossRef](#)]
123. Wilkens, R.H.; Westerhold, T.; Drury, A.J.; Lyle, M.; Gorgas, T.; Tian, J. Revisiting the Ceara Rise, equatorial Atlantic Ocean: Isotope stratigraphy of ODP Leg 154 from 0 to 5 Ma. *Clim. Past* **2017**, *13*, 779–793. [[CrossRef](#)]
124. Hayashi, H.; Idemitsu, K.; Wade, B.S.; Idehara, Y.; Kimoto, K.; Nishi, H.; Matsui, H. Middle Miocene to Pleistocene planktonic foraminiferal biostratigraphy in the eastern equatorial Pacific Ocean. *Paleontol. Res.* **2013**, *17*, 91–109. [[CrossRef](#)]
125. Ogg, J.G.; Ogg, G.M.; Gradstein, F.M. Neogene. In *A Concise Geologic Time Scale*; Ogg, J.G., Ogg, G.M., Gradstein, F.M., Eds.; Elsevier: Amsterdam, The Netherlands, 2016; pp. 201–203.
126. Drury, A.J.; Westerhold, T.; Frederichs, T.; Tian, J.; Wilkens, R.; Channell, J.E.; Röhl, U. Late Miocene climate and time scale reconciliation: Accurate orbital calibration from a deep-sea perspective. *Earth Planet. Sci. Lett.* **2017**, *475*, 254–266. [[CrossRef](#)]
127. Kuhnt, W.; Holbourn, A.; Hall, R.; Zuvella, M.; Käse, R. Neogene history of the Indonesian throughflow. In *Continent–Ocean Interactions within East Asian Marginal Seas. Geophysical Monograph*; Clift, P.D., Wang, P., Kuhnt, W., Hayes, D.E., Eds.; American Geophysical Union: Washington, DC, USA, 2004; Volume 149, pp. 299–320.
128. Vincent, E. Indian Ocean Neogene planktonic foraminiferal biostratigraphy and its paleoceanographic implications. *Indian Ocean. Geol. Biostratigraphy* **1977**, *20*, 469–584.
129. Srinivasan, M.S. Recent advances in Neogene planktonic foraminiferal biostratigraphy, chemostratigraphy and paleoceanography, Northern Indian Ocean. *J. Palaeontol. Soc. India* **1989**, *34*, 1–18.
130. Sinha, D.K.; Singh, A.K. Late Neogene planktic foraminiferal biochronology of the ODP Site 763a, Exmouth Plateau, southeast Indian Ocean. *J. Foraminif. Res.* **2008**, *38*, 251–270. [[CrossRef](#)]
131. Groeneveld, J.; De Vleeschouwer, D.; McCaffrey, J.C.; Gallagher, S.J. Dating the northwest shelf of Australia since the Pliocene. *Geochem. Geophys. Geosyst.* **2021**, *22*, e2020GC009418. [[CrossRef](#)]
132. de Vargas, C.; Norris, R.; Zaninetti, L.; Gibb, S.W.; Pawlowski, J. Molecular evidence of cryptic speciation in planktonic foraminifers and their relation to oceanic provinces. *Proc. Natl. Acad. Sci. USA* **1999**, *96*, 2864–2868. [[CrossRef](#)]
133. Norris, R.D. Hydrographic and tectonic control of plankton distribution and evolution. In *Reconstructing Ocean History*; Abrantes, F., Mix, A.C., Eds.; Springer: Berlin/Heidelberg, Germany, 1999; pp. 173–193.
134. Darling, K.F.; Wade, C.M.; Kroon, D.; Brown AJ, L.; Bijma, J. The diversity and distribution of modern planktic foraminiferal small subunit ribosomal RNA genotypes and their potential as tracers of present and past ocean circulations. *Paleoceanography* **1999**, *14*, 3–12. [[CrossRef](#)]
135. Norris, R.D. Species diversity, biogeography, and evolution in the pelagic realm. In *Deep Time: Paleobiology's Perspective*; Erwin, D.H., Wing, S.L., Eds.; Paleontological Society: Baltimore, MA, USA, 2000; pp. 237–258.
136. de Vargas, C.; Bonzon, M.; Rees, N.W.; Pawlowski, J.; Zaninetti, L. A molecular approach to biodiversity and biogeography in the planktonic foraminifer *Globigerinella siphonifera* (d'Orbigny). *Mar. Micropaleontol.* **2002**, *45*, 101–116. [[CrossRef](#)]
137. Sexton, P.F.; Norris, R.D. Dispersal and biogeography of marine plankton: Long-distance dispersal of the foraminifer *Truncorotalia truncatulinoides*. *Geology* **2008**, *36*, 899–902. [[CrossRef](#)]
138. Bradshaw, J.S. Ecology of living planktonic foraminifera in the north and equatorial Pacific Ocean. *Contrib. Cushman Found. Foraminif. Res.* **1959**, *10*, 25–64.
139. Schneider, C.E.; Kennett, J.P. Isotopic evidence for interspecies habitat differences during evolution of the Neogene planktonic foraminiferal clade *Globoconella*. *Paleobiology* **1996**, *22*, 282–303. [[CrossRef](#)]

140. Rutherford, S.; D'Hondt, S.; Prell, W. Environmental controls on the geographic distribution of zooplankton diversity. *Nature* **1999**, *400*, 749–753. [[CrossRef](#)]
141. Tittensor, D.P.; Mora, C.; Jetz, W.; Lotze, H.K.; Ricard, D.; Berghe, E.V.; Worm, B. Global patterns and predictors of marine biodiversity across taxa. *Nature* **2010**, *466*, 1098–1101. [[CrossRef](#)]
142. Yasuhara, M.; Hunt, G.; Dowsett, H.J.; Robinson, M.M.; Stoll, D.K. Latitudinal species diversity gradient of marine zooplankton for the last three million years. *Ecol. Lett.* **2012**, *15*, 1174–1179. [[CrossRef](#)]
143. Fenton, I.S.; Pearson, P.N.; Dunkley Jones, T.; Purvis, A. Environmental predictors of diversity in recent planktonic foraminifera as recorded in marine sediments. *PLoS ONE* **2016**, *11*, e0165522. [[CrossRef](#)]
144. Fenton, I.S.; Pearson, P.N.; Jones, T.D.; Farnsworth, A.; Lunt, D.J.; Markwick, P.; Purvis, A. The impact of Cenozoic cooling on assemblage diversity in planktonic foraminifera. *Philos. Trans. R. Soc. B Biol. Sci.* **2016**, *371*, 20150224. [[CrossRef](#)]
145. Scott, G.H. *Globorotalia inflata* lineage and *G. crassaformis* from Blind River, New Zealand: Recognition, relationship, and use in uppermost Miocene-lower Pliocene biostratigraphy. *N. Z. J. Geol. Geophys.* **1980**, *23*, 665–677.
146. DeConto, R.M.; Pollard, D. Rapid Cenozoic glaciation of Antarctica induced by declining atmospheric CO₂. *Nature* **2003**, *421*, 245–249. [[CrossRef](#)]
147. Kennett, J.P. Cenozoic evolution of Antarctic glaciation, the circum-Antarctic Ocean, and their impact on global paleoceanography. *J. Geophys. Res.* **1977**, *82*, 3843–3860. [[CrossRef](#)]
148. Kennett, J.P. The development of planktonic biogeography in the Southern Ocean during the Cenozoic. *Mar. Micropaleontol.* **1978**, *3*, 301–345. [[CrossRef](#)]
149. Zhang, Y.; Chen, X.; Dong, C. Anatomy of a cyclonic eddy in the Kuroshio extension based on high-resolution observations. *Atmosphere* **2019**, *10*, 553. [[CrossRef](#)]
150. Kennett, J.P.; Keller, G.; Srinivasan, M.S. Miocene planktonic foraminiferal biogeography and pale-oceanographic development of the Indo-Pacific region. In *The Miocene Ocean: Paleooceanography and Biogeography*; Kennett, J.P., Ed.; Geological Society of America: Boulder, CO, USA, 1985; Volume 163, pp. 197–236.
151. Wu, L.; Cai, W.; Zhang, L.; Nakamura, H.; Timmermann, A.; Joyce, T.; Giese, B. Enhanced warming over the global subtropical western boundary currents. *Nat. Clim. Chang.* **2012**, *2*, 161–166. [[CrossRef](#)]
152. Matsui, H.; Horikawa, K.; Chiyonobu, S.; Itaki, T.; Ikehara, M.; Kawagata, S.; Okazaki, Y. Integrated Neogene biochemostratigraphy at DSDP Site 296 on the Kyushu-Palau Ridge in the western North Pacific. *Newsl. Stratigr.* **2020**, *53*, 313–331. [[CrossRef](#)]